Copyright Warning & Restrictions

The copyright law of the United States (Title 17, United States Code) governs the making of photocopies or other reproductions of copyrighted material.

Under certain conditions specified in the law, libraries and archives are authorized to furnish a photocopy or other reproduction. One of these specified conditions is that the photocopy or reproduction is not to be "used for any purpose other than private study, scholarship, or research." If a, user makes a request for, or later uses, a photocopy or reproduction for purposes in excess of "fair use" that user may be liable for copyright infringement,

This institution reserves the right to refuse to accept a copying order if, in its judgment, fulfillment of the order would involve violation of copyright law.

Please Note: The author retains the copyright while the New Jersey Institute of Technology reserves the right to distribute this thesis or dissertation

Printing note: If you do not wish to print this page, then select "Pages from: first page # to: last page #" on the print dialog screen

NJIT New Jersey's Science & Technology University

The Van Houten library has removed some of the personal information and all signatures from the approval page and biographical sketches of theses and dissertations in order to protect the identity of NJIT graduates and faculty.

ABSTRACT

I/Q IMBALANCE MITIGATION FOR SPACE-TIME BLOCK CODED COMMUNICATION SYSTEMS

by
Mingzheng Cao

Multiple-input multiple-output (MIMO) space-time block coded (STBC) wireless communication systems provide reliable data transmissions by exploiting the spatial diversity in fading channels. However, due to component imperfections, the in-phase/quadrature (I/Q) imbalance caused by the non-ideal matching between the relative amplitudes and phases of the I and Q branches always exists in the practical implementation of MIMO STBC communication systems. Such distortion results in a complex conjugate term of the intended signal in the time domain, hence a mirror-image term in the frequency domain, in the data structure. Consequently, I/Q imbalance increases the symbol error rate (SER) drastically in MIMO STBC or STBC MIMO orthogonal frequency division multiplexing (OFDM) communication systems, where both the signal and its complex conjugate are utilized for the information transmission, hence should be mitigated effectively.

In this dissertation, the impact of I/Q imbalance in MIMO STBC systems over flat fading channels, the impact of I/Q imbalance in STBC MIMO-OFDM systems and in time-reversal STBC (TR-STBC) systems over frequency-selective fading channels are studied systematically. With regard to the MIMO STBC and the STBC MIMO-OFDM systems with I/Q imbalance, orthogonal space-time block codes (OSTBCs), quasi-orthogonal STBCs (QOSTBCs) and rotated QOSTBCs (RQOSTBCs) are studied, respectively. By exploiting the special structure of the received signal, low-complexity solutions are provided to mitigate the distortion induced by I/Q imbalance successfully. In addition, to mitigate I/Q imbalance while at the same time to exploit the multipath diversity for STBC OFDM systems over frequency-selective fading channels, a new encoding/decoing scheme for the grouped linear constellation precoded (GLCP) OFDM systems with I/Q imbalance is studied.

In Chapter 1, the objectives of the research are elaborated. In Chapter 2, the various I/Q imbalance models are introduced, and the model used in this dissertation is established. In Chapter 3, the performance degradation caused by I/Q imbalance of the transceivers in MIMO STBC wireless communication systems over flat fading channels and the solutions are studied. A 2 Tx Alamouti system, a 4 Tx quasi-orthogonal STBC (QOSTBC) system, and a 4 Tx rotated QOSTBC (RQOSTBC) system with I/Q imbalance are studied in detail. By exploiting the special structure of the received signal, low-complexity solutions are proposed to mitigate I/Q imbalance successfully.

Since STBCs are developed for frequency-flat fading channels, to achieve the spatial diversity in frequency-selective fading channels, MIMO-OFDM arrangements have been suggested, where STBCs are used across different antennas in conjunction with OFDM. In Chapter 4, the performance degradation caused by I/Q imbalance in STBC MIMO-OFDM wireless systems over frequency-selective fading channels and the solutions are studied. Similarly, a 2 Tx Alamouti system, a 4 Tx quasi-orthogonal STBC (QOSTBC) system, and a 4 Tx rotated QOSTBC (RQOSTBC) system with I/Q imbalance are studied in detail, and low-complexity solutions are proposed to mitigate the distortion effectively.

However, OFDM systems suffer from the loss of the multipath diversity by converting frequency-selective fading channels into parallel frequency-flat fading subchannels. To exploit the multipath diversity and reduce the decoding complexity, GLCP OFDM systems with I/Q imbalance are studied. By judiciously assigning the mirror-subcarrier pair into one group, a new encoding/decoding scheme with a low-complexity is proposed to mitigate I/Q imbalance for GLCP OFDM systems in Chapter 5.

Since OFDM communication systems have high peak-to-average power ratio (PAPR) problem and are sensitive to carrier frequency offset (CFO), to achieve both the spatial and multipath diversity, time-reversal STBC (TR-STBC) communication systems are introduced. In Chapter 6, the I/Q imbalance mitigating solutions in TR-STBC systems, both in the time domain and in the frequency domain, are studied.

I/Q IMBALANCE MITIGATION FOR SPACE-TIME BLOCK CODED COMMUNICATION SYSTEMS

by
Mingzheng Cao

A Dissertation
Submitted to the Faculty of
New Jersey Institute of Technology
in Partial Fulfillment of the Requirements for the Degree of
Doctor of Philosophy in Electrical Engineering

Department of Electrical and Computer Engineering

May 2009

Copyright © 2009 by Mingzheng Cao

ALL RIGHTS RESERVED

APPROVAL PAGE

I/Q IMBALANCE MITIGATION FOR SPACE-TIME BLOCK CODED COMMUNICATION SYSTEMS

Mingzheng Cao

11/14/08

Hongya Ge, Dissertation Advisor — Date
Associate Professor, ECE Dept., New Jersey Institute of Technology

11/14/08

Yeheskel Bar-Ness, Committee Member — Date
Distinguished Professor, ECE Dept., New Jersey Institute of Technology

11/14/08

Ali Abdi, Committee Member — Date
Associate Professor, ECE Dept., New Jersey Institute of Technology

11/14/08

Osvaldo Simeone, Committee Member — Date
Assistant Professor, ECE Dept., New Jersey Institute of Technology

11/14/08

Hongbin Li, Committee Member — Date
Associate Professor, ECE Dept., Stevens Institute of Technology

BIOGRAPHICAL SKETCH

Author: Mingzheng Cao

Degree: Doctor of Philosophy

Date: May 2009

Undergraduate and Graduate Education:

- Doctor of Philosophy in Electrical Engineering,
  New Jersey Institute of Technology, Newark, NJ, USA, 2009
- Master of Science in Electrical Engineering,
  National University of Singapore, Singapore, 2004
- Bachelor of Science in Electrical Engineering,
  Tianjin University, Tianjin, China, 1996

Major: Electrical Engineering

Presentations and Publications:

Mingzheng Cao and Hongya Ge, "I/Q Imbalance Mitigation for STBC Communication Systems," submitted to *IEEE Trans. on Wireless Communications.*

Mingzheng Cao and Hongya Ge, "GLCP OFDM System With I/Q Imbalance," *IEEE Communications Letters*, Vol. 13, No. 4, April 2009.

Mingzheng Cao and Hongya Ge, "I/Q Imbalance Mitigation for Time-Reversal STBC Systems Over Frequency-Selective Fading Channels," *in Proc. of IEEE International Conference on Acoustics, Speech, and Signal Processing (ICASSP)*, Taipei, Taiwan, April 2009.

Mingzheng Cao and Hongya Ge, "I/Q Imbalance in MIMO STBC Communication Systems: Impact and Solution," *in Proc. of IEEE Military Communications Conference (Milcom)*, San Diego, CA, Nov. 2008.

Mingzheng Cao and Hongya Ge, "CP Based Time-Reversal QOSTBC Transmissions Over Frequency-Selective Fading Channels," *in Proc. of IEEE Military Communications Conference (Milcom)*, San Diego, CA, Nov. 2008.

Mingzheng Cao and Hongya Ge, "I/Q Imbalance Mitigation for STBC MIMO-OFDM Communication Systems," *in Proc. of IEEE International Conference on Acoustics, Speech, and Signal Processing (ICASSP)*, Las Vegas, NV, April 2008.

Mingzheng Cao, Hongya Ge, Hong Zhang, and Ali Abdi, "Parametric Doppler Spread Estimation in Mobile Fading Channels," *in Proc. of IEEE Military Communications Conference (Milcom)*, Orlando, FL, Oct. 2007.

Mingzheng Cao, Xiaoli Wang, and Hongya Ge, "Experimental Study on the Performance of the Reduced Rank Timing Acquisition Scheme for Multiple Access Communications," *in Proc. of IEEE Sarnoff Symposium*, Princeton, NJ, April 2007.

Mingzheng Cao and Hongya Ge, "Parametric Modeling in Mitigating I/Q Mismatch: Estimation, Equalization and Performance Analysis," *in Proc. of the 40th Annual Conference on Information Sciences and Systems (CISS)*, Princeton, NJ, March 2006.

To my parents

Guangquan Cao and Chundi Liao,

my sisters

Mingrong, Minghua, Mingxia, Minghong,

and my brother

Mingfei.

ACKNOWLEDGMENT

I would like to acknowledge all the people who have made this dissertation possible.

First, I would like to express my sincere gratitude to my advisor, Dr. Hongya Ge, for her guidance and financial support throughout my Ph.D. study. She gave me an insightful view of the signal processing for wireless communications I never had before, and the correct way to conduct a scientific research. What I have learned from her is invaluable and will continue to guide me in the future. It is no doubt that my pursuing of Ph.D. could be impossible without her support and guidance. Also, I would like to give my special acknowledge to Dr. Nirwan Ansari, for his support during the period of my study.

In addition, I would also like to thank Dr. Yeheskel Bar-Ness, Dr. Ali Abdi, Dr. Osvaldo Simeone and Dr. Hongbin Li for their serving as my committee members.

Moreover, I would like to give the special acknowledge to Dr. Yeheskel Bar-Ness, the director of the Center for Wireless Communication and Signal Processing Research (CWCSPR), for accepting me as a member of the center, where I met many wonderful researchers. The interactions with them greatly expanded my knowledge in wireless communications and signal processing. Also I would like to give special thanks to Dr. Shengshan Cui, Dr. Jordi Diaz, Huaihai Gauo, Dr. Hong Li, Bo Niu, Dr. Hongshan Sheng, Miao Shi, Igor Stanojev, Nicola Varanese, Dr. Shuangquan Wang, Xiaoli Wang, Dr. Hong Zhang, Dr. Jianming Zhu and all the other students in the center for their help in my research, and Ms. Marlene Toeroek for her administrative assistance.

Last, but not the least, I would like to thank my family for their unconditional support throughout my life.

TABLE OF CONTENTS

TABLE OF CONTENTS
(Continued)

TABLE OF CONTENTS
(Continued)

Chapter **Page**

LIST OF FIGURES

LIST OF FIGURES
(Continued)

Figure **Page**

LIST OF FIGURES
(Continued)

Figure **Page**

ABBREVIATIONS

AWGN:	additive white Gaussian noise
BER:	bit error rate
CDMA:	code division multiple access
CFO:	carrier frequency offset
CP:	cyclic prefix
CRLB:	Cramer-Rao lower bound
DFE:	decision feedback equalizer
DFT:	discrete Fourier transform
ECSI:	effective channel state information
FD:	frequency domain
FIR:	finite-impulse-response
GLCP:	grouped linear constellation precoded
ISI:	inter-symbol-interference
ICI:	inter-carrier interference
I/Q:	in-phase/quadrature
LMMSE:	linear minimum-mean-square-error
LO:	local oscillator
LPF:	lowpass filter
LS:	least squares
MC-CDMA:	multi-carrier code division multiple access
MIMO:	multiple-input multiple-output
ML:	maximum likelihood
MLSE:	maximum likelihood sequence estimate
MMSE:	minimum-mean-squared-error
MRC:	maximum ratio combining

OFDM:	orthogonal frequency division multiplexing
OSTBC:	orthogonal space-time block coded
OSTBCs:	orthogonal space-time block codes
PAPR:	peak-to-average power ratio
PEP:	pair-wise error probability
PLS:	polygon local searching
PMF:	probability mass function
PSK:	phase-shift keying
QAM:	quadrature amplitude modulation
QOSTBC:	quasi-orthogonal space-time block coded
QOSTBCs:	quasi-orthogonal space-time block codes
RQOSTBC:	rotated quasi-orthogonal space-time block coded
RQOSTBCs:	rotated quasi-orthogonal space-time block codes
Rx:	receiver
SER:	symbol error rate
SFBC:	space-frequency block coded
SIR:	signal-to-interference ratio
SISO:	single-input single-output
SNR:	signal-to-noise ratio
STBC:	space-time block coded
STBCs:	space-time block codes
TR:	time-reversal
TRC:	time-reversal conjugate
Tx:	transmitter
ZF:	zero-forcing

NOTATION

$\mathbf{A}^*$:	complex-conjugate of $\mathbf{A}$
$\mathbf{A}^T$:	transpose of $\mathbf{A}$
$\mathbf{A}^H$:	complex-conjugate and transpose of $\mathbf{A}$
$\mathbf{A}^{-1}$:	inverse of $\mathbf{A}$
rank($\mathbf{A}$):	rank of matrix $\mathbf{A}$
det($\mathbf{A}$):	determinant of matrix $\mathbf{A}$
circ{$\mathbf{x}$}:	a circulant matrix with $\mathbf{x}$ as its first column
diag{$\mathbf{x}$}:	a diagonal matrix with elements of $\mathbf{x}$ as its diagonal entries
$\mathcal{F}\{\mathbf{x}\}$:	discrete Fourier transform of $\mathbf{x}$
$\Re\{\mathbf{x}\}$:	real part of $\mathbf{x}$
$\Im\{\mathbf{x}\}$:	imaginary part of $\mathbf{x}$
$\mathbf{x}_I$:	in-phase part of $\mathbf{x}$
$\mathbf{x}_Q$:	quadrature part of $\mathbf{x}$
$\circledast$:	convolution product
$\otimes$:	Kronecker product
$E\{x\}$:	statistical expectation of x
j:	$\sqrt{-1}$
$\mathbf{I}_N$:	identity matrix of size $N \times N$
$\mathbf{0}_{M\times N}$:	all-zero matrix of size $M \times N$
$\|\mathbf{x}\|^2$:	Euclidean norm of $\mathbf{x}$

CHAPTER 1

INTRODUCTION

1.1 Problem Statement

In wireless communication systems, as a result of the multipath propagation, the amplitude and phase of the received signal vary significantly in time due to the constructive and destructive superpositions of the replicas of the transmitted signal. The corresponding channel is called fading channel, and the transmitted signal can not be recovered reliably when the channel is in a deep fade [1] [2] [3] [4] [5]. In multiple-input multiple-output (MIMO) communication systems, when the multiple antennas are put far away, different channels fade independently, making the spatial diversity available. Recently, the MIMO space-time block coded (STBC) system is introduced to improve the reliability of the transmission by exploiting the spatial diversity [6] [7] [8].

Within various space-time block codes (STBCs), orthogonal STBCs (OSTBCs) are studied extensively since they can provide the full spatial diversity with simple linear maximum likelihood (ML) decodings. Their drawback is that only Alamouti scheme can provide a full rate transmission if a complex constellation is used. To achieve the full rate transmission while sacrificing the full spatial diversity, quasi-orthogonal STBCs (QOSTBCs) are proposed, with low computational pair-wise ML decodings feasible. By choosing some symbols from a rotated constellation, the rotated QOSTBCs (RQOSTBCs) can provide the full spatial diversity, full rate, and pair-wise ML decoding properties [9] [6].

Since STBCs are developed for frequency-flat fading channels, to achieve the spatial diversity in frequency-selective fading channels, MIMO orthogonal frequency division multiplexing (OFDM) arrangements have been suggested, where STBCs are used across different antennas in conjunction with OFDM [10] [11] [12] [13]. Consequently, the inter-

symbol-interference (ISI) can be removed by converting the frequency-selective fading channels into the flat fading channels.

However, OFDM systems suffer from the loss of the multipath diversity by converting the frequency-selective fading channels into the parallel flat fading subchannels. To exploit the multipath diversity, the coding across subcarriers of STBC MIMO-OFDM systems is needed [14]. To reduce the decoding complexity while exploit the multipath diversity, grouped linear constellation precoded (GLCP) OFDM systems are studied and an optimal subcarrier grouping is proposed in [15] [16].

Since OFDM systems have the high peak-to-average power ratio (PAPR) problem [17] [18] and are sensitive to the carrier frequency offset (CFO) [19] [20], to achieve both the spatial and multipath diversity over frequency-selective fading channels, time-reversal STBC (TR-STBC) communication systems with equalization, either in the time domain or in the frequency domain, are studied [21] [22] [23] [24].

Practically, due to the component imperfections, some analog processing problems result from the low-cost, low-power, and highly integrated implementation of MIMO STBC systems. The associated impairments with the analog processing should be compensated in the digital baseband domain. One of the problems is the in-phase/quadrature (I/Q) imbalance caused by the non-ideal matching between the relative amplitudes and phases of the I and Q branches, especially in the direct conversion transceiver design [25] [26]. This distortion results in a complex conjugate term of the intended signal in the time domain and a mirror-image term in the frequency domain in the data structure, increasing symbol error rate (SER) dramatically, especially in STBC systems utilizing both the transmitted symbol and its complex conjugate, hence should be mitigated effectively.

In this dissertation, the impact of I/Q imbalance in MIMO STBC systems over flat fading channels, the impact of I/Q imbalance in STBC MIMO-OFDM systems and in TR-STBC systems over frequency-selective fading channels are studied systematically. Since I/Q imbalance results in a complex conjugate term of the intended signal in the time

domain, by reformulating the complex-valued signal into a real-valued form with its in-phase and quadrature parts separately, low-complexity solutions are provided to mitigate the distortion successfully in MIMO STBC communication systems with I/Q imbalance. In the frequency domain, I/Q imbalance causes the inter-carrier interference (ICI) between the mirror-subcarrier pair, by reformulating the received signal over the mirror-subcarrier pair together, similar low-complexity solutions are provided to mitigate the distortion effectively in STBC MIMO-OFDM communication systems with I/Q imbalance. In addition, to mitigate I/Q imbalance and to exploit the multipath diversity for STBC OFDM systems over frequency-selective fading channels, a new encoding/decoing scheme for GLCP OFDM systems with I/Q imbalance is studied. Moreover, in cyclic prefix (CP) based TR-STBC communication systems with I/Q imbalance over frequency-selective fading channels, by using the circulant property of the effective channel matrix, low-complexity solutions, both in the time domain and in the frequency domain, are proposed to mitigate I/Q imbalance and to achieve the multipath diversity.

1.2 Organization of Dissertation

The dissertation is organized as follows. The I/Q imbalance models in MIMO systems, both in the time domain and in the frequency domain are established in Chapter 2. In Chapter 3, the performance degradation caused by I/Q imbalance of the transceivers in MIMO STBC wireless communication systems over frequency-flat fading channels and the solutions are studied. A 2 Tx Alamouti system, a 4 Tx quasi-orthogonal STBC (QOSTBC) system, and a 4 Tx rotated QOSTBC (RQOSTBC) system with I/Q imbalance are examined in detail. By exploiting the special structure of the received signal, low-complexity solutions are proposed to mitigate the distortion successfully. In Chapter 4, the performance degradation caused by I/Q imbalance in STBC MIMO-OFDM wireless communication systems over frequency-selective fading channels and the solutions are studied. Similarly, a 2 Tx Alamouti system, a 4 Tx QOSTBC system, and a 4 Tx RQOSTBC system with I/Q

imbalance are examined in detail, and low-complexity solutions are proposed to mitigate the distortion successfully. In Chapter 5, to mitigate I/Q imbalance while at the same time to exploit the multipath diversity in OFDM systems over frequency-selective fading channels, a new subcarrier grouping is proposed with a low-complexity decoding feasible in the presence of I/Q imbalance. In Chapter 6, the solutions, both in the time domain and in the frequency domain, of I/Q imbalance mitigation in TR-STBC systems are studied.

CHAPTER 2

I/Q IMBALANCE MODEL OF TRANSCEIVER

2.1 Introduction

Due to the physical characteristics of the capacitor and the resistor used to implement the analog components, the error in the nominal 90^o phase shift and the imbalance between the amplitudes of the I and Q branches will corrupt the up-converted and down-converted signal constellations [25]. The imbalance caused by the different amplitudes of the I and Q channels and by the phase shift error is termed as I/Q imbalance, or I/Q mismatch. Without being compensated, I/Q imbalance will increase SER of a communication system.

Many methods have been proposed to compensate I/Q imbalance based on different models [27] [28] [29] [30] [31]. In [27] and [28], a four-parameter model of I/Q imbalance is used, two describing the amplitude gains of the I and Q channels and the other two describing the corresponding phases, respectively. Based on this model, the gain and phase parameters for each channel are grouped together and then are estimated by a nonlinear regression technique [28]. In [30], an adaptive scheme is proposed to mitigate I/Q imbalance based on a model involving three parameters where two parameters describe the amplitude gains of the I and Q channels, and one parameter describes the phase imbalance, respectively. With the same three-parameter model, the amplitude and phase imbalance can be estimated first with the Cramer-Rao lower bound (CRLB) derived, and then be mitigated [32]. However, since only the relative value of the amplitude imbalance and the phase shift are needed to mitigate the resulting distortions, a two-parameter model becomes widely used [31]. By introducing different filter responses to the I and Q branches, a frequency-dependent I/Q imbalance model is established and mitigation solutions are provided in [33] and [34].

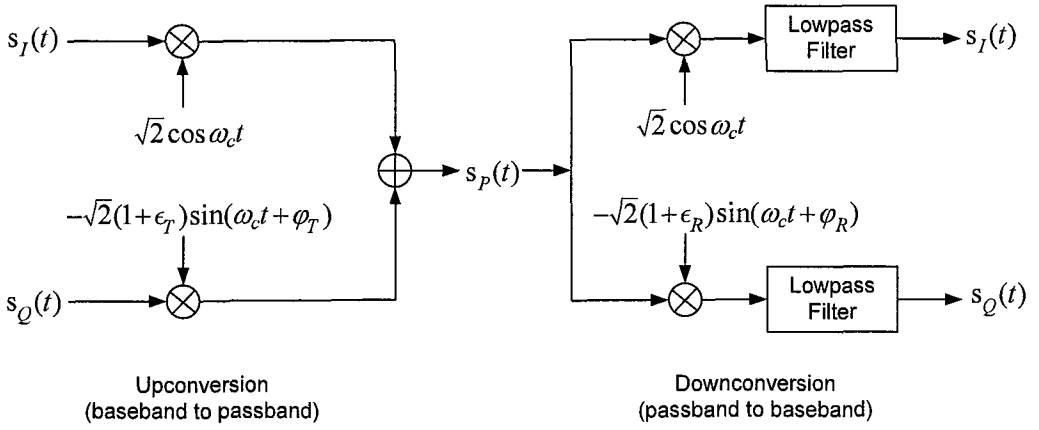

Figure 2.1 Upconversion from baseband to passband and downconversion from passband to baseband. A two-parameter I/Q imbalance model is used.

In this dissertation, a two-parameter frequency-independent I/Q imbalance model is adopted, and the same transmitter/receiver I/Q imbalance parameters are assumed for all the transmitting/receiving antennas sharing *the same* local oscillator (LO). It helps us to have a deep insight of the impact of I/Q imbalance in different encoding/decoing schemes.

2.2 I/Q Imbalance Model and Effect in Time Domain

As shown in Fig. 2.1, let ϵ_T and φ_T represent the amplitude and phase imbalance parameters of the transmitter, then the LO output at the transmitter can be expressed as

$$\begin{aligned} c_T(t) &= \cos(\omega_c t) + j(1+\epsilon_T)\sin(\omega_c t + \varphi_T) \\ &= \alpha_T e^{j\omega_c t} + \beta_T^* e^{-j\omega_c t}, \end{aligned} \tag{2.1}$$

where $\alpha_T = \frac{1}{2}[1 + (1+\epsilon_T)e^{j\varphi_T}]$, and $\beta_T = \frac{1}{2}[1 - (1+\epsilon_T)e^{j\varphi_T}]$. Consequently, the up-converted passband signal for the intended transmission $s(t)$ becomes $\Re\{\sqrt{2}s(t)c_T(t)\} = \Re\{\sqrt{2}s_T(t)e^{j\omega_c t}\}$, resulting in the equivalent baseband signal

$$s_T(t) = \alpha_T s(t) + \beta_T s^*(t), \tag{2.2}$$

containing both the intended signal and its complex-conjugate term.

In the absence of the transmitter I/Q imbalance, $\epsilon_T = 0$ and $\varphi_T = 0$, then $\alpha_T = 1$ and $\beta_T = 0$. Consequently, the LO output of the transmitter $c_T(t) = e^{j\omega_c t}$ is ideal, and the equivalent baseband signal $s_T(t)$ is the intended transmission $s(t)$.

Similarly, the LO output at the receiver can be expressed as

$$\begin{aligned} c_R(t) &= \cos(\omega_c t) - j(1+\epsilon_R)\sin(\omega_c t + \varphi_R) \\ &= \alpha_R^* e^{-j\omega_c t} + \beta_R e^{j\omega_c t}, \end{aligned} \tag{2.3}$$

where $\alpha_R = \frac{1}{2}[1+(1+\epsilon_R)e^{j\varphi_R}]$, and $\beta_R = \frac{1}{2}[1-(1+\epsilon_R)e^{j\varphi_R}]$, with ϵ_R and φ_R representing the amplitude and phase imbalance parameters of the receiving antennas. In the absence of the receiver I/Q imbalance, $\epsilon_R = 0$, $\varphi_R = 0$, $\alpha_R = 1$ and $\beta_R = 0$, then the LO output of the receiver becomes ideal with $c_R(t) = e^{-j\omega_c t}$.

Taking into account the effect of the channel $h(t)$ and the additive noise $n(t)$, the received data down-converted by $c_R(t)$ takes the equivalent baseband form,

$$r(t) = \alpha_R^*[h(t) \circledast s_T(t)] + \beta_R[h(t) \circledast s_T(t)]^* + n(t). \tag{2.4}$$

As shown in (2.2) and (2.4), the target signal is interfered by its own complex-conjugate due to I/Q imbalance either at the transmitter or receiver side. Note that the additive noise $n(t)$ contains the distortion caused by the receiver I/Q imbalance.

The relation between the transmitted signal and the received signal in (2.2) and (2.4) can be illustrated in Fig.2.2. In the absence of the transceiver I/Q imbalance, $\alpha_T = \alpha_R = 1$, and $\beta_T = \beta_R = 0$, the distortion illustrated by the dashed line disappears, and the relation boils down to $r(t) = h(t) \circledast s(t) + n(t)$.

The detailed derivation of the transceiver I/Q imbalance can be found in Appendix A.

I/Q imbalance causes distortion to the received signal, hence increases SER, especially when the high order modulation such as 16-QAM, 16-PSK, 64-QAM constellations are

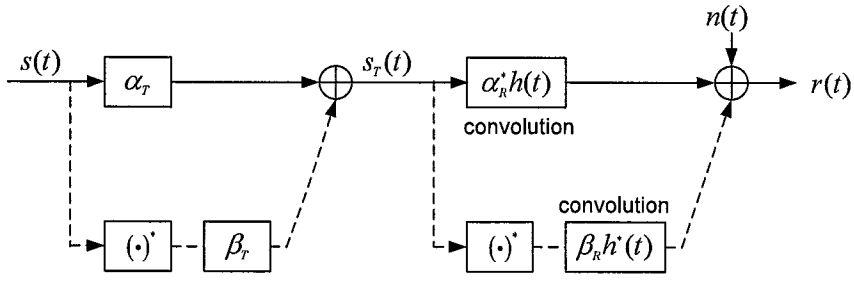

Figure 2.2 Block diagram of the received signal in the presence of the transceiver I/Q imbalance in the time domain.

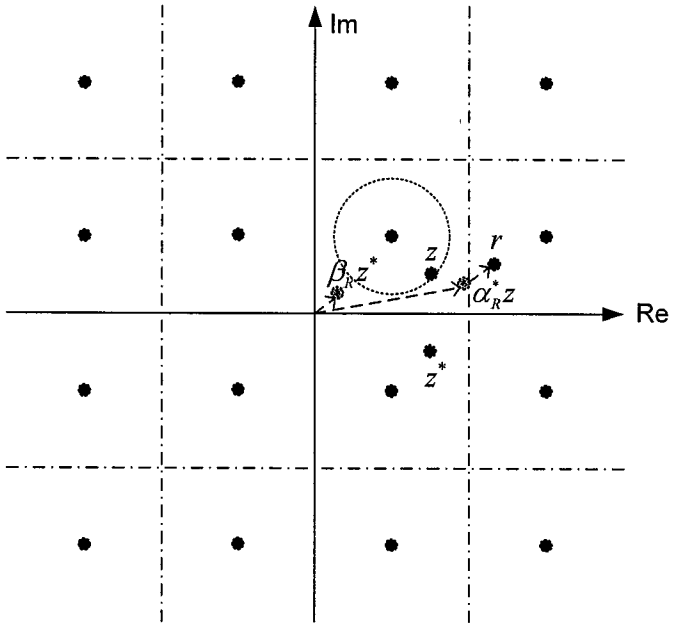

Figure 2.3 Possible observation of the received signal in the presence of I/Q imbalance. A 16-QAM constellation is used.

used. Let $z(t)$ denotes the signal with the additive noise in the absence of the receiver I/Q imbalance. As shown in Fig.2.3, the received signal $r(t)$ in the presence of I/Q imbalance falls into the wrong decision zone. It shows that I/Q imbalance changes both the amplitude and phase of the received signal.

2.3 I/Q Imbalance Model and Effect in Frequency Domain

To study the impact of I/Q imbalance in OFDM systems, the I/Q imbalance model and effect in the frequency domain are needed to be formulated out.

With regard to an OFDM system in the absence of I/Q imbalance, assuming the length of CP is longer than the channel delay spread, after the removal of CP, the relation between the transmitted signal and the received signal in the frequency domain can be formulated as

$$R[k] = H[k]S[k] + \tilde{N}[k] \qquad (k = 0, 1, \cdots, K-1), \tag{2.5}$$

where $R[k]$, $H[k]$, $S[k]$ and $\tilde{N}[k]$ denotes the received signal, channel response, transmitted signal and additive white Gaussian noise (AWGN) over the subcarrier k in the frequency domain, respectively. k is the subcarrier index and K is the size of the discrete/fast Fourier transform (DFT/FFT) used. The time-domain channel is modeled as a finite-impulse-response (FIR) filter with $L+1$ taps, and the transmission and reception schemes of an OFDM system are illustrated in Fig. 2.4.

With regard to an OFDM system in the presence of I/Q imbalance, according to (2.2) and (2.4), it can be derived that

$$S_T[k] = \alpha_T S[k] + \beta_T S^*[k'], \tag{2.6}$$

and

$$R[k] = \alpha_R^* H[k] S_T[k] + \beta_R H^*[k'] S_T^*[k'] + N[k], \tag{2.7}$$

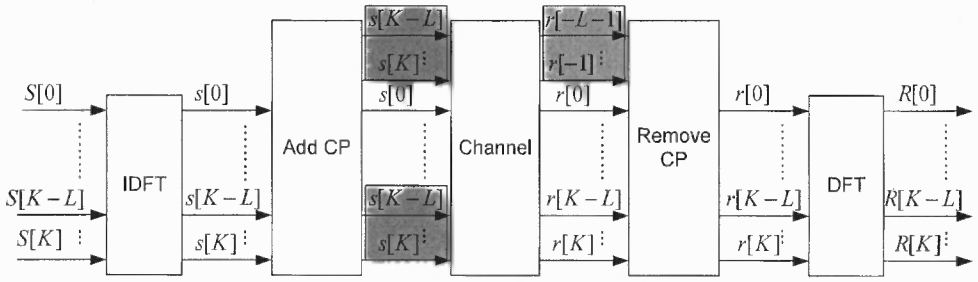

Figure 2.4 The OFDM transmission and reception schemes.

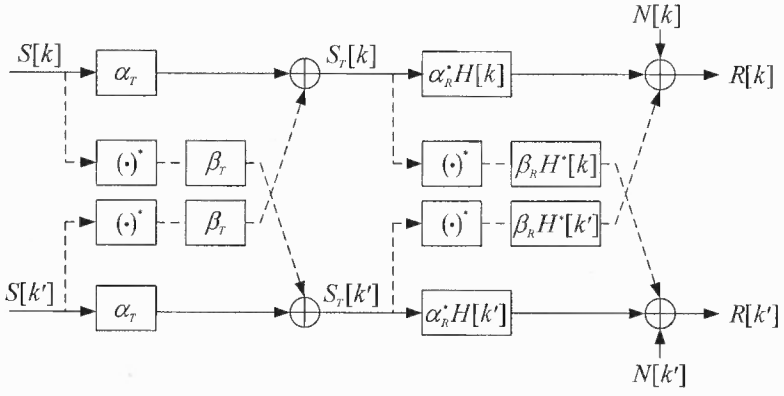

Figure 2.5 Block diagram of the received signal in the presence of the transceiver I/Q imbalance in the frequency domain.

where $k' = (-k)_K$. Eqs. (2.6)-(2.7) show that in the frequency domain, I/Q imbalance of the transmitter/receiver results in the inter-carrier interference (ICI) between the mirror-subcarrier pairs $\{k, k'\}$. The detailed derivation of the transceiver I/Q imbalance in the frequency domain can be found in Appendix B.

The relation between the transmitted signal and the received signal in (2.6) and (2.7) can be illustrated in Fig.2.5. In the absence of the transceiver I/Q imbalance, $\alpha_T = \alpha_R = 1$, and $\beta_T = \beta_R = 0$, ICI illustrated by the dashed line disappears, and the relation boils down to equation (2.5).

CHAPTER 3

I/Q IMBALANCE IN MIMO STBC SYSTEMS OVER FREQUENCY-FLAT FADING CHANNELS

3.1 Introduction

I/Q imbalance, or I/Q mismatch, has been studied extensively. The impact of the receiver I/Q imbalance is studied in [27] [28]. With training sequences, a method based on the adaptive interference canceler for the receiver I/Q imbalance compensation is studied in [29] [35] [36], and a least squares (LS) method is studied to mitigate both the receiver I/Q imbalance and DC offset in [31]. In addition, a widely linear minimum mean squared error (MMSE) method is proposed to mitigate the receiver I/Q imbalance in [37]. With no training sequences used, a blind method using the circular nature of the signal in the absence of I/Q imbalance is studied in [38] [39] [40]. This kind of blind method is also extended to the frequency-dependent I/Q imbalance model in [41]. In addition, a blind maximum likelihood (ML) method is studied to compensate the receiver I/Q imbalance in [42]. Taking into account I/Q imbalance of the transmitter, a calibration method for the transceiver I/Q imbalance assisted by a low-cost phase-shifter is studied in [43], and an adaptive compensation method for the transceiver I/Q imbalance is studied in [44]. Apart from the above work in single-input single-output (SISO) systems, there are lots of work dealing with I/Q imbalance in multiple-input multiple-out (MIMO) systems as well. For example, the impact of the transceiver I/Q imbalance on a 2×1 Alamouti system is studied in [45], and the performance analysis in terms of signal-to-interference ratio (SIR) of a STBC MIMO-OFDM system is studied in [46], respectively.

In this chapter, taking into account the noise corrupted by I/Q imbalance, the impact of the transceiver I/Q imbalance on MIMO STBC communication systems is studied, and the mitigating solutions are proposed. By exploiting the special structure of the received

signal, computationally efficient LS methods are provided to mitigate I/Q imbalance in MIMO OSTBC and MIMO QOSTBC systems. To mitigate I/Q imbalance and achieve the full spatial diversity in MIMO RQOSTBC systems, a low-complexity polygon local searching (PLS) solution is applied. Since only the effective channel state information (ECSI) is needed in the proposed solutions, the tasks of separately estimating the channel parameters as well as the I/Q imbalance parameters can be combined, reducing the computational complexity of the parameter estimation. Simulation results demonstrate that the distortions caused by I/Q imbalance in MIMO STBC systems can be successfully mitigated by the proposed solutions.

3.2 Signal and System Models

3.2.1 MIMO OSTBC Systems Without I/Q Imbalance

In MISO/MIMO wireless communication systems, STBCs are used to achieve the spatial diversity. The technique is categorized into the transmit diversity. Compared to the receive diversity technique such as maximum ratio combining (MRC) [5], the advantage of the transmit diversity technique is that the transmitter can be equipped with much more antennas than the receiver due to the small size of the receiver. Within various STBCs, the 2×1 OSTBC scheme, known as Alamouti scheme, is the most popular one [47]. In this subsection, the 2×1 Alamouti scheme will be briefly reviewed before the impact and solution of I/Q imbalance in STBC MIMO wireless communication systems are studied.

In a 2×1 wireless communication system, let the antenna-one transmit s_1 and the antenna-two transmit s_2 at the time slot 1, then let the antenna-one transmit $-s_2^*$ and the antenna-two transmit s_1^* at the time slot 2, as shown in Fig. 3.1. The corresponding codeword can be expressed as

$$\mathbf{C} = \begin{pmatrix} s_1 & s_2 \\ -s_2^* & s_1^* \end{pmatrix} \quad \begin{matrix} \longrightarrow \text{space} \\ \downarrow \text{time} \end{matrix} . \tag{3.1}$$

Assuming channel h_i $(i = 1, 2)$ is block flat fading (channel keeps constant during the encoded block interval), then it can be obtained that

$$\begin{bmatrix} r[1] \\ r^*[2] \end{bmatrix} = \begin{bmatrix} h_1 & h_2 \\ h_2^* & -h_1^* \end{bmatrix} \begin{bmatrix} s_1 \\ s_2 \end{bmatrix} + \begin{bmatrix} \tilde{n}[1] \\ \tilde{n}^*[2] \end{bmatrix}, \tag{3.2}$$

where $r[l]$ denotes the received signal at time slot l, and $\tilde{n}[l] \sim \mathcal{CN}(0, \sigma_{\tilde{n}}^2)$ is proper additive white Gaussian noise (AWGN).

- Since

$$\begin{bmatrix} h_1 & h_2 \\ h_2^* & -h_1^* \end{bmatrix}^H \begin{bmatrix} h_1 & h_2 \\ h_2^* & -h_1^* \end{bmatrix} = (\|h_1\|^2 + \|h_2\|^2)\mathbf{I}_2,$$

multiply the received data vector in (3.2) with the Hermitian of the channel matrix, it can be obtained that

$$r'[l] = s_l + n'[l], \qquad (l = 1, 2)$$

with $r'[l]$ and $n'[l]$ denote the output of the received signal and the noise after the multiplication. It is easy to show $n'[l] \sim \mathcal{CN}(0, \sigma_{\tilde{n}}^2)$. Consequently, $\{s_l\}_{i=1}^2$ can be decoded separately by linear ML method as

$$\hat{s}_{l,\mathrm{M}} = \arg \max_{s_l \in \mathcal{C}} \|r'[l] - n'[l]\|^2 \qquad l = 1, 2.$$

Here $\mathcal{C}$ is the symbol constellation set. Since each symbol $\{s_i\}_{i=1}^2$ is transmitted through two independent fading channels h_1 and h_2, the diversity order of two can be achieved. The related theoretical results can be found in [6] [8].

3.2.2 MIMO OSTBC Systems With I/Q Imbalance

With regard to OSTBC systems in the presence of the transceiver I/Q imbalance, the structure of the received signal is very complicated since in OSTBC systems, both the

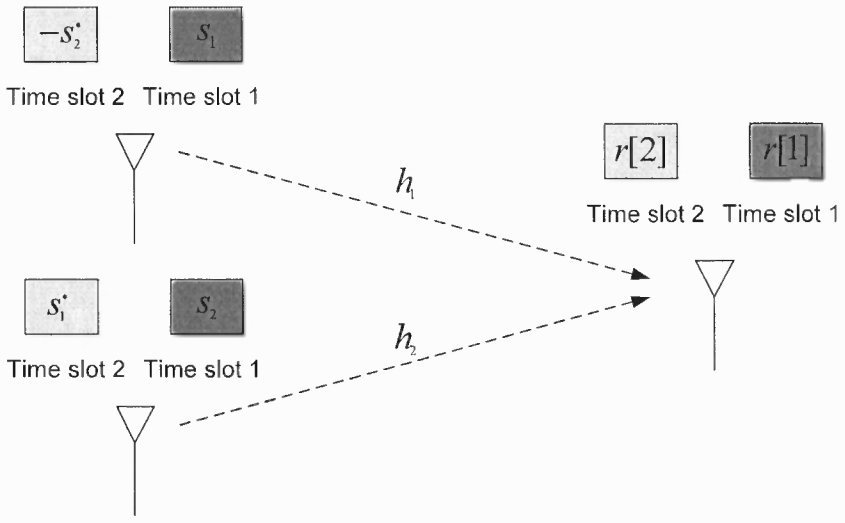

Figure 3.1 A 2×1 wireless communication system with Alamouti scheme used.

symbol and its complex-conjugate are utilized, and I/Q imbalance induces the complex-conjugate term in the data structure as well.

Without loss of generality, assume the same codeword as in (3.1) is used, taking into account the noise corrupted by I/Q imbalance, the received signal can be obtained from (2.2) and (2.4) as

$$\underbrace{\begin{bmatrix} r[1] \\ r^*[2] \end{bmatrix}}_{\mathbf{r}_a} = \underbrace{\begin{bmatrix} u_1 & u_2 \\ u_2^* & -u_1^* \end{bmatrix}}_{\mathbf{U}_a} \underbrace{\begin{bmatrix} s_1 \\ s_2 \end{bmatrix}}_{\mathbf{s}_a} + \underbrace{\begin{bmatrix} v_1 & v_2 \\ v_2^* & -v_1^* \end{bmatrix}}_{\mathbf{V}_a} \begin{bmatrix} s_1^* \\ s_2^* \end{bmatrix} + \underbrace{\begin{bmatrix} n[1] \\ n^*[2] \end{bmatrix}}_{\mathbf{n}_a}, \tag{3.3}$$

where

$$\begin{aligned} u_i &= \alpha_T \alpha_R^* h_i + \beta_T \beta_R^* h_i^* \\ v_i &= \beta_T^* \alpha_R^* h_i + \alpha_T^* \beta_R^* h_i^* \end{aligned}, \qquad i = 1, 2, \tag{3.4}$$

with $n[l] = \alpha_R^* \tilde{n}[l] + \beta_R \tilde{n}^*[l]$. Here only 2×1 OSTBC systems with I/Q imbalance is studied for simplicity, and the extension to MIMO OSTBC systems is straightforward.

In the absence of I/Q imbalance, the equation (3.3) boils down to (3.2). It shows that due to the term $\mathbf{s}_a^*$ induced by I/Q imbalance, the simple linear ML decoding is no longer applicable to MIMO OSTBC systems.

3.2.3 Extension to MIMO QOSTBC/RQOSTBC Systems

Without loss of generality, a 4×1 QOSTBC system with codeword

$$\mathbf{C} = \begin{pmatrix} s_1 & s_2 & s_3 & s_4 \\ -s_2^* & s_1^* & -s_4^* & s_3^* \\ -s_3^* & -s_4^* & s_1^* & s_2^* \\ s_4 & -s_3 & -s_2 & s_1 \end{pmatrix} \tag{3.5}$$

is studied, then the received signal corrupted by I/Q imbalance becomes

$$\underbrace{\begin{bmatrix} r[1] \\ r^*[2] \\ r^*[3] \\ r[4] \end{bmatrix}}_{\mathbf{r}_q} = \mathbf{U}_q \underbrace{\begin{bmatrix} s_1 \\ s_2 \\ s_3 \\ s_4 \end{bmatrix}}_{\mathbf{s}_q} + \mathbf{V}_q \begin{bmatrix} s_1^* \\ s_2^* \\ s_3^* \\ s_4^* \end{bmatrix} + \underbrace{\begin{bmatrix} n[1] \\ n^*[2] \\ n^*[3] \\ n[4] \end{bmatrix}}_{\mathbf{n}_q}, \tag{3.6}$$

where $\mathbf{U}_q$ and $\mathbf{V}_q$ have the following expressions as

$$\mathbf{U}_q = \begin{bmatrix} u_1 & u_2 & u_3 & u_4 \\ u_2^* & -u_1^* & u_4^* & -u_3^* \\ u_3^* & u_4^* & -u_1^* & -u_2^* \\ u_4 & -u_3 & -u_2 & u_1 \end{bmatrix}, \quad \mathbf{V}_q = \begin{bmatrix} v_1 & v_2 & v_3 & v_4 \\ v_2^* & -v_1^* & v_4^* & -v_3^* \\ v_3^* & v_4^* & -v_1^* & -v_2^* \\ v_4 & -v_3 & -v_2 & v_1 \end{bmatrix}.$$

Here $\{u_i\}_{i=1}^4$ and $\{v_i\}_{i=1}^4$ can be obtained from (3.4) by letting $i = 1, \cdots, 4$.

To achieve full spatial diversity, assume the same codeword in (3.5) is used, but now $s_1, s_2 \in \mathcal{C}$ and $s_3, s_4 \in e^{j\theta}\mathcal{C}$, where $\mathcal{C}$ is the symbol constellation set. Then the received signal becomes

$$\mathbf{r}_q = \tilde{\mathbf{U}}_q \mathbf{s}_q + \tilde{\mathbf{V}}_q \mathbf{s}_q^* + \mathbf{n}_q, \tag{3.7}$$

where

$$\tilde{\mathbf{U}}_q = \begin{bmatrix} \mathbf{u}_{q,1} & \mathbf{u}_{q,2} & \mathbf{u}_{q,3}e^{j\theta} & \mathbf{u}_{q,4}e^{j\theta} \end{bmatrix}$$
$$\tilde{\mathbf{V}}_q = \begin{bmatrix} \mathbf{v}_{q,1} & \mathbf{v}_{q,2} & \mathbf{v}_{q,3}e^{-j\theta} & \mathbf{v}_{q,4}e^{-j\theta} \end{bmatrix}.$$

Here $\mathbf{u}_{q,i}$ and $\mathbf{v}_{q,i}$ are the i-th column of $\mathbf{U}_q$ and $\mathbf{V}_q$, respectively.

Due to the term $\mathbf{s}_q^*$ induced by I/Q imbalance, the pair-wise ML decoding is no longer applicable to MIMO QOSTBC/RQOSTBC systems as well.

As a summary, the presence of I/Q imbalance forces us to take into consideration a widely linear relation to effectively decode the transmitted symbols.

3.3 Solutions

3.3.1 Computationally Efficient LS Estimator

To fully capture the symbol information in the presence of I/Q imbalance, both the symbol terms in (3.3) can be rewritten as

$$\underbrace{\begin{bmatrix} \Re\{\mathbf{r}_a\} \\ \Im\{\mathbf{r}_a\} \end{bmatrix}}_{\vec{\mathbf{r}}_a} = \underbrace{\begin{bmatrix} \Re\{\mathbf{U}_a+\mathbf{V}_a\} & \Im\{\mathbf{V}_a-\mathbf{U}_a\} \\ \Im\{\mathbf{U}_a+\mathbf{V}_a\} & \Re\{\mathbf{U}_a-\mathbf{V}_a\} \end{bmatrix}}_{\mathbf{H}_a} \underbrace{\begin{bmatrix} \Re\{\mathbf{s}_a\} \\ \Im\{\mathbf{s}_a\} \end{bmatrix}}_{\vec{\mathbf{s}}_a} + \underbrace{\begin{bmatrix} \Re\{\mathbf{n}_a\} \\ \Im\{\mathbf{n}_a\} \end{bmatrix}}_{\vec{\mathbf{n}}_a}.$$

The least squares (LS) estimate of $\vec{\mathbf{s}}_a$ can be obtained from

$$\hat{\vec{\mathbf{s}}}_a = (\mathbf{H}_a^T\mathbf{H}_a)^{-1}\mathbf{H}_a^T\vec{\mathbf{r}}_a. \tag{3.8}$$

The corresponding Gram matrix can be expressed as

$$\mathbf{H}_a^T\mathbf{H}_a = \begin{bmatrix} \mathbf{\Lambda}_1 & \mathbf{G}_a \\ \mathbf{G}_a & \mathbf{\Lambda}_2 \end{bmatrix},$$

where

$$\mathbf{G}_a = \begin{bmatrix} g_1 & g_2 \\ g_2 & -g_1 \end{bmatrix},$$

$\mathbf{\Lambda}_1 = \lambda_1\mathbf{I}_2$, $\mathbf{\Lambda}_2 = \lambda_2\mathbf{I}_2$, and $\mathbf{G}_a\mathbf{G}_a = \lambda_3\mathbf{I}_2$. Here $\{\lambda_i\}_{i=1}^3$ and $\{g_i\}_{i=1}^2$ are real constants. The property of the Gram matrix $\mathbf{H}_a^T\mathbf{H}_a$ comes from the special structure induced by the Alamouti coding scheme [48]. Using the matrix inversion formula

$$\begin{bmatrix} \mathbf{\Lambda}_1 & \mathbf{G}_a \\ \mathbf{G}_a & \mathbf{\Lambda}_2 \end{bmatrix}^{-1} = \begin{bmatrix} \mathbf{\Lambda}^{-1} & -\mathbf{\Lambda}^{-1}\mathbf{G}_a\mathbf{\Lambda}_2^{-1} \\ -\mathbf{\Lambda}_2^{-1}\mathbf{G}_a\mathbf{\Lambda}^{-1} & \mathbf{\Lambda}_2^{-1} + \mathbf{\Lambda}_2^{-1}\mathbf{G}_a\mathbf{\Lambda}^{-1}\mathbf{G}_a\mathbf{\Lambda}_2 \end{bmatrix},$$

where $\mathbf{\Lambda} = \mathbf{\Lambda}_1 - \mathbf{G}_a\mathbf{\Lambda}_2^{-1}\mathbf{G}_a = (\lambda_1 - \lambda_3/\lambda_2)\mathbf{I}_2$, all the matrices to be inverted are diagonal. Consequently, the computational complexity to invert $\mathbf{H}_a^T\mathbf{H}_a$ is reduced.

Similarly, rewrite both symbol terms in (3.6) as

$$\underbrace{\begin{bmatrix} \Re\{\mathbf{r}_q\} \\ \Im\{\mathbf{r}_q\} \end{bmatrix}}_{\vec{\mathbf{r}}_q} = \underbrace{\begin{bmatrix} \Re\{\mathbf{U}_q+\mathbf{V}_q\} & \Im\{\mathbf{V}_q-\mathbf{U}_q\} \\ \Im\{\mathbf{U}_q+\mathbf{V}_q\} & \Re\{\mathbf{U}_q-\mathbf{V}_q\} \end{bmatrix}}_{\mathbf{H}_q} \underbrace{\begin{bmatrix} \Re\{\mathbf{s}_q\} \\ \Im\{\mathbf{s}_q\} \end{bmatrix}}_{\vec{\mathbf{s}}_q} + \underbrace{\begin{bmatrix} \Re\{\mathbf{n}_q\} \\ \Im\{\mathbf{n}_q\} \end{bmatrix}}_{\vec{\mathbf{n}}_q},$$

the LS estimate of $\vec{\mathbf{s}}_q$ can be obtained from

$$\hat{\vec{\mathbf{s}}}_q = (\mathbf{H}_q^T\mathbf{H}_q)^{-1}\mathbf{H}_q^T\vec{\mathbf{r}}_q. \tag{3.9}$$

The 8×8 Gram matrix $\mathbf{H}_q^T\mathbf{H}_q$ can be expressed by four 4×4 sub-matrices as

$$\mathbf{H}_q^T\mathbf{H}_q = \begin{bmatrix} \mathbf{A}_q & \mathbf{E}_q \\ \mathbf{E}_q & \mathbf{B}_q \end{bmatrix}. \tag{3.10}$$

Let $\mathbf{D}_q = \mathbf{A}_q - \mathbf{E}_q\mathbf{B}_q^{-1}\mathbf{E}_q$, according to the matrix inversion formula, $\mathbf{B}_q^{-1}$ and $\mathbf{D}_q^{-1}$ are involved to compute the inversion of $\mathbf{H}_q^T\mathbf{H}_q$. Since all the 2×2 sub-matrices composing $\mathbf{A}_q$, $\mathbf{B}_q$ and $\mathbf{E}_q$ have the similar structure of $\mathbf{G}_a$, and the summation or multiplication of matrices with this structure still keeps the structure [48], it is easy to show that $\mathbf{B}_q$ and $\mathbf{D}_q$ have the similar property of the Gram matrix $\mathbf{H}_a^T\mathbf{H}_a$. Consequently, the sub-matrices to be inverted to have $\mathbf{B}_q^{-1}$ and $\mathbf{D}_q^{-1}$ are diagonal, resulting in a low computational matrix inversion.

The computational efficient LS estimator is applicable as well when multiple receiving antennas are used.

3.3.2 Polygon Local Searching Method

However, for MIMO RQOSTBC systems, the full spatial diversity can not be achieved by only implementing LS estimator. To mitigate I/Q imbalance and achieve the full spatial diversity, based on the initial estimates obtained by LS estimator, the polygon local searching (PLS) method proposed in [49] is applied here. The basic idea is the same as the sphere decoding [50] [51], i.e, searching the candidate symbols within a shrunk area around the initial estimates.

Similarly, the received signal of a 4×1 RQOSTBC system can be obtained as

$$\vec{\mathbf{r}}_q = \tilde{\mathbf{H}}_q \vec{\mathbf{s}}_q + \vec{\mathbf{n}}_q,$$

where

$$\tilde{\mathbf{H}}_q = \begin{bmatrix} \Re\{\tilde{\mathbf{U}}_q + \tilde{\mathbf{V}}_q\} & \Im\{\tilde{\mathbf{V}}_q - \tilde{\mathbf{U}}_q\} \\ \Im\{\tilde{\mathbf{U}}_q + \tilde{\mathbf{V}}_q\} & \Re\{\tilde{\mathbf{U}}_q - \tilde{\mathbf{V}}_q\} \end{bmatrix}.$$

Let $p(\vec{\mathbf{r}}_q; \vec{\mathbf{s}}_q)$ denote the probability mass function (PMF) of $\vec{\mathbf{r}}_q$ parameterized by the unknown parameter $\vec{\mathbf{s}}_q$, the ML estimate of $\vec{\mathbf{s}}_q$ from $\vec{\mathbf{r}}_q$ is

$$\hat{\vec{\mathbf{s}}}_{q,\mathrm{M}} = \arg \max_{\vec{\mathbf{s}}_q \in \mathcal{S}} p(\vec{\mathbf{r}}_q; \vec{\mathbf{s}}_q), \tag{3.11}$$

where the set $\mathcal{S}$ contains all the possible signal vectors from a given symbol constellation. Since $n_I[l] = \tilde{n}_I[l]$, and $n_Q[l] = (1+\epsilon_R)\cos\varphi_R \tilde{n}_Q[l] - (1+\epsilon_R)\sin\varphi_R \tilde{n}_I[l]$, it can be obtained that $n_I[l] \sim \mathcal{N}(0, \sigma_{n_I}^2)$, and $n_Q[l] \sim \mathcal{N}(0, \sigma_{n_Q}^2)$, where $\sigma_{n_I}^2 = \sigma_{\tilde{n}}^2/2$, and $\sigma_{n_Q}^2 = (1+\epsilon_R)^2\sigma_{\tilde{n}}^2/2$, respectively. Consequently, $n[l]$ is not proper complex Gaussian due to I/Q imbalance. In addition, $n_I[l]$ and $n_Q[l]$ are correlated with the correlation coefficient $\rho = E\{n_I[l]n_Q[l]\}/(\sigma_{n_I}\sigma_{n_Q}) = -\sin\varphi_R$. Since the practical values of the amplitude and phase imbalances are around $1\% \sim 5\%$ and $1^\circ \sim 5^\circ$, respectively, i.e., $\rho \approx 0$ and

$\sigma_{n_I}^2 \approx \sigma_{n_Q}^2$, it is reasonable to treat $n[l]$ as proper, especially in high signal-to-noise ratio (SNR) scenario, then (3.11) boils down to

$$\hat{\vec{\mathbf{s}}}_{q,\mathrm{M}} = \arg \min_{\vec{\mathbf{s}}_q \in \mathcal{S}} \|\vec{\mathbf{r}}_q - \tilde{\mathbf{H}}_q \vec{\mathbf{s}}_q\|^2. \tag{3.12}$$

The initial estimate of $\vec{\mathbf{s}}_q$ can be obtained from

$$\hat{\vec{\mathbf{s}}}_q = (\tilde{\mathbf{H}}_q^T \tilde{\mathbf{H}}_q)^{-1} \tilde{\mathbf{H}}_q^T \vec{\mathbf{r}}_q.$$

Let $\{\mathbf{g}_i\}_{i=1}^8$ denotes the i-th row vector of matrix $(\tilde{\mathbf{H}}_q^T \tilde{\mathbf{H}}_q)^{-1} \tilde{\mathbf{H}}_q^T$, according to [49], the boundary of the shrunk area can be given by

$$-d \leq \frac{\vec{s}_i - \hat{\vec{s}}_i}{\|\mathbf{g}_i\|} \leq d, \qquad i = 1, \cdots, 8, \tag{3.13}$$

where $\vec{s}_i$ and $\hat{\vec{s}}_i$ denote the i-th elements of the column vector $\vec{\mathbf{s}}_q$ and $\hat{\vec{\mathbf{s}}}_q$, respectively. Treating the noise as a proper Gaussian, d can be determined by

$$d = \|\vec{\mathbf{r}}_q - \tilde{\mathbf{H}}_q \hat{\vec{\mathbf{s}}}_q\|.$$

By searching the candidates within the area defined by (3.13), the ML estimate of $\vec{\mathbf{s}}_q$ can be obtained.

3.3.3 Estimation of Channel and I/Q Imbalance

Since only ECSI such as u_i and v_i are needed in the proposed solutions, the tasks of separately estimating the channel parameters as well as the I/Q imbalance parameters can be combined.

In a 2×1 Alamouti system, stack $\mathbf{s}_a$ and $\mathbf{s}_a^*$ into the new transmitted signal vector, according to (3.3), the effective channel matrix can be formulated as $\begin{bmatrix} \mathbf{U}_a & \mathbf{V}_a \end{bmatrix}$. Consequently, the relation between the received signal and the transmitted signal keeps the same, except the change of the dimensionality of the channel matrix and the transmitted signal vector. Hence, all the channel estimation methods for MIMO OSTBC communication

systems in the literatures can be applied directly. In this work, the LS channel estimation based on training is adopted [52] [53]. Reformulate (3.3) as

$$\begin{bmatrix} r[1] \\ r[2] \end{bmatrix} = \begin{bmatrix} s_1 & s_2 & s_1^* & s_2^* \\ -s_2^* & s_1^* & -s_2 & s_1 \end{bmatrix} \underbrace{\begin{bmatrix} u_1 \\ u_2 \\ v_1 \\ v_2 \end{bmatrix}}_{\boldsymbol{\theta}} + \begin{bmatrix} n[1] \\ n[2] \end{bmatrix},$$

stack N_t received data vector into a new vector $\mathbf{r}_t$, the corresponding *observation matrix* is denoted as $\mathbf{S}_t$ [53], then the LS estimate of the effective channel parameters can be obtained as

$$\hat{\boldsymbol{\theta}} = (\mathbf{S}_t^T \mathbf{S}_t)^{-1} \mathbf{S}^T \mathbf{r}_t.$$

To study the performance degradation caused by I/Q imbalance without the compensation, only the effective channel $\mathbf{U}_a$ is estimated by ignoring the term $\mathbf{V}_a \mathbf{s}_a^*$ in (3.3), i.e.,

$$\begin{bmatrix} \hat{\tilde{u}}_1 \\ \hat{\tilde{u}}_2 \end{bmatrix} = (\tilde{\mathbf{S}}_t^T \tilde{\mathbf{S}}_t)^{-1} \tilde{\mathbf{S}}_t^T \mathbf{r}_t.$$

Here $\tilde{\mathbf{S}}_t$ is the truncated matrix containing the first two columns of $\mathbf{S}_t$. Once $\hat{\tilde{\mathbf{U}}}_a$, the estimate of $\mathbf{U}_a$ without considering the effect of I/Q imbalance is available, the linear ML decoding is applied directly to the output of $\hat{\tilde{\mathbf{U}}}_a^H \mathbf{r}_a$.

The extension to MIMO QOSTBC/RQOSTBC systems is straightforward.

3.4 Simulation Results

In the simulations, the worst case, the amplitude imbalance $\epsilon = 5\%$ and the phase imbalance $\varphi = 5^\circ$ at both of the transmitter and receiver are studied. In addition, the block flat Rayleigh fading channels are assumed. Moreover, The number of training symbol block $N_t = 10$, and the number of receiving antennas $M = \{1, 2\}$ are used. Furthermore,

$\theta = \pi/4$, the optimal rotation for the QAM constellation is chosen for RQOSTBC systems [9].

Fig. 3.2$\sim$Fig. 3.5 show that by applying the linear ML decoding to 2-Tx Alamouti systems, or to the pair-wise ML decoding to 4-Tx QOSTBC/RQOSTBC systems in the presence of I/Q imbalance based on $\hat{\tilde{\mathbf{U}}}_a$ or $\hat{\tilde{\mathbf{U}}}_q$, the SER performance degrades dramatically. Fig. 3.2 also shows that the Tx I/Q imbalance and Rx I/Q imbalance cause the similar performance degradation.

When ECSI is known, I/Q imbalance in 2-Tx Alamouti and 4-Tx QOSTBC systems can be successfully mitigated by applying the LS estimator, with only a small performance loss in 4-Tx QOSTBC systems. In addition, based on the initial estimates obtained by LS estimator, I/Q imbalance in 4-Tx RQOSTBC systems can be successfully mitigated by applying the PLS approach.

Based on the estimated ECSI, I/Q imbalance can be effectively mitigated by the proposed approaches as well.

3.5 Conclusions

In this chapter, the impact of I/Q imbalance on MIMO STBC communication systems is studied, and the effectiveness of the proposed mitigating solutions is verified. The results show that I/Q imbalance causes severe distortion in MIMO STBC communication systems, and the resulting distortion can be successfully mitigated by the proposed methods.

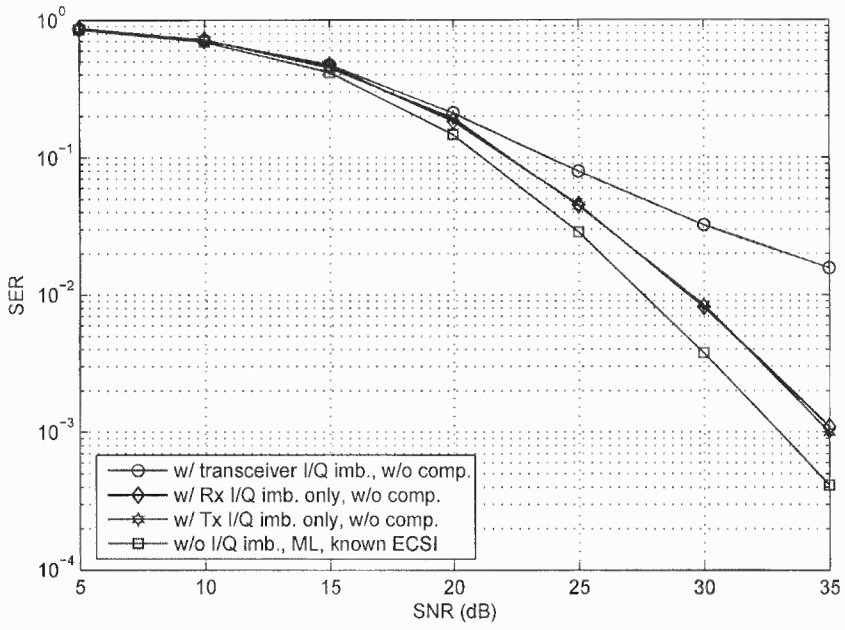

Figure 3.2 SER versus SNR of a 2×1 Alamouti system with I/Q imbalance. $\epsilon_T = 5\%$, $\varphi_T = 5°$, $\epsilon_R = 5\%$, $\varphi_R = 5°$, $M = 1$, and $N_t = 10$. A 64-QAM constellation is used. The number of independent trials is 10^6.

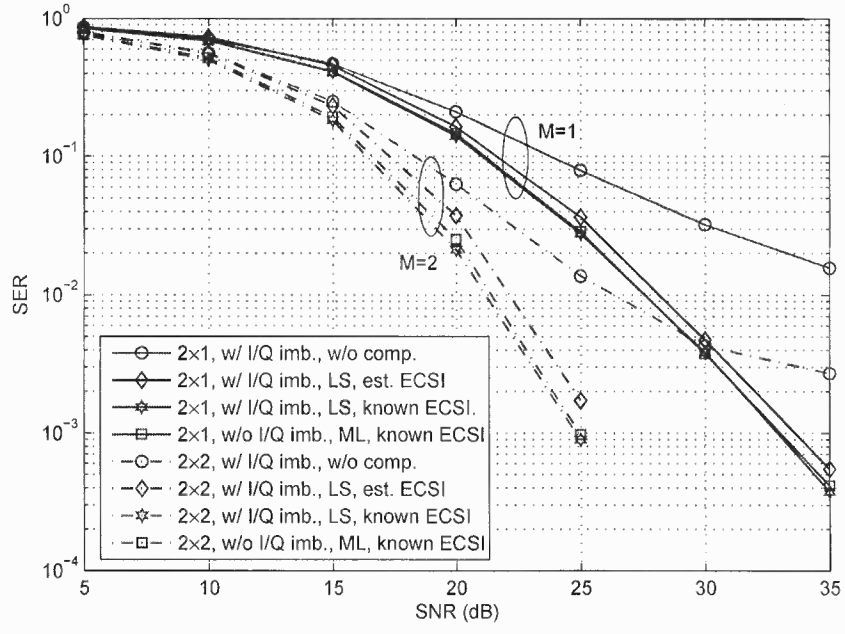

Figure 3.3 SER versus SNR of a 2-Tx Alamouti system with I/Q imbalance. $\epsilon_T = 5\%$, $\varphi_T = 5°$, $\epsilon_R = 5\%$, $\varphi_R = 5°$, $M = \{1, 2\}$, and $N_t = 10$. A 64-QAM constellation is used. The number of independent trials is 10^6.

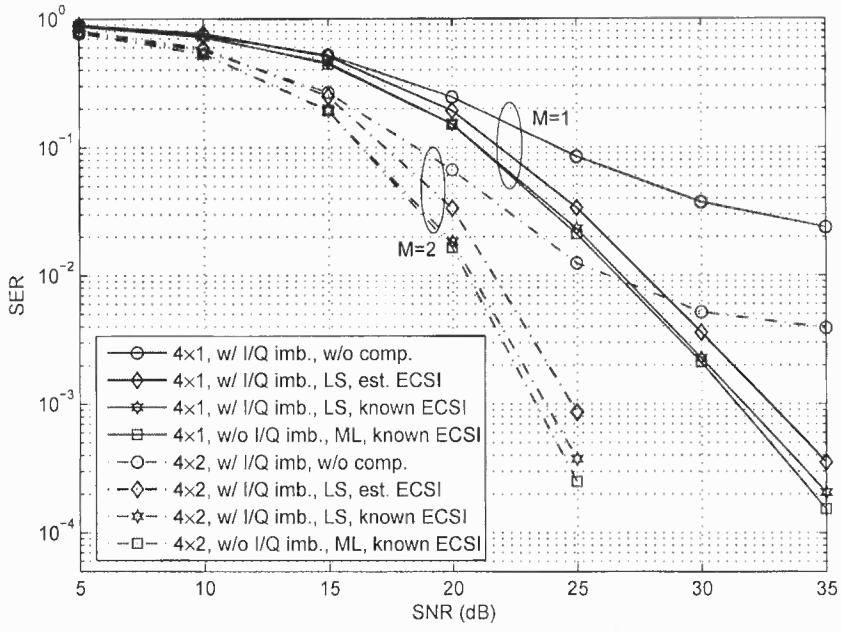

Figure 3.4 SER versus SNR of a 4-Tx QOSTBC system with I/Q imbalance. $\epsilon_T = 5\%$, $\varphi_T = 5°$, $\epsilon_R = 5\%$, $\varphi_R = 5°$, $M = \{1, 2\}$, and $N_t = 10$. A 64-QAM constellation is used. The number of independent trials is 10^6.

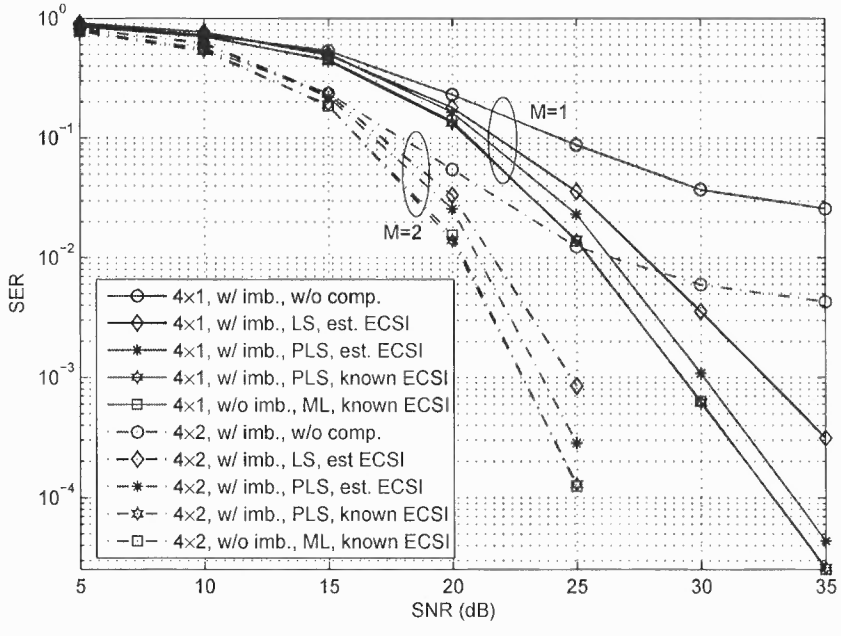

Figure 3.5 SER versus SNR of a 4-Tx RQOSTBC system with I/Q imbalance. $\epsilon_T = 5\%$, $\varphi_T = 5°$, $\epsilon_R = 5\%$, $\varphi_R = 5°$, $M = \{1, 2\}$, and $N_t = 10$. A 64-QAM constellation is used. The number of independent trials is 10^6.

CHAPTER 4

I/Q IMBALANCE IN STBC MIMO-OFDM SYSTEMS OVER FREQUENCY-SELECTIVE FADING CHANNELS

4.1 Introduction

Since STBCs are originally developed for frequency-flat fading channels, to achieve the spatial diversity in frequency selective fading channels, STBC MIMO-OFDM systems have been suggested, where STBCs are used across different antennas in conjunction with OFDM [10] [11] [12] [13]. However, in the implementation of OFDM systems, there are some challenges caused by the RF impairments such as I/Q imbalance, phase noise and carrier frequency offset (CFO), and lots of researchers have been devoted into the mitigation of them in OFDM systems [54] [55] [19] [20].

Compared to that in the time domain, I/Q imbalance in OFDM systems causes more distortions, and more works dealing I/Q imbalance in OFDM systems can be found in the literatures. The impacts of the receiver I/Q imbalance on OFDM, code division multiple access (CDMA), and multi-carrier MC-CDMA systems are studied in [56] [57], and a novel code is designed to mitigate the receiver I/Q imbalance for MC-CDMA system in [58]. A method to improve the channel and the receiver I/Q imbalance parameters in OFDM systems by using unbiased training sequences is studied in [59]. An compensation method for the transmitter I/Q imbalance in OFDM systems in studied in [60]. The capacity of OFDM systems with the receiver I/Q imbalance is studied in [61]. An analytical approach to evaluate the M-QAM bit error rate (BER) as well as the channel capacity of Alamouti space-time coded OFDM systems with the receiver I/Q imbalance is studied in [62]. Using the frequency-dependent I/Q imbalance model, optimal training sequences for the joint channel and I/Q imbalance estimation in OFDM systems are designed in [63].

Taking into account both I/Q imbalance and CFO, an expectation maximization (EM) based method and a ML method to mitigate the receiver I/Q imbalance and CFO for OFDM systems are proposed in [64] and [65], respectively. In addition, taking into account I/Q imbalance and the phase noise simultaneously, the joint mitigation of phase noise and I/Q imbalance is studied in [66] [67] [68]. Moreover, an I/Q imbalance mitigation method for mobile space-frequency block coded (SFBC) OFDM systems is studied in [69] [70].

Taking into account the transmitter I/Q imbalance, a widely linear MMSE method is proposed to mitigate the transceiver I/Q imbalance in OFDM systems in [71]. In addition, the joint CFO and transceiver I/Q imbalance mitigation in OFDM systems is studied in [72]. Moreover, the effect of the transceiver I/Q imbalance on STBC MIMO systems is studied with no mitigating solutions provided in [45], and the performance analysis in terms of signal-to-interference ratio (SIR) of STBC MIMO-OFDM systems with I/Q imbalance is studied in [46], respectively.

Since the distortion caused by the transceiver I/Q imbalance in STBC MIMO-OFDM systems increases symbol error rate (SER) drastically, especially in high order modulations or with higher carrier frequencies, hence should be effectively compensated. Inspired by the work in [73] [74], taking into account the noise corrupted by I/Q imbalance, the impact of the transceiver I/Q imbalance on the STBC MIMO-OFDM communication systems is studied systematically, and low-complexity solutions are proposed to mitigate the distortion. Similar to the work in Chapter 3, exploiting the special structure of the received signal induced by Alamouti scheme, low-complexity LS solutions are proposed to mitigate I/Q imbalance in OSTBC/QOSTBC OFDM systems. In addition, the low-complexity PLS method is applied to RQOSTBC OFDM systems to mitigate the distortions.

4.2 Signal and System Models

4.2.1 MIMO OSTBC OFDM Systems Without I/Q Imbalance

First a 2×1 Alamouti OFDM system in the absence of I/Q imbalance is reviewed. As we know, OFDM systems convert a frequency-selective channel in the time domain into K parallel frequency-flat channels in the frequency domain when a K-point DFT/FFT is performed. Consequently, one SISO OFDM system can be treated as K SISO parallel communication systems. By introducing another transmitting antenna, apply Alamouti scheme to any subcarrier k of the two transmitting antennas, the spatial diversity can be achieved with a linear ML decoding within each subcarrier at the receiver side. The transmission and reception of a 2×1 Alamouti OFDM system are illustrated in Fig. 4.1. Correspondingly, the codeword can be expressed as

$$\mathbf{C} = \begin{pmatrix} S_1 & S_2 \\ -S_2^* & S_1^* \end{pmatrix} \quad \begin{matrix} \longrightarrow \text{space} \\ \downarrow \text{time} \end{matrix} .$$

That is, the transmitter sends $S_1[k]$ from the antenna-one and $S_2[k]$ from the antenna-two at the time 1 over the subcarrier k, then at the time 2, it sends $-S_2^*[k]$ and $S_1^*[k]$ from the antenna-one and the antenna-two over the subcarrier k, respectively. Assume the lenth of CP is longer than the channel delay spread, and the channel keeps steady within the coded block interval. Let $H_i[k]$ denote the frequency-domain channel response between the i-th transmit antenna and the receive antenna over the subcarrier k, the received signal at the time 1 and 2 over the subcarrier k after the removal of CP can be obtained as

$$\begin{bmatrix} R_1[k] \\ R_2^*[k] \end{bmatrix} = \begin{bmatrix} H_1[k] & H_2[k] \\ H_2^*[k] & -H_1^*[k] \end{bmatrix} \begin{bmatrix} S_1[k] \\ S_2[k] \end{bmatrix} + \begin{bmatrix} \tilde{N}_1[k] \\ \tilde{N}_2^*[k] \end{bmatrix} . \tag{4.1}$$

Here $R_l[k]$ denotes the received signal at the time l over the subcarrier k, and $\tilde{N}[k] \sim \mathcal{CN}(0, \sigma_{\tilde{N}}^2)$ denotes the proper AWGN in the frequency domain at the subcarrier k. Since the channel matrix is orthogonal, multiplying the received signal vector with the Hermitian

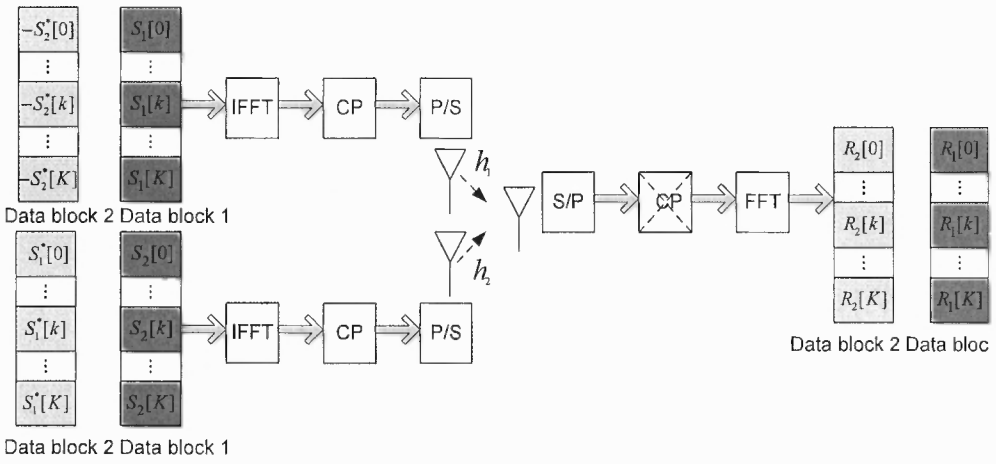

Figure 4.1 A 2×1 OFDM communication system with Alamouti scheme used in the frequency domain.

of the channel matrix, $\{S_i[k]\}_{i=1}^{2}$ can be decoded separately with the ML method. The detailed derivation has been given in Chapter 3.

Since Alamouti scheme is performed in the frequency domain, this system sometimes is named as space-frequency block coded (SFBC) OFDM system [75] [76] [77]. In this work, the name STBC OFDM system is used for consistence.

4.2.2 MIMO OSTBC OFDM Systems With I/Q Imbalance

In the presence of the transceiver I/Q imbalance, taking into account the noise corrupted by I/Q imbalance, the received signal at the time 1 and 2 over the subcarrier k (except for $k = 0$ and $k = K/2$) after the removal of CP can be obtained from (2.6) and (2.7) as

$$\underbrace{\begin{bmatrix} R_1[k] \\ R_2^*[k] \end{bmatrix}}_{R_a[k]} = \mathbf{U}_{\bar{a}}[k] \underbrace{\begin{bmatrix} S_1[k] \\ S_2[k] \end{bmatrix}}_{S_a[k]} + \mathbf{V}_{\bar{a}}[k] \underbrace{\begin{bmatrix} S_1^*[k'] \\ S_2^*[k'] \end{bmatrix}}_{S_{\bar{a}}^*[k']} + \underbrace{\begin{bmatrix} N_1[k] \\ N_2^*[k] \end{bmatrix}}_{N_a[k]}, \tag{4.2}$$

where

$$\mathbf{U}_{\bar{a}}[k] = \begin{bmatrix} u_1[k] & u_2[k] \\ u_2^*[k] & -u_1^*[k] \end{bmatrix}, \quad \mathbf{V}_{\bar{a}}[k] = \begin{bmatrix} v_1[k] & v_2[k] \\ v_2^*[k] & -v_1^*[k] \end{bmatrix},$$

where $N[k] = \alpha_R^* \tilde{N}[k] + \beta_R \tilde{N}^*[k']$. Note that $S_a[k]$ and $S_a[k']$ are different data vectors. The elements of $\mathbf{U}_{\bar{a}}[k]$ and $\mathbf{V}_{\bar{a}}[k]$ can be obtained by

$$\begin{aligned} u_i[k] &= \alpha_T \alpha_R^* H_i[k] + \beta_T \beta_R^* H_i^*[k'] \\ v_i[k] &= \beta_T^* \alpha_R^* H_i[k] + \alpha_T^* \beta_R^* H_i^*[k'] \end{aligned}, \quad i = 1, 2. \tag{4.3}$$

It shows that in the absence of the transmitter I/Q imbalance, i.e., $\beta_T = 0$, $H_i^*[k']$ and $H_i[k]$ will not be involved in $w_i[k]$ and $u_i[k]$, respectively, hence the model reduces to the model used in [74]. In addition, in the absence of the transceiver I/Q imbalance, (4.2) boils down to (4.1)

Similar to in the time domain, the simple linear ML decoding is no longer applicable due to $S_a^*[k']$ induced by I/Q imbalance.

4.2.3 Extension to MIMO QOSTBC/RQOSTBC OFDM Systems

Without loss of generality, a 4×1 QOSTBC system with the same codeword as (3.5) is studied, then the received signal corrupted by I/Q imbalance can be expressed as

$$\underbrace{\begin{bmatrix} R_1[k] \\ R_2^*[k] \\ R_3^*[k] \\ R_4[k] \end{bmatrix}}_{R_q[k]} = \mathbf{U}_{\bar{q}}[k] \underbrace{\begin{bmatrix} S_1[k] \\ S_2[k] \\ S_3[k] \\ S_4[k] \end{bmatrix}}_{S_q[k]} + \mathbf{V}_{\bar{q}}[k] \underbrace{\begin{bmatrix} S_1^*[k'] \\ S_2^*[k'] \\ S_3^*[k'] \\ S_4^*[k'] \end{bmatrix}}_{S_q^*[k']} + \underbrace{\begin{bmatrix} N_1[k] \\ N_2^*[k] \\ N_3^*[k] \\ N_4[k] \end{bmatrix}}_{N_q[k]}, \tag{4.4}$$

where

$$\mathbf{U}_{\bar{q}}[k] = \begin{bmatrix} u_1[k] & u_2[k] & u_3[k] & u_4[k] \\ u_2^*[k] & -u_1^*[k] & u_4^*[k] & -u_3^*[k] \\ u_3^*[k] & u_4^*[k] & -u_1^*[k] & -u_2^*[k] \\ u_4[k] & -u_3[k] & -u_2[k] & u_1[k] \end{bmatrix}, \quad \mathbf{V}_{\bar{q}}[k] = \begin{bmatrix} v_1[k] & v_2[k] & v_3[k] & v_4[k] \\ v_2^*[k] & -v_1^*[k] & v_4^*[k] & -v_3^*[k] \\ v_3^*[k] & v_4^*[k] & -v_1^*[k] & -v_2^*[k] \\ v_4[k] & -v_3[k] & -v_2[k] & v_1[k] \end{bmatrix}.$$

Here $\{u_i[k]\}_{i=1}^4$ and $\{v_i[k]\}_{i=1}^4$ can be obtained from (4.3) by letting $i = 1, \cdots, 4$.

To achieve the full spatial diversity, assume the same codeword in (3.5) is used, $S_1, S_2 \in \mathcal{C}$ and $S_3, S_4 \in e^{j\theta}\mathcal{C}$. Then the corresponding received signal becomes

$$R_q[k] = \tilde{\mathbf{U}}_{\bar{q}}[k]S_q[k] + \tilde{\mathbf{V}}_{\bar{q}}[k]S_q^*[k'] + N_q[k], \tag{4.5}$$

where

$$\tilde{\mathbf{U}}_{\bar{q}}[k] = \begin{bmatrix} \mathbf{u}_{\bar{q},1}[k] & \mathbf{u}_{\bar{q},2}[k] & \mathbf{u}_{\bar{q},3}[k]e^{j\theta} & \mathbf{u}_{\bar{q},4}[k]e^{j\theta} \end{bmatrix}$$
$$\tilde{\mathbf{V}}_{\bar{q}}[k] = \begin{bmatrix} \mathbf{v}_{\bar{q},1}[k] & \mathbf{v}_{\bar{q},2}[k] & \mathbf{v}_{\bar{q},3}[k]e^{-j\theta} & \mathbf{v}_{\bar{q},4}[k]e^{-j\theta} \end{bmatrix}.$$

Here $\mathbf{w}_{\bar{q},i}[k]$ and $\mathbf{u}_{\bar{q},i}[k]$ denote the i-th column of $\mathbf{W}_{\bar{q}}[k]$ and $\mathbf{U}_{\bar{q}}[k]$, respectively.

Due to $S_q^*[k']$ induced by I/Q imbalance, the pair-wise ML decoding is no longer applicable to MIMO QOSTBC/RQOSTBC OFDM systems.

4.3 Solutions

4.3.1 Computationally Efficient LS Estimator

Rewrite (4.2) as

$$\underbrace{\begin{bmatrix} R_a[k] \\ R_a^*[k'] \end{bmatrix}}_{\vec{R}_a[k]} = \underbrace{\begin{bmatrix} \mathbf{U}_{\bar{a}}[k] & \mathbf{V}_{\bar{a}}[k] \\ \mathbf{V}_{\bar{a}}^*[k'] & \mathbf{U}_{\bar{a}}^*[k'] \end{bmatrix}}_{\mathbf{H}_{\bar{a}}[k]} \underbrace{\begin{bmatrix} S_a[k] \\ S_a^*[k'] \end{bmatrix}}_{\vec{S}_a[k]} + \begin{bmatrix} N_a[k] \\ N_a^*[k'] \end{bmatrix}. \tag{4.6}$$

The LS estimate of $\vec{S}_a[k]$ can be given as

$$\hat{\vec{S}}_a[k] = (\mathbf{H}_{\bar{a}}^H[k]\mathbf{H}_{\bar{a}}[k])^{-1}\mathbf{H}_{\bar{a}}^H[k]\vec{R}_a[k]. \tag{4.7}$$

Since the 2×2 sub-matrices to be inverted to obtain $(\mathbf{H}_{\bar{a}}^H[k]\mathbf{H}_{\bar{a}}[k])^{-1}$ are diagonal, the low-complexity LS estimator is available, and it is applicable to MIMO OSTBC OFDM systems as well [48].

Similarly, it can be obtained from (4.4) that

$$\underbrace{\begin{bmatrix} R_q[k] \\ R_q^*[k'] \end{bmatrix}}_{\vec{R}_q[k]} = \underbrace{\begin{bmatrix} \mathbf{U}_{\bar{q}}[k] & \mathbf{V}_{\bar{q}}[k] \\ \mathbf{V}_{\bar{q}}^*[k'] & \mathbf{U}_{\bar{q}}^*[k'] \end{bmatrix}}_{\mathbf{H}_{\bar{q}}[k]} \underbrace{\begin{bmatrix} S_q[k] \\ S_q^*[k'] \end{bmatrix}}_{\vec{S}_q[k]} + \underbrace{\begin{bmatrix} N_q[k] \\ N_q^*[k'] \end{bmatrix}}_{\vec{N}_q[k]}. \tag{4.8}$$

Similar to (3.10), a low computational inversion of matrix $\mathbf{H}_{\bar{q}}^H[k]\mathbf{H}_{\bar{q}}[k]$ can be obtained.

4.3.2 Polygon Local Searching Method

However, for MIMO RQOSTBC OFDM systems, the distortion can not be mitigated satisfactorily by only employing the LS method. Again, the PLS method can be applied.

The received signal of a 4×1 RQOSTBC scheme can be obtained from (4.5) and (4.8) as

$$\vec{R}_q[k] = \tilde{\mathbf{H}}_{\bar{q}}[k]\vec{S}_q[k] + \vec{N}_q[k], \tag{4.9}$$

where

$$\tilde{\mathbf{H}}_{\bar{q}}[k] = \begin{bmatrix} \tilde{\mathbf{U}}_{\bar{q}}[k] & \tilde{\mathbf{V}}_{\bar{q}}[k] \\ \tilde{\mathbf{V}}_{\bar{q}}^*[k'] & \tilde{\mathbf{U}}_{\bar{q}}^*[k'] \end{bmatrix}.$$

Let $p(\vec{R}_q[k]; \vec{S}_q[k])$ denote the PMF of $\vec{R}_q[k]$ parameterized by the unknown parameter $\vec{S}_q[k]$, according to (4.9), the ML estimate of $\vec{S}_q[k]$ from $\vec{R}_q[k]$ is

$$\hat{\vec{S}}_{q,\mathrm{M}}[k] = \arg \max_{\vec{S}_q[k] \in \mathcal{S}} p(\vec{R}_q[k]; \vec{S}_q[k]). \tag{4.10}$$

Since $N[k]$ is a linear superposition of two independent proper Gaussian variables, $N[k]$ is still a proper Gaussian variable. However, $N[k]$ and $N^*[k']$ are correlated. It can be obtained that

$$E\{N_I[k]N_I[k']\} = E\{N_Q[k]N_Q[k']\} = -\frac{\sigma_{\tilde{N}}^2}{4}(2\epsilon_R + \epsilon_R^2),$$
$$E\{N_I[k]N_Q[k']\} = -E\{N_Q[k]N_I[k']\} = \frac{\sigma_{\tilde{N}}^2}{2}(1+\epsilon_R)\sin\phi_R.$$

Since ϵ_R and ϕ_R are small, it is reasonable to treat $N[k]$ and $N^*[k']$ as independent, then (4.10) boils down to

$$\hat{\vec{S}}_{q,\mathrm{M}}[k] = \arg \min_{\vec{S}_q[k] \in \mathcal{S}} \|\vec{R}_q[k] - \tilde{\mathbf{H}}_{\bar{q}}[k]\vec{S}_q[k]\|^2. \tag{4.11}$$

Let $\hat{\vec{S}}_q[k] = (\tilde{\mathbf{H}}_{\bar{q}}^H[k]\tilde{\mathbf{H}}_{\bar{q}}[k])^{-1}\tilde{\mathbf{H}}_{\bar{q}}^H[k]\vec{R}_q[k] = \bar{\mathbf{G}}[k]\vec{R}_q[k]$, to avoid the global searching within $\mathcal{S}$, the PLS method based on $\hat{\vec{S}}_q[k]$ can be applied. It holds that

$$\|\vec{R}_q[k] - \tilde{\mathbf{H}}_{\bar{q}}[k]\hat{\vec{S}}_{q,\mathrm{M}}[k]\|^2 \leq \|\vec{R}_q[k] - \tilde{\mathbf{H}}_{\bar{q}}[k]\hat{\vec{S}}_q[k]\|^2 = \tilde{d}^2. \tag{4.12}$$

Let $\{\bar{\mathbf{g}}_i[k]\}_{i=1}^8$ denote the i-th row of $\bar{\mathbf{G}}[k]$, according to [49], the boundary of the shrunk area can be given by

$$-\tilde{d} \leq \Re\left\{\frac{\vec{R}_{q,i}[k] - \hat{\vec{R}}_{q,i}[k]}{\|\bar{\mathbf{g}}_i[k]\|}\right\} \leq \tilde{d}, \quad -\tilde{d} \leq \Im\left\{\frac{\vec{R}_{q,i}[k] - \hat{\vec{R}}_{q,i}[k]}{\|\bar{\mathbf{g}}_i[k]\|}\right\} \leq \tilde{d}\ , \tag{4.13}$$

where $\vec{R}_{q,i}[k]$ and $\hat{\vec{R}}_{q,i}[k]$ denote the i-th elements of $\vec{R}_q[k]$ and $\hat{\vec{R}}_q[k]$, respectively.

4.4 Simulation Results

In the simulations, the worst case, the amplitude imbalance $\epsilon = 5\%$ and the phase imbalance $\varphi = 5^\circ$ at both of the transmitter and receiver side are studied. In addition, the FFT size $K = 64$, the number of training symbol block $N_t = 10$, the length of CP $L_{\mathrm{cp}} = 3$, and 4-tap FIR channels with $\mathbf{h}_i \sim \mathcal{CN}(\mathbf{0}, \mathbf{I}_4)$ are used. Moreover, $\theta = \pi/4$, the optimal rotation for a QAM constellation is chosen for the RQOSTBC scheme [9].

Fig. 4.2 shows that I/Q imbalance of the receiver causes more distortion than that of the transmitter. Fig. 4.3~Fig. 4.5 show that by using the linear ML estimator for Alamouti system or the pair-wise ML estimator for QOSTBC and RQOSTBC systems with I/Q imbalance without the compensation, respectively, SER of the estimated signal increases dramatically compared to that of the estimated signal without I/Q imbalance, resulting in an error floor. However, the resulting distortion can be successfully mitigated by the proposed solutions.

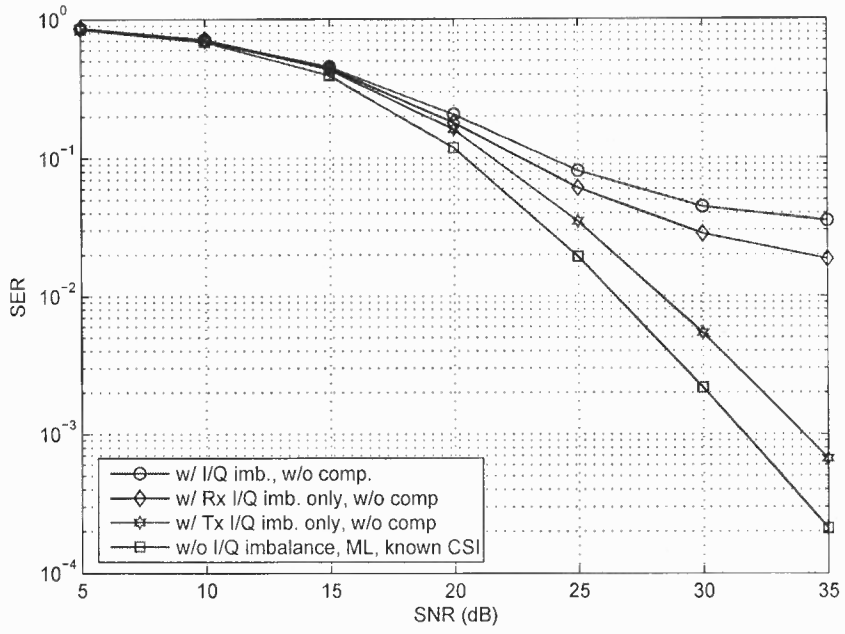

Figure 4.2 SER versus SNR of a 2×1 Alamouti OFDM system with I/Q imbalance. System parameters are: $\epsilon_T = 5\%$, $\varphi_T = 5°$, $\epsilon_R = 5\%$, $\varphi_R = 5°$, $M = 1$, $K = 64$, $L_{\text{cp}} = 3$, and $N_t = 10$. A 64-QAM constellation is used. The number of independent trials is 10^6.

4.5 Conclusions

In this chapter, the performance degradation caused by the transceiver I/Q imbalance in STBC MIMO-OFDM communication systems and solutions are studied. It shows that I/Q imbalance causes severe distortions in STBC MIMO-OFDM communication systems, and the resulting distortion can be successfully mitigated by the proposed methods.

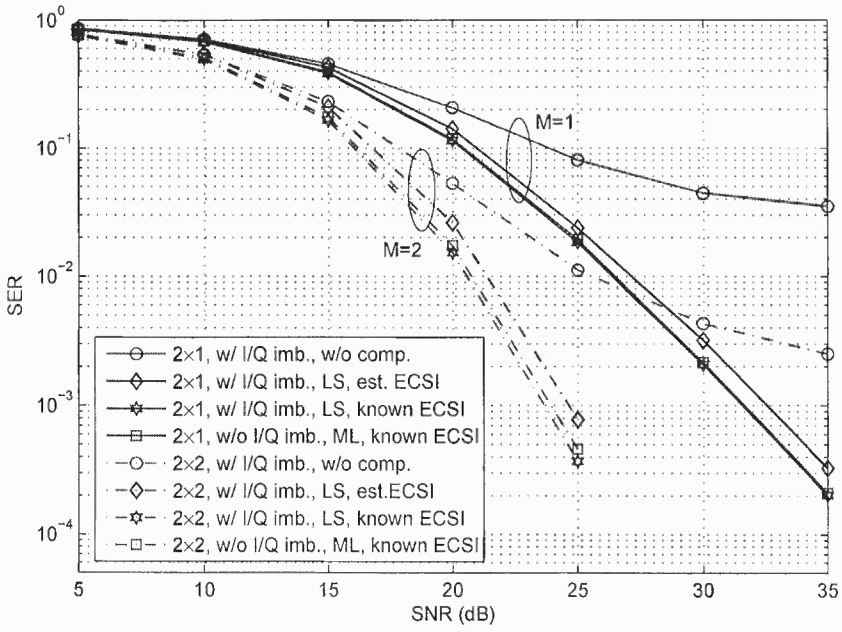

Figure 4.3 SER versus SNR of 2-Tx Alamouti OFDM systems with I/Q imbalance. System parameters are: $\epsilon_T = 5\%$, $\varphi_T = 5°$, $\epsilon_R = 5\%$, $\varphi_R = 5°$, $M = \{1, 2\}$, $K = 64$, $L_{\text{cp}} = 3$, and $N_t = 10$. A 64-QAM constellation is used. The number of independent trials is 10^6.

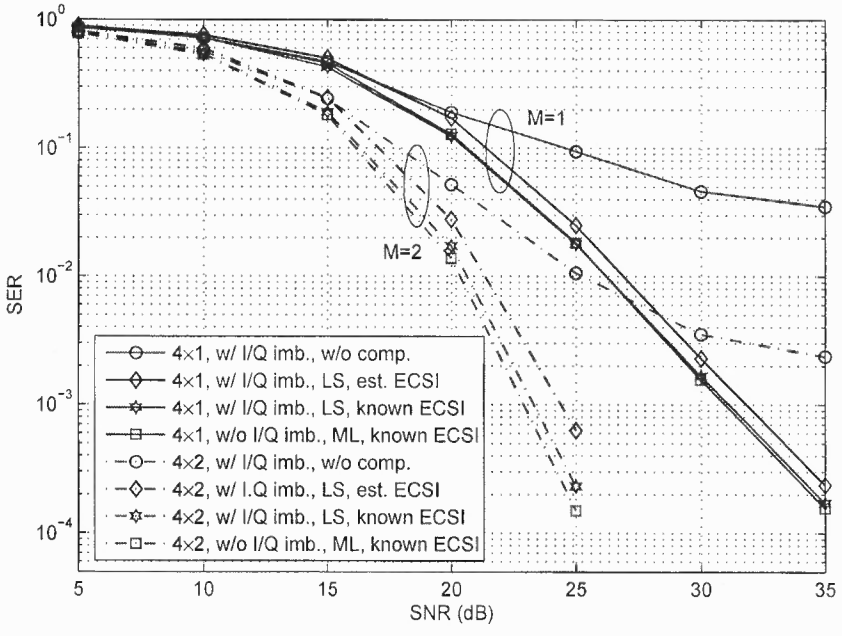

Figure 4.4 SER versus SNR of 4-Tx QOSTBC OFDM systems with I/Q imbalance. System parameters are: $\epsilon_T = 5\%$, $\varphi_T = 5°$, $\epsilon_R = 5\%$, $\varphi_R = 5°$, $M = \{1, 2\}$, $K = 64$, $L_{\text{cp}} = 3$, and $N_t = 10$. A 64-QAM constellation is used. The number of independent trials is 10^6.

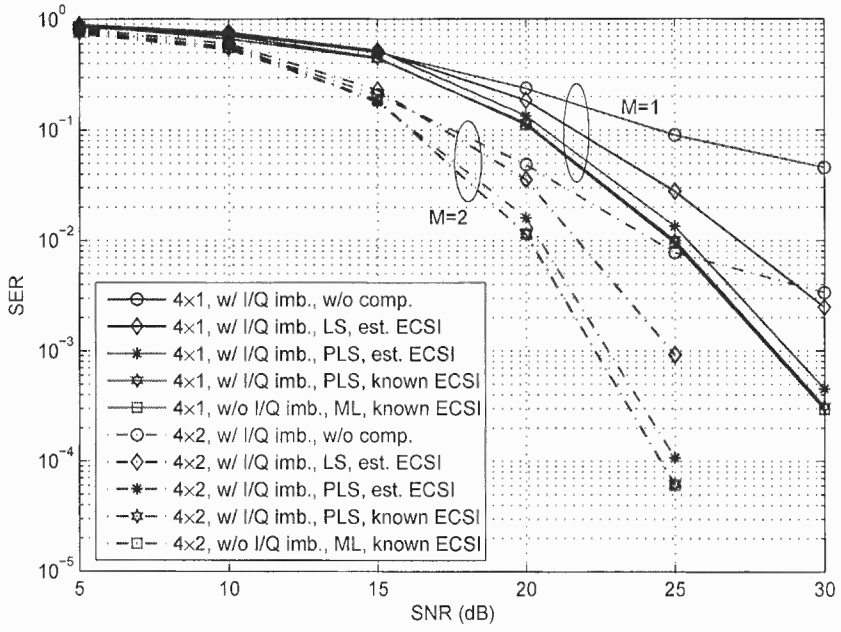

Figure 4.5 SER versus SNR of 4-Tx RQOSTBC OFDM systems with I/Q imbalance. System parameters are: $\epsilon_T = 5\%$, $\varphi_T = 5°$, $\epsilon_R = 5\%$, $\varphi_R = 5°$, $M = \{1, 2\}$, $K = 64$, $L_{\text{cp}} = 3$, and $N_t = 10$. A 64-QAM constellation is used. The number of independent trials is 5×10^6.

CHAPTER 5

A NEW SUBCARRIER GROUPING SCHEME FOR GLCP OFDM SYSTEMS WITH I/Q IMBALANCE

5.1 Introduction

OFDM systems convert a frequency-selective fading channel into parallel frequency-flat fading channels, so a simple single-tap equalizer can be applied in the frequency domain to decode the signals. However, the penalty is that the embedded multipath diversity is lost at the same time. To exploit the multipath diversity embedded in the frequency-selective fading channel, the coding across the subcarriers is needed [78]. However, the decoding complexity is formidable if the coding over all subcarriers is performed. To reduce the decoding complexity while at the same time to achieve the full multipath diversity, the grouped linear constellation precoded (GLCP) OFDM communication system is studied in [15] [16] [79]. In addition, the optimal subcarrier grouping scheme is proposed in [16].

As we know, I/Q imbalance results in a mirror-image term in the data structure in the frequency domain. In GLCP OFDM systems, the mirror-image term links different subcarrier groups, hence the symbols transmitted over these subcarriers should be decoded jointly. In addition, symbols within the same data block have to be decoded jointly as well due to I/Q imbalance, increasing the decoding complexity dramatically. In this chapter, a new subcarrier grouping scheme is developed for GLCP OFDM communication systems in the presence of I/Q imbalance to exploit the potential system diversity existing in multipath frequency-selective fading channels. Different from existing works along this line [15] [16], in this chapter the existence of the system I/Q imbalance is specifically considered.

Although there are various I/Q mitigation methods can be found in the literature, when I/Q imbalance of both the transmitter and receiver is taken into account, the frequency-domain mitigation method in [74] [80] for OFDM systems is preferred. This method can

mitigate the transceiver I/Q imbalance at the receiver with only the estimated effective channel state information (ECSI) available, hence the tasks to estimate the parameters of the transmitter I/Q imbalance, channels and receiver I/Q imbalance are combined. In this chapter, adopting this method, a new strategy for subcarrier grouping for GLCP OFDM systems with I/Q imbalance is proposed by judiciously assigning the mirror-subcarrier pair into one group, therefore a low-complexity solution to the I/Q imbalance mitigation at the receiver is applicable. Compared to the optimal subcarrier grouping, the proposed subcarrier grouping can achieve the full diversity gain with some loss of the coding gain in the absence of I/Q imbalance. However, in the presence of I/Q imbalance, the proposed solution can mitigate the distortion and provide a performance comparable to (or better than) the optimal subcarrier grouping scheme with no I/Q imbalance.

5.2 GLCP OFDM System With I/Q Imbalance

Without loss of generality, a 2×1 space-time-frequency coded (STFC) OFDM system with I/Q imbalance over the frequency-selective block fading channel $\mathbf{h}_i = [h_i(0) \ \cdots \ h_i(L)]^T$ with $L = 1$ (Here L is the order of the FIR channel model) is considered. Correspondingly, the codeword

$$\mathbf{C} = \begin{pmatrix} S_1 & S_2 \\ -S_2^* & S_1^* \end{pmatrix} \qquad \begin{matrix} \longrightarrow \text{space} \\ \downarrow \text{time} \end{matrix}$$

is used. i.e., the transmitter sends $S_1[k]$ from the antenna-one and $S_2[k]$ from the antenna-two at the time 1 over the subcarrier k, then at time 2, it sends $-S_2^*[k]$ and $S_1^*[k]$ from the antenna-one and the antenna-two over the subcarrier k, respectively. Assume the length of CP is longer than the channel delay spread, and the channel keeps steady within the symbol block interval. Let $H_i[k]$ denote the frequency-domain channel response between the i-th transmitting antenna and the receiving antenna over the subcarrier k, the received signal within two consecutive time slots over the subcarrier k after the removal of CP can

be obtained as

$$\underbrace{\begin{bmatrix} R_1[k] \\ R_2^*[k] \end{bmatrix}}_{\bar{R}[k]} = \mathbf{U}[k] \underbrace{\begin{bmatrix} S_1[k] \\ S_2[k] \end{bmatrix}}_{\bar{S}[k]} + \mathbf{V}[k] \underbrace{\begin{bmatrix} S_1^*[k'] \\ S_2^*[k'] \end{bmatrix}}_{\bar{S}^*[k']} + \underbrace{\begin{bmatrix} N_1[k] \\ N_2^*[k] \end{bmatrix}}_{\bar{N}[k]}, \tag{5.1}$$

where

$$\mathbf{U}[k] = \begin{bmatrix} u_1[k] & u_2[k] \\ u_2^*[k] & -u_1^*[k] \end{bmatrix}, \mathbf{V}[k] = \begin{bmatrix} v_1[k] & v_2[k] \\ v_2^*[k] & -v_1^*[k] \end{bmatrix},$$

with

$$\begin{aligned} u_i[k] &= \alpha_T \alpha_R^* H_i[k] + \beta_T \beta_R^* H_i^*[k'] \\ v_i[k] &= \beta_T^* \alpha_R^* H_i[k] + \alpha_T^* \beta_R^* H_i^*[k'] \end{aligned}, \quad i = 1, 2.$$

Here $\bar{S}[k]$ and $\bar{S}[k']$ are different data vectors except for $k = 0$ and $k = K/2$ (Note that the DC subcarrier $k = K/2$ is usually not used in practical systems, i.e., $S_i[K/2] = 0$).

Applying the optimal subcarrier grouping [16] to the above transmission system with $M = 2$ ($M \geq L + 1$) subcarriers in each group, the precoded symbols become

$$\begin{bmatrix} \tilde{S}_i[k] \\ \tilde{S}_i[\frac{K}{2}+k] \end{bmatrix} = \mathbf{\Theta} \begin{bmatrix} S_i[k] \\ S_i[\frac{K}{2}+k] \end{bmatrix}, \qquad i=1,2, \;\; k=0,\cdots,\frac{K}{2}-1,$$

where $\mathbf{\Theta}$ is the 2×2 GLCP matrix.

In the presence of I/Q imbalance, symbols within different subcarrier groups are coupled together and should be decoded jointly. For example, the eight groups with the optimal subcarrier grouping for $K=16$ are $\{0, 8\}$, $\{1, 9\}$, $\{2, 10\}$, $\{3, 11\}$, $\{4, 12\}$, $\{5, 13\}$, $\{6, 14\}$ and $\{7, 15\}$ (here each number is the subcarrier index). However, due to the coupling induced by I/Q imbalance, the decoding has to be performed within the five groups $\{0, 8\}$, $\{1, 7, 9, 15\}$, $\{2, 6, 10, 14\}$, $\{3, 5, 11, 13\}$ and $\{4, 12\}$. Note $S_1[k]$ and $S_2[k]$ can not be decoded separately due to I/Q imbalance, hence the maximum number of symbols to be decoded jointly becomes 8.

5.3 Proposed Encoding/Decoding Scheme

Since I/Q imbalance only induces ICI between mirror-subcarrier pairs, assign each mirror-subcarrier pair $\{k, k'\}$ into one group, I/Q imbalance can be mitigated with a low-complexity decoding. As a special case, $\{0, K/2\}$ are grouped together. Then the symbol vector after precoding becomes

$$\begin{bmatrix} \tilde{S}_i[k] \\ \tilde{S}_i[k'] \end{bmatrix} = \mathbf{\Theta} \begin{bmatrix} S_i[k] \\ S_i[k'] \end{bmatrix}, \qquad i=1,2, \;\; k=0,\cdots,\frac{K}{2}-1.$$

As mentioned above, the symbols $\{S_i[k]\}_{i=1}^{2}$ can not be decoded separately due to I/Q imbalance. In addition, the proposed precoding links $S_i[k]$ and $S_i[k']$ together, consequently, $\{S_i[k], S_i[k']\}_{i=1}^{2}$ have to be decoded jointly by the ML decoding to achieve the full diversity.

After precoding, (5.1) can be reformulated as

$$\underbrace{\begin{bmatrix} \bar{R}[k] \\ \bar{R}^*[k'] \end{bmatrix}}_{\vec{R}[k]} = \underbrace{\begin{bmatrix} \mathbf{U}[k] & \mathbf{V}[k] \\ \mathbf{V}^*[k'] & \mathbf{U}^*[k'] \end{bmatrix}}_{\mathbf{H}[k]} \underbrace{\begin{bmatrix} \bar{\tilde{S}}[k] \\ \bar{\tilde{S}}^*[k'] \end{bmatrix}}_{\vec{S}[k]} + \begin{bmatrix} \bar{N}[k] \\ \bar{N}^*[k'] \end{bmatrix}, \tag{5.2}$$

where $\bar{\tilde{S}}[k] = \begin{bmatrix} \tilde{S}_1[k] & \tilde{S}_2[k] \end{bmatrix}^T$. Based on the proper AWGN assumption, the maximum likelihood sequence estimate (MLSE) can be obtained as

$$\hat{\vec{S}}_{\mathrm{ML}}[k] = \arg \min_{\vec{S}[k] \in \mathcal{S}} \|\vec{R}[k] - \mathbf{H}[k]\vec{S}[k]\|^2,$$

where the set $\mathcal{S}$ contains all possible signal vectors from a given symbol constellation set. Note the number of symbols to be jointly decoded is reduced from 8 to 4. Generally, using a $N-$QAM constellation, the number of searching to decode each signal vector is reduced from N^{4M} with the optimal grouping to N^{2M} with the proposed grouping with I/Q imbalance.

To sacrifice the optimal performance and reduce the complexity, the least squares (LS) estimate of $\vec{S}[k]$ can be obtained as

$$\hat{\vec{S}}_{\text{LS}}[k] = (\mathbf{H}^H[k]\mathbf{H}[k])^{-1}\mathbf{H}^H[k]\vec{R}[k].$$

Since only the effective channel state information (ECSI) such as $u_i[k]$ and $v_i[k]$ are needed in the proposed solution, the task to estimate the channel $H_i[k]$ and the I/Q imbalance parameters $\{\alpha_T, \beta_T, \alpha_R, \beta_R\}$ can be combined [74]. Because $R_i[k]$ is a linear superposition of $u_i[k]$ and $v_i[k]$, their estimates, $\hat{u}_i[k]$ and $\hat{v}_i[k]$, can be obtained by sending training sequences [52].

5.4 Performance Analysis

First, the loss of the coding gain by introducing the proposed grouping in the absence of I/Q Imbalance is studied, since the full diversity can be achieved with arbitrary subcarrier grouping as long as $M \geq L+1$ [15]. A 4×1 channel vector $\mathbf{h} := [\mathbf{h}_1^T \ \mathbf{h}_2^T]^T \sim \mathcal{CN}(0, \frac{1}{2}\mathbf{R}_h)$ is used, and $\mathbf{R}_h = \mathbf{B}_h\mathbf{B}_h^H \in \mathbb{C}^{4\times4}$, with $\text{rank}(\mathbf{R}_h) = 4$.

With no I/Q imbalance, it can be obtained that

$$\begin{bmatrix} R_1[k] R_2[k] \end{bmatrix} = \begin{bmatrix} H_1[k] H_2[k] \end{bmatrix} \underbrace{\begin{bmatrix} \tilde{S}_1[k] & -\tilde{S}_2^*[k] \\ \tilde{S}_2[k] & \tilde{S}_1^*[k] \end{bmatrix}}_{\tilde{\mathbf{S}}[k]} + \begin{bmatrix} N_1[k] N_2[k] \end{bmatrix}.$$

For any group $k \in \{k_1, k_2\}$, the follows are defined

$$\begin{aligned} \boldsymbol{\Delta}[k] &:= \tilde{\mathbf{S}}[k] - \tilde{\mathbf{S}}'[k] \in \mathbb{C}^{2\times2}, \\ \boldsymbol{\Omega}[k] &:= \mathbf{I}_2 \otimes [1 \ \ e^{-j2k\pi/K}]^T \in \mathbb{C}^{4\times2}, \\ \boldsymbol{\Lambda}_e &:= \textstyle\sum_{k\in\{k_1,k_2\}} \boldsymbol{\Omega}[k]\boldsymbol{\Delta}[k]\boldsymbol{\Delta}^H[k]\boldsymbol{\Omega}^H[k] \in \mathbb{C}^{4\times4}, \\ \tilde{\boldsymbol{\Lambda}}_e &:= \mathbf{B}_h^T\boldsymbol{\Lambda}_e\mathbf{B}_h^* \in \mathbb{C}^{4\times4}. \end{aligned}$$

Follow the derivation of the pairwise error probability (PEP) of erroneously decoding $\tilde{\mathbf{S}}[k]$ to be $\tilde{\mathbf{S}}'[k]$ in [15], the achievable diversity gain and coding gain can be obtained as

$$\begin{aligned} G_d &= \text{rank}(\tilde{\mathbf{\Lambda}}_e), \\ G_c &= \frac{1}{2}\big(\det(\mathbf{R}_h)\det(\mathbf{\Lambda}_e)\big)^{\frac{1}{4}}, \quad \text{when } \tilde{\mathbf{\Lambda}}_e \text{ is full rank.} \end{aligned}$$

With the optimal subcarrier grouping, i.e., $k_2 = K/2 + k_1$, based on the detailed derivation in Appendix C, it can be obtained that

$$\det(\mathbf{\Lambda}_e) = (4d[k_1]d[k_2])^2,$$

while with the proposed subcarrier grouping, i.e., $k_2 = (-k_1)_K$, it can be obtained that

$$\det(\mathbf{\Lambda}_e) = \begin{cases} (4d[k_1]d[k_2])^2 & k_1 = 0, k_2 = \frac{K}{2}, \\ \left(4d[k_1]d[k_2]\left(\frac{1-\cos(2\theta)}{2}\right)\right)^2 & \text{others}, \end{cases}$$

with $d[k] := \|\tilde{S}_1[k] - \tilde{S}_1'[k]\|^2 + \|\tilde{S}_2[k] - \tilde{S}_2'[k]\|^2$, and $\theta := 2\pi k_1/K$ $(k_1 = 1, \cdots, K/2-1)$. It shows that $\det(\mathbf{\Lambda}_e) = 0$ only when $\{S_i[k]\}_{i=1}^2$ $(k \in \{k_1, k_2\})$ are correctly decoded with the linear precoding. Since $\mathbf{R}_h$ is assumed full rank, $\tilde{\mathbf{\Lambda}}_e$ is full rank as well when $\det(\mathbf{\Lambda}_e) \neq 0$. Consequently, the maximum diversity gain $G_d = 2(L+1) = 4$ can be achieved. However, the coding gain decreases (except $k \in \{0, K/2\}$) since

$$\sqrt{\frac{1-\cos(2\theta)}{2}} \leq 1.$$

It is consistent with the result in [81] that the optimum solution of subcarrier grouping is unique for $M = L + 1$.

When compared to the case with no I/Q imbalance, a better performance may be achieved due to the coupling between mirror-subcarrier pairs induced by I/Q imbalance. The penalty is that the dimensionality of the signal vectors to be decoded is doubled. Since we have not been able to provide a general proof, the performance is studied through simulations.

Next, the study is extended to other scenario such as $L = 3$ and $M = 4$. Correspondingly, $\text{rank}(\mathbf{R}_h) = 8$ is assumed. Accordingly, the achievable diversity gain and coding gain become

$$\begin{aligned} G_d &= \text{rank}(\tilde{\mathbf{\Lambda}}_e), \\ G_c &= \frac{1}{4}\big(\det(\mathbf{R}_h)\det(\mathbf{\Lambda}_e)\big)^{\frac{1}{8}}, \qquad \text{when } \tilde{\mathbf{\Lambda}}_e \text{ is full rank.} \end{aligned}$$

With the optimal subcarrier grouping, for any group $\{k_i\}_{i=1}^4$ ($k_i = (i-1)K/4 + k_1$), based on the detailed derivation in Appendix C, it can be obtained that

$$\det(\mathbf{\Lambda}_e) = \big(\prod_{i=1}^{4} 4d[k_i]\big)^2.$$

Similarly, the mirror-subcarrier pair is assigned into the same group. Follow the idea of the optimal grouping, the subcarrier pairs containing k and $k + K/4$ are assigned into one group, i.e., the subcarriers $\{k, k+K/4, -k+3K/4, -k+K\}$ ($k = 1, \cdots, K/4$) are selected and grouped. As the special case, $\{0, K/4, K/2, 3K/4\}$ become one group. Then it can be obtained

$$\det(\mathbf{\Lambda}_e) = \begin{cases} \big(\prod_{i=1}^{4} 4d[k_i]\big)^2, & k_i \in \{0, \frac{K}{4}, \frac{K}{2}, \frac{3K}{4}\} \\ \Big(\big(\prod_{i=1}^{4} 4d[k_i]\big)\big(\frac{1-e^{-j4\theta}}{2}\big)^2\big(\frac{e^{j2\theta}+j}{2}\big)^4\Big)^2, & \text{others} \end{cases}$$

where $\theta := 2\pi k_1/K$ ($k_1 = 1, \cdots, K/4 - 1$). Note $\det(\mathbf{\Lambda}_e)$ is a real value since $\mathbf{\Lambda}_e$ is Hermitian. It shows that $\det(\mathbf{\Lambda}_e) = 0$ only when $\{S_i[k]\}_{i=1}^2$ ($k \in \{k_1, k_2, k_3, k_4\}$) are correctly decoded, hence, the maximum diversity gain $G_d = 8$ can be achieved, with the factor causing the loss of coding gain being

$$\Big(\big(\frac{1-e^{-j4\theta}}{2}\big)^2\big(\frac{e^{j2\theta}+j}{2}\big)^4\Big)^{\frac{1}{4}} \leq 1.$$

5.5 Simulation Results

In the simulations, the worst case, the amplitude imbalance $\epsilon = 5\%$ and the phase imbalance $\varphi = 5^\circ$ at both of the transmitter and receiver side are adopted. In addition, the FFT size

$K = 64$, the number of training data block $N_t = 10$, and the $(L+1)$-tap $(L = \{1, 3\})$ blocking fading channel with each tap being Rayleigh fading are adopted. Moreover, the GLCP matrices

$$\Theta = \frac{1}{\sqrt{2}} \begin{bmatrix} 1 & e^{j\frac{\pi}{4}} \\ 1 & e^{j\frac{5\pi}{4}} \end{bmatrix} \qquad L = 1,$$

$$\Theta = \frac{1}{2} \begin{bmatrix} 1 & e^{j\frac{\pi}{8}} & e^{j\frac{2\pi}{8}} & e^{j\frac{3\pi}{8}} \\ 1 & e^{j\frac{5\pi}{8}} & e^{j\frac{10\pi}{8}} & e^{j\frac{15\pi}{8}} \\ 1 & e^{j\frac{9\pi}{8}} & e^{j\frac{18\pi}{8}} & e^{j\frac{27\pi}{8}} \\ 1 & e^{j\frac{13\pi}{8}} & e^{j\frac{26\pi}{8}} & e^{j\frac{39\pi}{8}} \end{bmatrix} \qquad L = 3$$

are used, respectively.

As shown in Fig. 5.1~Fig. 5.4, without compensation (the dashed curves), I/Q imbalance degrades the performance dramatically. With no I/Q imbalance, there is some performance loss by introducing the proposed grouping, compared to the optimal grouping. However, with I/Q imbalance, the proposed solution can provide a performance comparable to the optimal grouping scheme with no I/Q imbalance (see Fig. 5.1~Fig. 5.2), or a better performance (see Fig. 5.3~Fig. 5.4). In addition, the frequency diversity can not be exploited by the LS method. Moreover, I/Q imbalance can be mitigated successfully with the estimated ECSI as well, as shown in Fig. 5.5.

5.6 Conclusions

In this chapter, a new subcarrier grouping enabling a low-complexity decoding is proposed to mitigate I/Q imbalance for GLCP OFDM systems. Analysis and simulation results demonstrate that in the presence of I/Q imbalance, the proposed solution can provide a performance comparable to (or better than) the optimal grouping scheme with no I/Q imbalance.

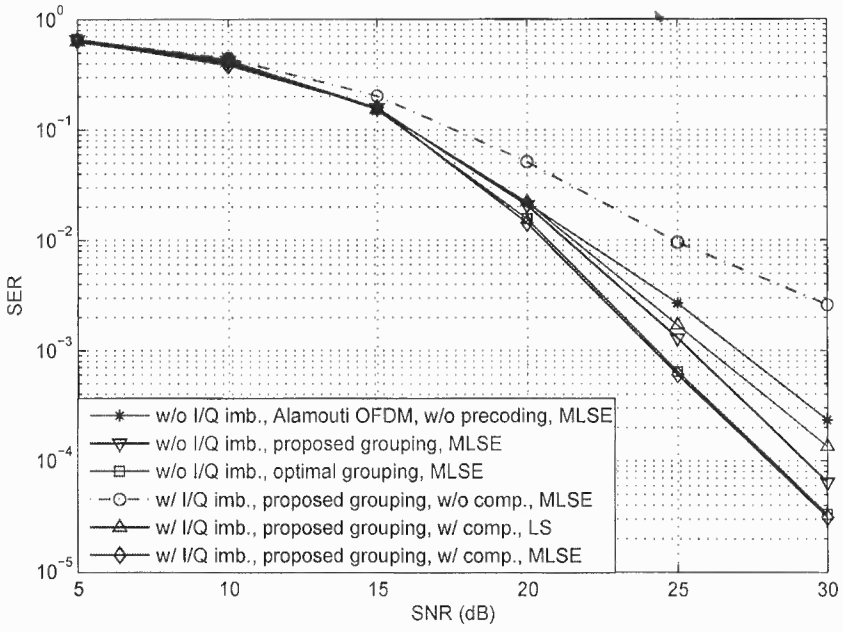

Figure 5.1 SER versus SNR of a 2×1 GLCP OFDM system with I/Q imbalance. System parameters are: $\epsilon_T = 5\%$, $\varphi_T = 5°$, $\epsilon_R = 5\%$, $\varphi_R = 5°$, $K = 64$, $L = 1$, and $M = 2$. A 16-PSK constellation is used. The number of independent trial is 10^6.

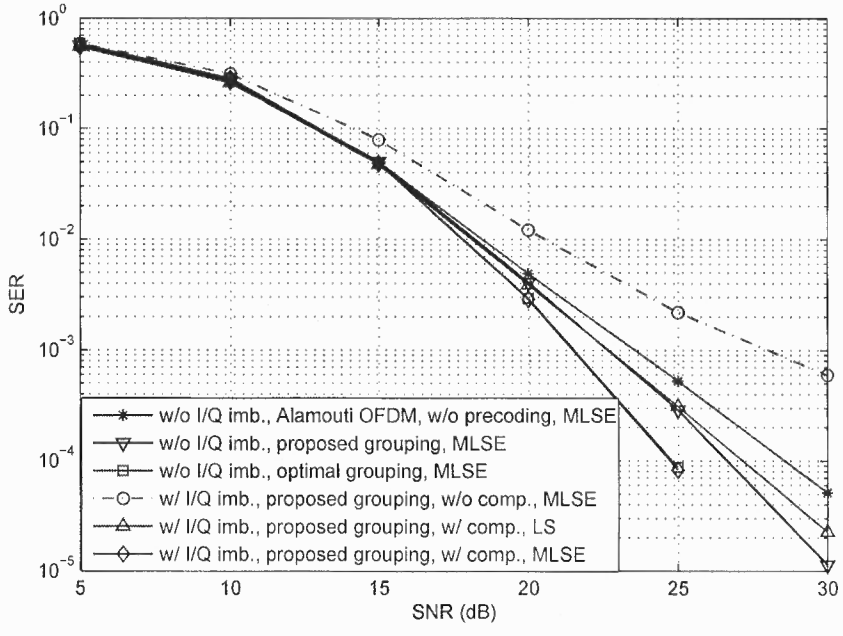

Figure 5.2 SER versus SNR of a 2×1 GLCP OFDM system with I/Q imbalance. System parameters are: $\epsilon_T = 5\%$, $\varphi_T = 5°$, $\epsilon_R = 5\%$, $\varphi_R = 5°$, $K = 64$, $L = 1$, and $M = 2$. A 16-QAM constellation is used. The number of independent trial is 10^6.

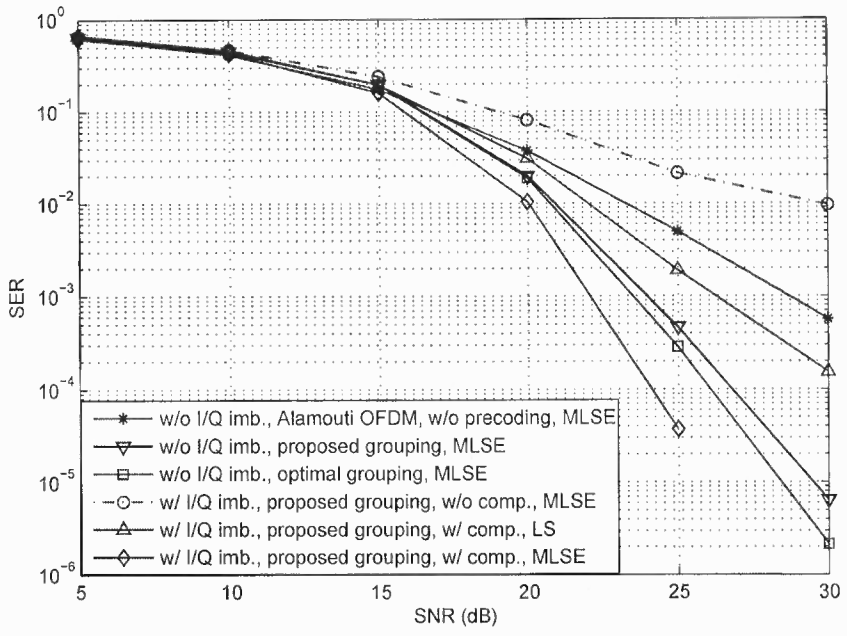

Figure 5.3 SER versus SNR of a 2×1 GLCP OFDM system with I/Q imbalance. System parameters are: $\epsilon_T = 5\%$, $\varphi_T = 5°$, $\epsilon_R = 5\%$, $\varphi_R = 5°$, $K = 64$, $L = 3$, and $M = 4$. A 16-PSK constellation is used. The number of independent trial is 10^6.

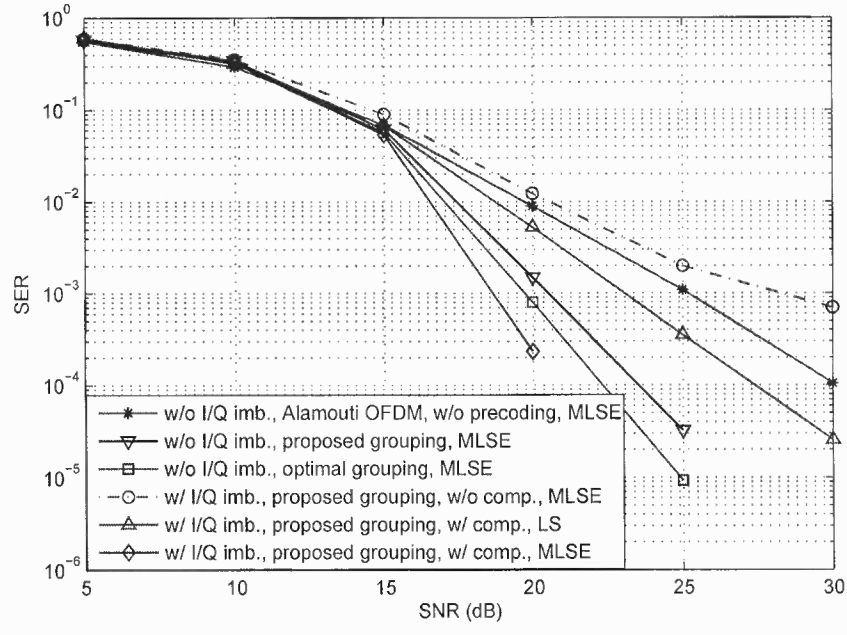

Figure 5.4 SER versus SNR of a 2×1 GLCP OFDM system with I/Q imbalance. System parameters are: $\epsilon_T = 5\%$, $\varphi_T = 5°$, $\epsilon_R = 5\%$, $\varphi_R = 5°$, $K = 64$, $L = 3$, and $M = 4$. A 16-QAM constellation is used. The number of independent trial is 10^6.

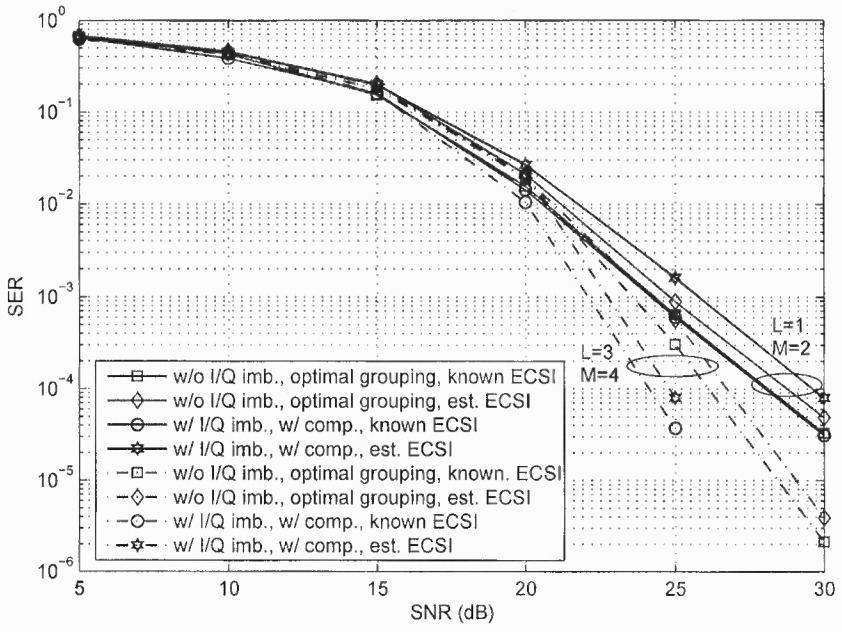

Figure 5.5 SER versus SNR of a 2×1 GLCP OFDM system with I/Q imbalance. System parameters are: $\epsilon_T = 5\%$, $\varphi_T = 5°$, $\epsilon_R = 5\%$, $\varphi_R = 5°$, $K = 64$, $L = \{1, 3\}$, $M = \{2, 4\}$, and $N_t = 5$. A 16-PSK constellation is used, and the MLSE method is employed. The number of independent trial is 10^6.

CHAPTER 6

I/Q IMBALANCE IN TIME-REVERSAL STBC SYSTEMS OVER FREQUENCY-SELECTIVE FADING CHANNELS

6.1 Introduction

Space-time block coded (STBC) wireless communication systems provide reliable data transmissions by exploiting the spatial diversity in flat fading channels [6]. To achieve the spatial diversity in frequency-selective fading channels, space-time block codes (STBCs) in conjunction with orthogonal frequency division multiplexing (OFDM) is proposed [82] [11] [12] [13]. To further exploit the embedded multipath diversity of frequency-selective fading channels, codings across subcarriers of STBC-OFDM systems are introduced [78] [14] [15]. However, OFDM has the high peak-to-average power ratio (PAPR) problem and is sensitive to the carrier frequency offset [83] [84] [20]. Consequently, to achieve both the spatial and multipath diversity, time-reversal STBC (TR-STBC) schemes are studied extensively [21] [22] [23] [24].

In time-reversal communication systems, both the signal and its complex-conjugate are utilized. As we know, I/Q imbalance induces the complex-conjugate term of the intended signal in the time domain, consequently, the presence of I/Q imbalance in time-reversal communication systems will change the properties of the original scheme, increase SER dramatically if no further advanced signal processing technique is employed.

In this work, a new transmission scheme that enables simple yet effective solutions, both in the time domain and in the frequency domain, is developed to mitigate the transceiver I/Q imbalance in TR-OSTBC systems over frequency-selective fading channels. Simulation results demonstrate that the transceiver I/Q imbalance can be compensated successfully by employing the proposed solutions with known or estimated effective channels.

6.2 Signal and System Models

6.2.1 Data Structure With CP Aided Transmission

When two transmit-antennas are used to simultaneously transmit $K \times 1$ data blocks $\mathbf{s}_i$ over frequency-selective fading channels $\mathbf{h}_i = \begin{bmatrix} h_i[0] & \cdots & h_i[L] \end{bmatrix}^T, (i = 1, 2,\ L \ll K)$, the received $K \times 1$ data vector containing I/Q imbalance has the following discrete-time baseband form,

$$\mathbf{r} = \sum_{i=1}^{2} (\mathbf{U}_i \mathbf{s}_i + \mathbf{V}_i \mathbf{s}_i^*) + \mathbf{n}. \tag{6.1}$$

The square matrices $\mathbf{U}_i$ and $\mathbf{V}_i$ in (6.1) are circulant due to the use of a cyclic-prefix (CP) preamble copying from the L trailing symbols of the data vector $\mathbf{s}_i$ at the transmitter. Specifically, matrices $\mathbf{U}_i = \text{circ}\{\mathbf{u}_i\}$ and $\mathbf{V}_i = \text{circ}\{\mathbf{v}_i\}$ are parameterized by the channel and the transceiver I/Q imbalance parameters as follows,

$$\begin{aligned} \mathbf{u}_i &= \alpha_T \alpha_R^* \tilde{\mathbf{h}}_i + \beta_T \beta_R^* \tilde{\mathbf{h}}_i^* \\ &\qquad\qquad , \qquad i = 1, 2. \\ \mathbf{v}_i &= \beta_T^* \alpha_R^* \tilde{\mathbf{h}}_i + \alpha_T^* \beta_R^* \tilde{\mathbf{h}}_i^* \end{aligned}$$

Here the $K \times 1$ vector $\tilde{\mathbf{h}}_i = \begin{bmatrix} \mathbf{h}_i^T & \mathbf{0}_{K-L+1}^T \end{bmatrix}^T$ is a zero-padded channel. Compared to the effect of I/Q imbalance on the signal, such effect on the noise is relatively small at reasonably high SNRs, hence a proper $\mathbf{n} \sim \mathcal{CN}(0, \sigma_n^2 \mathbf{I}_K)$ is adopted.

The matrices $\mathbf{U}_i$ and $\mathbf{V}_i$ can be diagonalized by the unitary discrete Fourier transform (DFT) matrix $\mathbf{W}$ as $\mathbf{U}_i = \mathbf{W}^H \mathbf{\Lambda}_{u_i} \mathbf{W}$, and $\mathbf{V}_i = \mathbf{W}^H \mathbf{\Lambda}_{v_i} \mathbf{W}$, with $\mathbf{\Lambda}_{u_i} = \text{diag}\{\mathbf{W}\mathbf{u}_i\}$, and $\mathbf{\Lambda}_{v_i} = \text{diag}\{\mathbf{W}\mathbf{v}_i\}$.

6.2.2 Data Model for the Proposed TR-OSTBC System With CP

In a 2×1 TR-OSTBC system, symbol vectors in the $2K \times 2$ codeword matrix

$$\mathbf{C}(\mathbf{s}_1, \mathbf{s}_2) = \begin{pmatrix} \mathbf{s}_1 & \mathbf{s}_2 \\ -J_c(\mathbf{s}_2) & J_c(\mathbf{s}_1) \end{pmatrix} \qquad \begin{matrix} \longrightarrow \text{space} \\ \downarrow \text{time} \end{matrix}$$

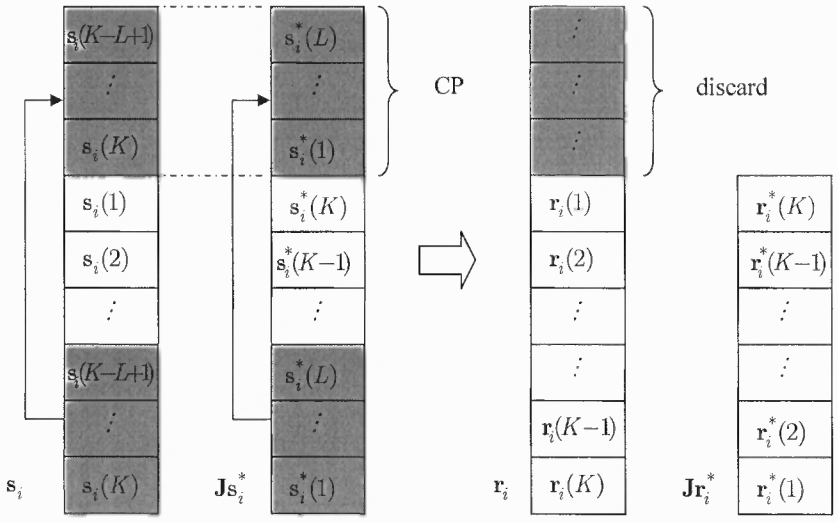

Figure 6.1 Structure of the data and its time-reversal complex-conjugate.

are transmitted over two consecutive time slots through two transmit-antennas. Here $J_c(\cdot)$ is a time-reversal conjugate (TRC) operator such that $J_c(\mathbf{s}_i) = \mathbf{J}\mathbf{s}_i^*$ with $\mathbf{J}$ being an exchange matrix, as shown in Fig. 6.1. For any circulant matrix $\mathbf{A}$, it holds that $\mathbf{J}\mathbf{A}^*\mathbf{J} = \mathbf{A}^H$. Using the results in (6.1), the received data block in a TR-OSTBC system over two consecutive time slots can be formulated as $\vec{\mathbf{r}} = \mathbf{U}\vec{\mathbf{s}} + \mathbf{V}\vec{\mathbf{s}}^* + \vec{\mathbf{n}}$, i.e.,

$$\begin{bmatrix} \mathbf{r}_1 \\ \mathbf{J}\mathbf{r}_2^* \end{bmatrix} = \begin{bmatrix} \mathbf{U}_1 & \mathbf{U}_2 \\ \mathbf{U}_2^H & -\mathbf{U}_1^H \end{bmatrix} \begin{bmatrix} \mathbf{s}_1 \\ \mathbf{s}_2 \end{bmatrix} + \begin{bmatrix} \mathbf{V}_1 & \mathbf{V}_2 \\ \mathbf{V}_2^H & -\mathbf{V}_1^H \end{bmatrix} \begin{bmatrix} \mathbf{s}_1^* \\ \mathbf{s}_2^* \end{bmatrix} + \begin{bmatrix} \mathbf{n}_1 \\ \mathbf{J}\mathbf{n}_2^* \end{bmatrix}. \tag{6.2}$$

The proposed 2×1 TR-OSTBC communication system is illustrated in Fig. 6.2. In the absence of I/Q imbalance, $\mathbf{V} = \mathbf{0}$, symbol blocks $\{\mathbf{s}_i\}_{i=1}^2$ can be decoded separately due to the circulant nature of matrices $\{\mathbf{U}_i\}_{i=1}^2$. However, the presence of I/Q imbalance forces us to take into consideration a widely linear relation containing both $\vec{\mathbf{s}}$ and its mirror-image $\vec{\mathbf{s}}^*$ in (6.2) to effectively decode symbols $\{\mathbf{s}_i\}_{i=1}^2$.

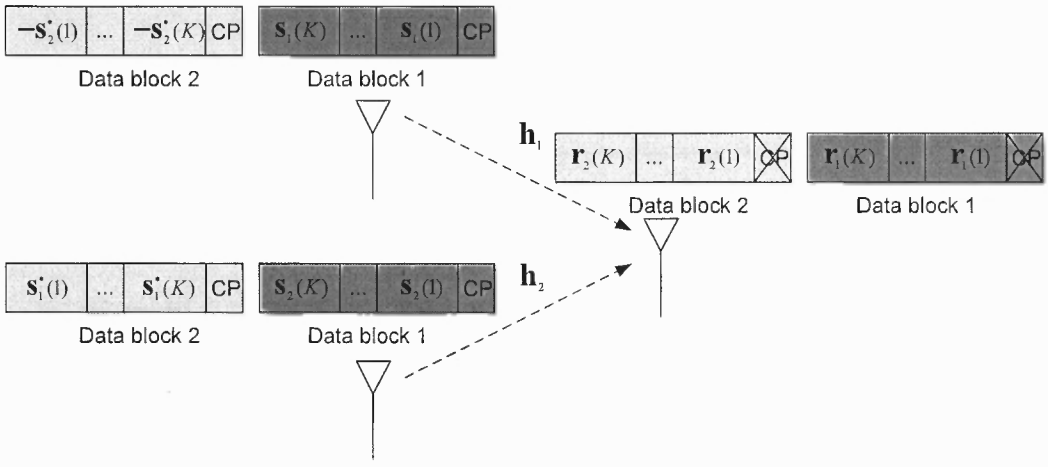

Figure 6.2 A 2×1 TR-OSTBC communication system.

6.3 Solutions

6.3.1 Time Domain Processing

In the presence of I/Q imbalance, to fully capture the symbol information contained in (6.2), the data can be re-arranged as

$$\underbrace{\begin{bmatrix} \Re\{\vec{\mathbf{r}}\} \\ \Im\{\vec{\mathbf{r}}\} \end{bmatrix}}_{\tilde{\mathbf{r}}} = \underbrace{\begin{bmatrix} \Re\{\mathbf{U}+\mathbf{V}\} & \Im\{\mathbf{V}-\mathbf{U}\} \\ \Im\{\mathbf{U}+\mathbf{V}\} & \Re\{\mathbf{U}-\mathbf{V}\} \end{bmatrix}}_{\mathbf{H}} \underbrace{\begin{bmatrix} \Re\{\vec{\mathbf{s}}\} \\ \Im\{\vec{\mathbf{s}}\} \end{bmatrix}}_{\tilde{\mathbf{s}}} + \underbrace{\begin{bmatrix} \Re\{\vec{\mathbf{n}}\} \\ \Im\{\vec{\mathbf{n}}\} \end{bmatrix}}_{\tilde{\mathbf{n}}}. \tag{6.3}$$

Under additive white Gaussian noise (AWGN) assumption, the optimal maximum-likelihood sequence estimate (MLSE) of $\{\mathbf{s}_i\}_{i=1}^2$ can be obtained from

$$\hat{\tilde{\mathbf{s}}}_{\mathrm{ML}} = \arg \min_{\tilde{\mathbf{s}} \in \mathcal{S}} \|\tilde{\mathbf{r}} - \mathbf{H}\tilde{\mathbf{s}}\|^2, \tag{6.4}$$

where the set $\mathcal{S}$ contains all possible $4K \times 1$ signal vectors $\tilde{\mathbf{s}}$ from a given symbol constellation. For a TR-OSTBC system with large data block size K (typically $K \gg L$), to reduce the computational complexity of MLSE, a low-complexity sub-optimal solution built upon the filtering idea can be found for the practical implementation.

Introducing a linear filter $\mathbf{F}$, $E\{\|\tilde{\mathbf{s}} - \mathbf{F}\tilde{\mathbf{r}}\|^2\}$ can be minimized to obtain the linear minimum-mean-square-error (LMMSE) estimates of $\{\mathbf{s}_i\}_{i=1}^2$,

$$\hat{\tilde{\mathbf{s}}}_{\text{LMMSE}} = \mathbf{F}_{\text{LMMSE}}\tilde{\mathbf{r}} = \mathbf{H}^T(\mathbf{H}\mathbf{H}^T + \sigma_n^2/\sigma_s^2\mathbf{I}_{4K})^{-1}\tilde{\mathbf{r}},$$

where σ_s^2 is the signal power per sample. The detailed derivation of $\mathbf{F}_{\text{LMMSE}}$ can be found in Appendix E. Its zero-forcing (ZF) counterpart is simply the result of dropping the diagonal loading factor,

$$\hat{\tilde{\mathbf{s}}}_{\text{ZF}} = \mathbf{F}_{\text{ZF}}\tilde{\mathbf{r}} = \mathbf{H}^T(\mathbf{H}\mathbf{H}^T)^{-1}\tilde{\mathbf{r}}.$$

Note that the inversion of the large-size $(4K \times 4K)$ matrices in the above LMMSE and ZF solutions can be avoided explicitly due to the proposed CP based TR-OSTBC scheme. The block structure of the matrix $\mathbf{H}$ in (6.3) results in a block Gram-matrix $\mathbf{G} = \mathbf{H}\mathbf{H}^T$ with the following structure,

$$\mathbf{G} = \begin{bmatrix} \mathbf{G}_{11} & \mathbf{G}_{12} \\ \mathbf{G}_{12}^T & \mathbf{G}_{22} \end{bmatrix} = \left[\begin{array}{cc|cc} \mathbf{A} & \mathbf{0}_K & \mathbf{C} & \mathbf{D} \\ \mathbf{0}_K & \mathbf{A} & \mathbf{D}^T & -\mathbf{C}^T \\ \hline \mathbf{C}^T & \mathbf{D} & \mathbf{B} & \mathbf{0}_K \\ \mathbf{D}^T & -\mathbf{C} & \mathbf{0}_K & \mathbf{B} \end{array}\right],$$

where matrices $\mathbf{A}$, $\mathbf{B}$, $\mathbf{C}$ and $\mathbf{D}$ are $K \times K$ circulant matrices. This can be seen from the fact that the matrices

$$\mathbf{A} = \sum_{i=1}^{2} \Big\{ \Re\{\mathbf{U}_i + \mathbf{V}_i\}\Re\{\mathbf{U}_i^H + \mathbf{V}_i^H\} - \Im\{\mathbf{V}_i - \mathbf{U}_i\}\Im\{\mathbf{V}_i^H - \mathbf{U}_i^H\} \Big\},$$

$$\mathbf{B} = \sum_{i=1}^{2} \Big\{ \Re\{\mathbf{U}_i - \mathbf{V}_i\}\Re\{\mathbf{U}_i^H - \mathbf{V}_i^H\} - \Im\{\mathbf{U}_i + \mathbf{V}_i\}\Im\{\mathbf{U}_i^H + \mathbf{V}_i^H\} \Big\},$$

$$\mathbf{C} = -\sum_{i=1}^{2} \Big\{ \Re\{\mathbf{U}_i + \mathbf{V}_i\}\Im\{\mathbf{U}_i^H + \mathbf{V}_i^H\} + \Im\{\mathbf{V}_i - \mathbf{U}_i\}\Re\{\mathbf{V}_i^H - \mathbf{U}_i^H\} \Big\},$$

$$\mathbf{D}=\Re\{\mathbf{U}_2+\mathbf{V}_2\}\Im\{\mathbf{U}_1+\mathbf{V}_1\}-\Re\{\mathbf{U}_1+\mathbf{V}_1\}\Im\{\mathbf{U}_2+\mathbf{V}_2\}$$
$$+\Im\{\mathbf{V}_2-\mathbf{U}_2\}\Re\{\mathbf{V}_1-\mathbf{U}_1\}-\Im\{\mathbf{V}_1-\mathbf{U}_1\}\Re\{\mathbf{V}_2-\mathbf{U}_2\},$$

are products and summations of circulant matrices. The Schur complement of $\mathbf{G}_{11}$ in $\mathbf{G}$ can be obtained as $\mathbf{G}_s = \mathbf{G}_{22}-\mathbf{G}_{12}^T\mathbf{G}_{11}^{-1}\mathbf{G}_{12} = \mathbf{I}_2\otimes\mathbf{E}$, where $\mathbf{E} = \mathbf{B}-(\mathbf{C}^T\mathbf{A}^{-1}\mathbf{C}+\mathbf{D}\mathbf{A}^{-1}\mathbf{D}^T)$ is also a $K \times K$ circulant matrix. Hence only $\mathbf{A}^{-1}$, $\mathbf{B}^{-1}$ and $\mathbf{E}^{-1}$ are involved to invert matrices $(\mathbf{H}\,\mathbf{H}^T + \sigma_n^2/\sigma_s^2\,\mathbf{I}_{4K})$ and $\mathbf{H}\,\mathbf{H}^T$. The circulant nature of matrices $\mathbf{A}$, $\mathbf{B}$ and $\mathbf{E}$ further indicates that their inversions can be easily calculated using the unitary DFT matrix, i.e., $\mathbf{A}^{-1} = \mathbf{W}^H\mathbf{\Lambda}_a^{-1}\mathbf{W}$ with diagonal elements of $\mathbf{\Lambda}_a$ being DFT of the first column of $\mathbf{A}$.

The performance of the linear filter solutions can be further improved by introducing *nonlinear* filters, such as MMSE decision feedback equalizer (MMSE-DFE) and/or ZF-DFE, to remove the remaining inter-symbol interference (ISI).

As shown in Fig. 6.3, let $\mathbf{F}_f = \mathbf{L}^T\mathbf{F}_{\text{LMMSE}}$ and $\mathbf{F}_b = \mathbf{L}^T-\mathbf{I}_{4K}$ denote the feedforward filter and feedback filter of MMSE-DFE, respectively, the $4K\times 4K$ lower-triangular matrix $\mathbf{L}$ can be explicitly obtained by the factorization,

$$\mathbf{H}^T\mathbf{H} + \sigma_n^2/\sigma_s^2\mathbf{I}_{4K} = \mathbf{L}\mathbf{\Lambda}_h\mathbf{L}^T.$$

Here $\mathbf{\Lambda}_h$ is a $4K \times 4K$ diagonal matrix used to normalize the diagonal entries of $\mathbf{L}$. The block symmetric matrix $\tilde{\mathbf{G}} = \mathbf{H}^T\mathbf{H}$, with the similar structure as $\mathbf{G}$, can be decomposed into

$$\tilde{\mathbf{G}}=\begin{bmatrix} \mathbf{I}_{2K} & \mathbf{0}_{2K} \\ \tilde{\mathbf{G}}_{12}^T\tilde{\mathbf{G}}_{11}^{-1} & \mathbf{I}_{2K} \end{bmatrix}\begin{bmatrix} \tilde{\mathbf{G}}_{11} & \mathbf{0}_{2K} \\ \mathbf{0}_{2K} & \tilde{\mathbf{G}}_s \end{bmatrix}\begin{bmatrix} \mathbf{I}_{2K} & \tilde{\mathbf{G}}_{11}^{-1}\tilde{\mathbf{G}}_{12} \\ \mathbf{0}_{2K} & \mathbf{I}_{2K} \end{bmatrix},$$

where $\tilde{\mathbf{G}}_{11} = \mathbf{I}_2\otimes\tilde{\mathbf{A}}$, and $\tilde{\mathbf{G}}_s = \tilde{\mathbf{G}}_{22}-\tilde{\mathbf{G}}_{12}^T\tilde{\mathbf{G}}_{11}^{-1}\tilde{\mathbf{G}}_{12} = \mathbf{I}_2\otimes\tilde{\mathbf{E}}$. Hence, obtaining matrix $\mathbf{L}$, only involves the inversions of $K \times K$ circulant matrices, whose computational complexity again can be dramatically reduced by the DFT operations.

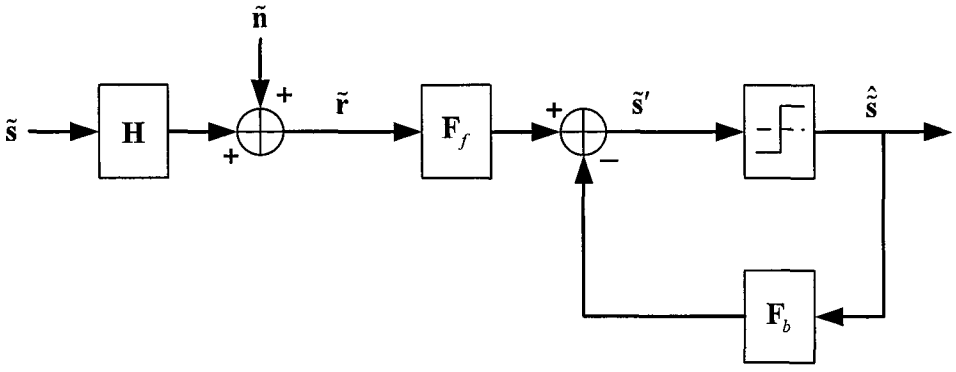

Figure 6.3 Block diagram of the decision feedback equalizer.

The detailed derivation of MMSE-DFE can be found in Appendix E. Dropping the diagonal loading factor, the implementation of ZF-DFE is straightforward.

6.3.2 Frequency Domain Processing

By exploiting the structure of (6.2), a frequency domain processing can be applied to mitigate I/Q imbalance. The equivalent frequency domain data model with a white noise vector can be formulated as

$$\begin{bmatrix} \mathbf{W}\mathbf{r}_1 \\ \mathbf{W}\mathbf{J}\mathbf{r}_2^* \end{bmatrix} = \begin{bmatrix} \mathbf{\Lambda}_{u_1} & \mathbf{\Lambda}_{u_2} \\ \mathbf{\Lambda}_{u_2}^* & -\mathbf{\Lambda}_{u_1}^* \end{bmatrix} \begin{bmatrix} \mathbf{W}\mathbf{s}_1 \\ \mathbf{W}\mathbf{s}_2 \end{bmatrix} + \begin{bmatrix} \mathbf{\Lambda}_{v_1} & \mathbf{\Lambda}_{v_2} \\ \mathbf{\Lambda}_{v_2}^* & -\mathbf{\Lambda}_{v_1}^* \end{bmatrix} \begin{bmatrix} \mathbf{W}\mathbf{s}_1^* \\ \mathbf{W}\mathbf{s}_2^* \end{bmatrix} + \begin{bmatrix} \mathbf{W}\mathbf{n}_1 \\ \mathbf{W}\mathbf{J}\mathbf{n}_2^* \end{bmatrix}.$$

For a K-point DFT, it holds that

$$\mathcal{F}\{\mathbf{s}_i[k]\} = \bar{\mathbf{s}}_i[k], \quad \mathcal{F}\{\mathbf{s}_i^*[k]\} = \bar{\mathbf{s}}_i^*[k'], \quad k=0,\cdots,K-1,$$

where $\bar{\mathbf{s}}$ is DFT of $\mathbf{s}$, and $k' = (-k)_K$. Assume K is even, let $\bar{\mathbf{r}}_1 = \mathbf{W}\mathbf{r}_1$, $\underline{\bar{\mathbf{r}}}_2 = \mathbf{W}\mathbf{J}\mathbf{r}_2^*$, $\bar{\mathbf{n}}_1 = \mathbf{W}\mathbf{n}_1$, and $\underline{\bar{\mathbf{n}}}_2 = \mathbf{W}\mathbf{J}\mathbf{n}_2^*$. For $k = 0, K/2$, it can be obtained that

$$\underbrace{\begin{bmatrix} \bar{\mathbf{r}}_1[k] \\ \underline{\bar{\mathbf{r}}}_2[k] \end{bmatrix}}_{\mathbf{r}_a} = \underbrace{\begin{bmatrix} \lambda_{u_1}[k] & \lambda_{u_2}[k] \\ \lambda_{u_2}^*[k] & -\lambda_{u_1}^*[k] \end{bmatrix}}_{\mathbf{E}_u} \underbrace{\begin{bmatrix} \bar{\mathbf{s}}_1[k] \\ \bar{\mathbf{s}}_2[k] \end{bmatrix}}_{\mathbf{s}_a} + \underbrace{\begin{bmatrix} \lambda_{v_1}[k] & \lambda_{v_2}[k] \\ \lambda_{v_2}^*[k] & -\lambda_{v_1}^*[k] \end{bmatrix}}_{\mathbf{E}_v} \begin{bmatrix} \bar{\mathbf{s}}_1^*[k] \\ \bar{\mathbf{s}}_2^*[k] \end{bmatrix} + \underbrace{\begin{bmatrix} \bar{\mathbf{n}}_1[k] \\ \underline{\bar{\mathbf{n}}}_2[k] \end{bmatrix}}_{\mathbf{n}_a}, \tag{6.5}$$

where $\lambda_{u_m}[k]$ and $\lambda_{v_m}[k]$ are the k-th diagonal entries of $\mathbf{\Lambda}_{u_m}$ and $\mathbf{\Lambda}_{v_m}$, respectively. Reformulate (6.5) as

$$\underbrace{\begin{bmatrix}\Re\{\mathbf{r}_a\}\\ \Im\{\mathbf{r}_a\}\end{bmatrix}}_{\bar{\mathbf{r}}_a}=\underbrace{\begin{bmatrix}\Re\{\mathbf{E}_u+\mathbf{E}_v\} & \Im\{\mathbf{E}_v-\mathbf{E}_u\}\\ \Im\{\mathbf{E}_u+\mathbf{E}_v\} & \Re\{\mathbf{E}_u-\mathbf{E}_v\}\end{bmatrix}}_{\mathbf{H}_a}\underbrace{\begin{bmatrix}\Re\{\mathbf{s}_a\}\\ \Im\{\mathbf{s}_a\}\end{bmatrix}}_{\bar{\mathbf{s}}_a}+\begin{bmatrix}\Re\{\mathbf{n}_a\}\\ \Im\{\mathbf{n}_a\}\end{bmatrix},$$

then the least-squares (LS) estimate of $\bar{\mathbf{s}}_a$ can be obtained as

$$\hat{\bar{\mathbf{s}}}_a=(\mathbf{H}_a^T\mathbf{H}_a)^{-1}\mathbf{H}_a^T\bar{\mathbf{r}}_a.$$

For other values of k, it can be obtained that

$$\underbrace{\begin{bmatrix}\bar{\mathbf{r}}_1[k]\\ \bar{\mathbf{r}}_2[k]\\ \bar{\mathbf{r}}_1^*[k']\\ \bar{\mathbf{r}}_2^*[k']\end{bmatrix}}_{\bar{\mathbf{r}}_b}=\underbrace{\begin{bmatrix}\lambda_{u_1}[k] & \lambda_{u_2}[k] & \lambda_{v_1}[k] & \lambda_{v_2}[k]\\ \lambda_{u_2}^*[k] & -\lambda_{u_1}^*[k] & \lambda_{v_2}^*[k] & -\lambda_{v_1}^*[k]\\ \lambda_{v_1}^*[k'] & \lambda_{v_2}^*[k'] & \lambda_{u_1}^*[k'] & \lambda_{u_2}^*[k']\\ \lambda_{v_2}[k'] & -\lambda_{v_1}[k'] & \lambda_{u_2}[k'] & -\lambda_{u_1}[k']\end{bmatrix}}_{\mathbf{H}_b}\underbrace{\begin{bmatrix}\bar{\mathbf{s}}_1[k]\\ \bar{\mathbf{s}}_2[k]\\ \bar{\mathbf{s}}_1^*[k']\\ \bar{\mathbf{s}}_2^*[k']\end{bmatrix}}_{\bar{\mathbf{s}}_b}+\begin{bmatrix}\bar{\mathbf{n}}_1[k]\\ \bar{\mathbf{n}}_2[k]\\ \bar{\mathbf{n}}_1^*[k']\\ \bar{\mathbf{n}}_2^*[k']\end{bmatrix}.$$

Then the LS estimate of $\bar{\mathbf{s}}_b$ can be obtained as

$$\hat{\bar{\mathbf{s}}}_b=(\mathbf{H}_b^H\mathbf{H}_b)^{-1}\mathbf{H}_b^H\bar{\mathbf{r}}_b.$$

It shows that $(K/2+1)$ inversions of a 4×4 matrix is needed in the frequency domain to obtain the LS estimate. In addition, due to the special structure of the matrix $\mathbf{H}_a$ and $\mathbf{H}_b$, by using the matrix inversion formula, all the sub-matrices to be inverted to obtain $(\mathbf{H}_a^T\mathbf{H}_a)^{-1}$ and $(\mathbf{H}_b^H\mathbf{H}_b)^{-1}$ are diagonal [48], reducing the computational complexity further.

The LS estimate of $\bar{\mathbf{s}}_i$, which is denoted as $\hat{\bar{\mathbf{s}}}_i$, can be obtained by stacking the elements of $\hat{\bar{\mathbf{s}}}_a$ and $\hat{\bar{\mathbf{s}}}_b$ correspondingly. Then LS estimate of $\mathbf{s}_i$ can be obtained from

$$\hat{\mathbf{s}}_{i,LS}=\mathbf{W}^H\hat{\bar{\mathbf{s}}}_i. \tag{6.6}$$

6.3.3 Estimation of Channel and I/Q Imbalance

Since only the effective channel state information (ECSI) such as $\mathbf{u}_i$ and $\mathbf{v}_i$ are needed in the proposed solutions, the tasks of separately estimating the channel parameters $\mathbf{h}_i$ as well as the I/Q imbalance parameters $\{\alpha_T, \beta_T, \alpha_R, \beta_R\}$ can be combined [74].

During the training period, according to (6.1) (6.2), it can be obtained

$$\underbrace{\begin{bmatrix} \mathbf{r}_{t,1} \\ \mathbf{r}_{t,2} \end{bmatrix}}_{\mathbf{r}_t} = \underbrace{\begin{bmatrix} \mathbf{S}_{t,1} & \mathbf{S}_{t,2} & \mathbf{S}_{t,1}^* & \mathbf{S}_{t,2}^* \\ -\mathbf{S}_{t,2}^* & \mathbf{S}_{t,1}^* & -\mathbf{S}_{t,2} & \mathbf{S}_{t,1} \end{bmatrix}}_{\mathbf{S}_t} \underbrace{\begin{bmatrix} \mathbf{u}_1 \\ \mathbf{u}_2 \\ \mathbf{v}_1 \\ \mathbf{v}_2 \end{bmatrix}}_{\boldsymbol{\theta}} + \begin{bmatrix} \mathbf{n}_{t,1} \\ \mathbf{n}_{t,2} \end{bmatrix}, \tag{6.7}$$

where the $N_t \times (L+1)$ matrix $\mathbf{S}_{t,i}$ is the first $L+1$ columns of a $N_t \times N_t$ circulant matrix $\text{circ}(\mathbf{s}_{t,i})$, with $\mathbf{s}_{t,i}$ being the $N_t \times 1$ training data vector sending from the i^{th} antenna. Consequently, the estimated ECSI can be obtained as

$$\hat{\boldsymbol{\theta}} = (\mathbf{S}_t^H \mathbf{S}_t)^{-1} \mathbf{S}_t^H \mathbf{r}_t. \tag{6.8}$$

To study the performance degradation caused by I/Q imbalance without compensation, only $\mathbf{u}_i$ is estimated, then $\boldsymbol{\theta}$ and $\mathbf{S}_t$ in (6.7) become

$$\tilde{\boldsymbol{\theta}} = \begin{bmatrix} \mathbf{u}_1 \\ \mathbf{u}_2 \end{bmatrix}, \qquad \tilde{\mathbf{S}}_t = \begin{bmatrix} \mathbf{S}_{t,1} & \mathbf{S}_{t,2} \\ -\mathbf{S}_{t,2}^* & \mathbf{S}_{t,1}^* \end{bmatrix}.$$

Once $\hat{\tilde{\boldsymbol{\theta}}}$ is available, the conventional detection for TR-OSTBC systems is performed.

6.4 Simulation Results

In the simulations, L-order channels with $\mathbf{h}_i \sim \mathcal{CN}(\mathbf{0}, \mathbf{I}_{L+1})$ and the data block length $K = 20$ with the length of CP $L = 2$ are used. In addition, SNR $\triangleq \sigma_s^2/\sigma_n^2$, and the power loss due to CP is neglected due to the fact $K + L \gg L$.

As shown in Fig. 6.4~Fig. 6.6, I/Q imbalance causes dramatic performance degradation without the compensation, and the receiver I/Q imbalance causes more performance degradation than the transmitter I/Q imbalance in such a system. In addition, as our analysis on the equivalent time and frequency domain model shows that the frequency domain LS (FD-LS) method provides the same performance as the time domain ZF method. The LMMSE method improves the performance compared to the above two. Moreover, further performance improvement can be achieved by introducing nonlinear processings such as ZF-DFE and MMSE-DFE, compared to their linear counterparts. Furthermore, the proposed solutions with estimated ECSI can mitigate I/Q imbalance as well, as shown in Fig. 6.7.

6.5 Conclusions

In this work, the solutions to the symbol detection, both in the time domain and in the frequency domain, for TR-STBC systems with I/Q imbalance over frequency-selective fading channels, are developed. Results demonstrate the effectiveness of the proposed approaches in mitigating I/Q imbalance and improving the SER performance.

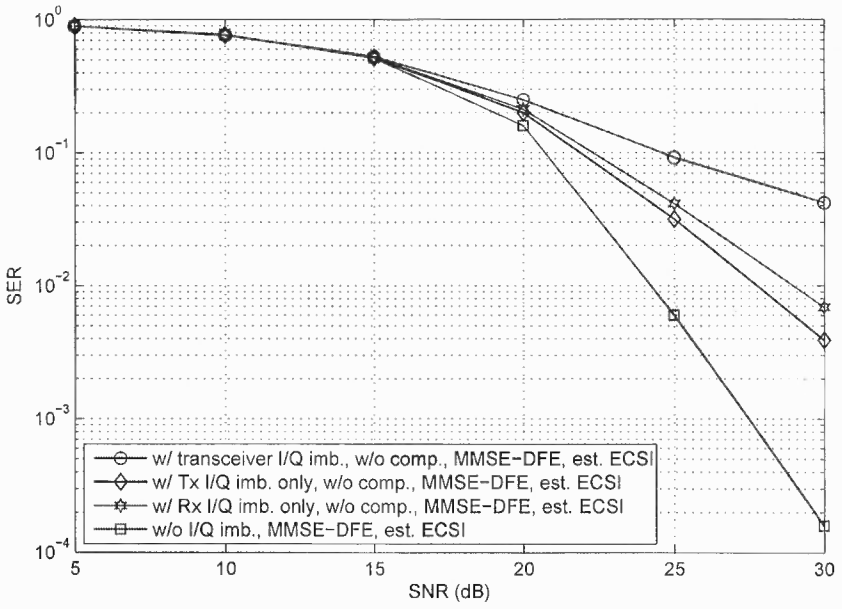

Figure 6.4 SER versus SNR of a 2×1 TR-OSTBC system with I/Q imbalance. System parameters are: $\epsilon_T = 5\%$, $\varphi_T = 5°$, $\epsilon_R = 5\%$, $\varphi_R = 5°$, $K = 20$, $L = 2$, and $N_t = 20$. A 64-QAM constellation is used. The number of independent trials is 10^5.

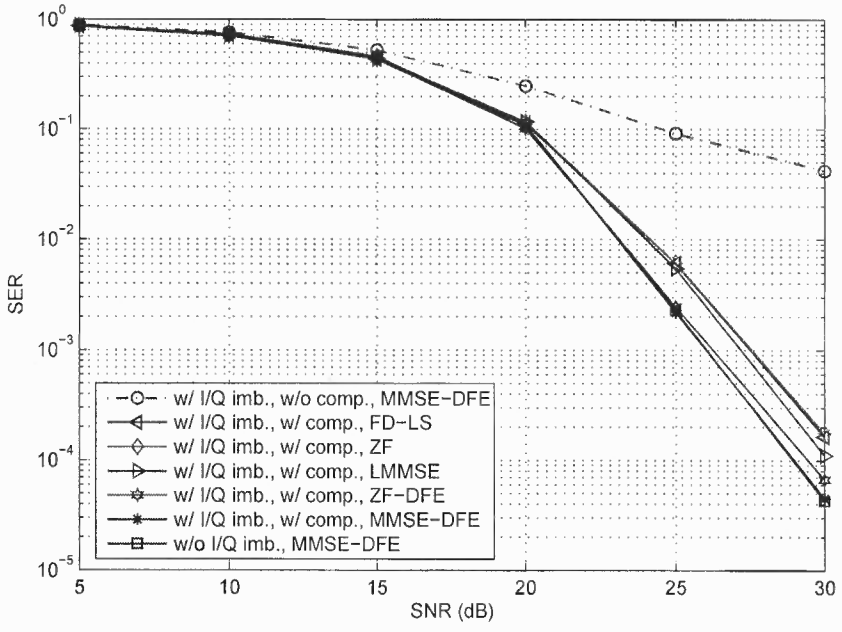

Figure 6.5 SER versus SNR of a 2×1 TR-OSTBC system with I/Q imbalance. System parameters are: $\epsilon_T = 5\%$, $\varphi_T = 5°$, $\epsilon_R = 5\%$, $\varphi_R = 5°$, $K = 20$, and $L = 2$. A 64-QAM constellation is used. The number of independent trials is 10^5.

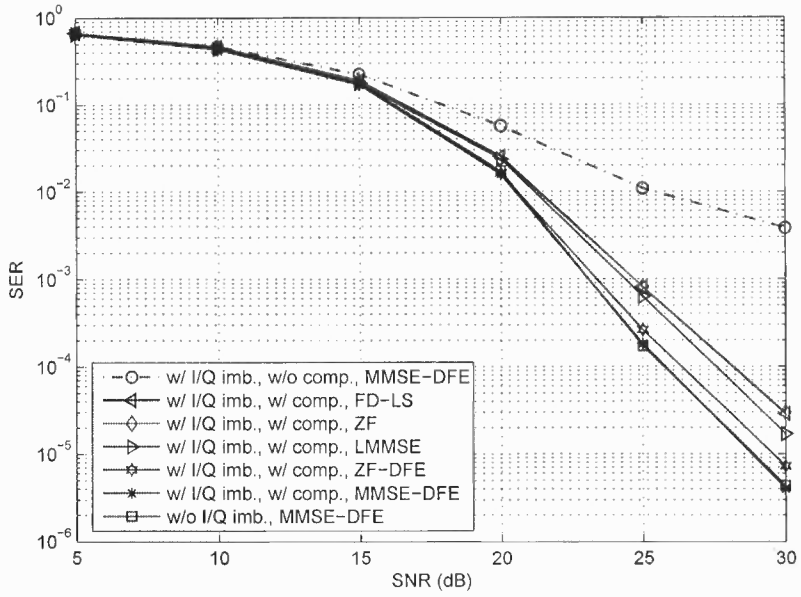

Figure 6.6 SER versus SNR of a 2×1 TR-OSTBC system with I/Q imbalance. System parameters are: $\epsilon_T = 5\%$, $\varphi_T = 5°$, $\epsilon_R = 5\%$, $\varphi_R = 5°$, $K = 20$, and $L = 2$. A 16-PSK constellation is used. The number of independent trials is 10^5.

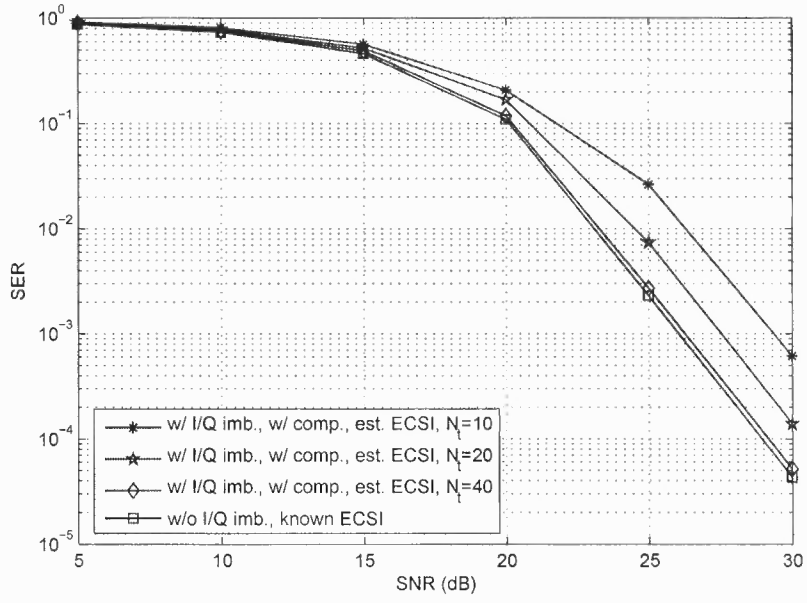

Figure 6.7 SER versus SNR of a 2×1 TR-OSTBC system with I/Q imbalance. System parameters are: $\epsilon_T = 5\%$, $\varphi_T = 5°$, $\epsilon_R = 5\%$, $\varphi_R = 5°$, $K = 20$, $L = 2$, and $N_t = \{10, 20, 40\}$. A 64-QAM constellation is used, and MMSE-DFE is performed. The number of independent trials is 10^5.

APPENDIX A

DERIVATION OF TRANSCEIVER I/Q IMBALANCE MODEL IN TIME DOMAIN

A.1 Derivation of Transmitter I/Q Imbalance Model in Time Domain

Assume the baseband signal intended to be transmitted is

$$s(t) = s_I(t) + js_Q(t).$$

In the absence of the transmitter I/Q imbalance, $\epsilon_T = 0$ and $\varphi_T = 0$, then the up-converted passband signal is

$$\Re\{\sqrt{2}s(t)c_T(t)\} = \Re\{\sqrt{2}s(t)e^{j\omega_c t}\}.$$

However, in the presence of the transmitter I/Q imbalance, $c_T(t)$ becomes

$$c_T(t) = \alpha_T e^{j\omega_c t} + \beta_T^* e^{-j\omega_c t},$$

therefore, the up-converted passband signal becomes

$$\Re\{\sqrt{2}s(t)(\alpha_T e^{j\omega_c t} + \beta_T^* e^{-j\omega_c t})\} = \Re\{\sqrt{2}\alpha_T s(t)e^{j\omega_c t}\} + \Re\{\sqrt{2}[\beta_T s^*(t)e^{j\omega_c t}]^*\}.$$

Since $\Re\{(\cdot)^*\} = \Re\{(\cdot)\}$, it can be obtained that

$$\begin{aligned}\Re\{\sqrt{2}s(t)(\alpha_T e^{j\omega_c t} + \beta_T^* e^{-j\omega_c t})\} &= \Re\{\sqrt{2}[\alpha_T s(t) + \beta_T s^*(t)]e^{j\omega_c t}\} \\ &= \Re\{\sqrt{2}s_T(t)e^{j\omega_c t}\},\end{aligned}$$

with the equivalent baseband signal in the presence of the transmitter I/Q imbalance being

$$s_T(t) = \alpha_T s(t) + \beta_T s^*(t).$$

A.2 Derivation of Receiver I/Q Imbalance Model in Time Domain

At the receiver side, in the absence of the receiver I/Q imbalance, the down-converted signal $\Re\{\sqrt{2}s(t)e^{j\omega_c t}\}\sqrt{2}c_R(t)$ is

$$\begin{aligned}\Re\{\sqrt{2}s(t)e^{j\omega_c t}\}\sqrt{2}e^{-j\omega_c t} &= 2[s_I(t)\cos^2\omega_c t + js_Q(t)\sin^2\omega_c t - js^*(t)\cos\omega_c t\sin\omega_c t] \\ &= s(t) + \underbrace{\{s^*(t)\cos 2\omega_c t - js^*(t)]\sin 2\omega_c t\}}_{\text{high frequency part}}.\end{aligned}$$

After the lowpass filter (LPF), the high frequency part is removed, hence the transmitted signal $s(t)$ can be obtained.

However, in the presence of the receiver I/Q imbalance, the down-converted signal becomes

$$2\Re\{s(t)e^{j\omega_c t}\}[\alpha_R^* e^{-j\omega_c t} + \beta_R e^{j\omega_c t}] = 2[\underbrace{\alpha_R^*\Re\{s(t)e^{j\omega_c t}\}e^{-j\omega_c t}}_{\text{first part}} + \underbrace{\beta_R\Re\{s(t)e^{j\omega_c t}\}e^{j\omega_c t}}_{\text{second part}}].$$

Based on the above derivation, it is straightforward to show that the down-converted signal of the first part is $\alpha_R^* s(t)$. With regard to the second part, since

$$\begin{aligned}2\beta_R\Re\{s(t)e^{j\omega_c t}\}e^{j\omega_c t} &= 2\beta_R\{s_I(t)\cos^2\omega_c t - js_Q(t)\sin^2\omega_c t + js^*(t)\cos\omega_c t\sin\omega_c t]\} \\ &= \beta_R\big\{s^*(t) + \underbrace{\{s(t)\cos 2\omega_c t + js(t)\sin 2\omega_c t\}}_{\text{high frequency part}}\big\},\end{aligned}$$

the corresponding down-converted signal is $\beta_R s^*(t)$.

Consequently, combine the above results, due to the receiver I/Q imbalance, the equivalent baseband signal can be expressed as

$$s_R(t) = \alpha_R^* s(t) + \beta_R s^*(t).$$

APPENDIX B

DERIVATION OF TRANSCEIVER I/Q IMBALANCE MODEL IN FREQUENCY DOMAIN

B.1 Derivation of Transmitter I/Q Imbalance Model in Frequency Domain

Let $\mathbf{s}_T = \begin{bmatrix} s_T[0] & s_T[1] & \cdots & s_T[K-1] \end{bmatrix}^T$ and $\mathbf{s} = \begin{bmatrix} s[0] & s[1] & \cdots & s[K-1] \end{bmatrix}^T$ denote the discrete data vectors of the equivalent baseband signal and the intended signal, respectively. Take the Discrete Fourier Transform (DFT) to equation (2.2), it can be obtained

$$\mathcal{F}\{\mathbf{s}_T\} = \alpha_T \mathcal{F}\{\mathbf{s}\} + \beta_T \mathcal{F}\{\mathbf{s}^*\},$$

where $\mathcal{F}\{\cdot\}$ denotes the K-point DFT operation.

Let $\vec{S}_T = \begin{bmatrix} S_T[0] & S_T[1] & \cdots & S_T[K-1] \end{bmatrix}^T$ and $\vec{S} = \begin{bmatrix} S[0] & S[1] & \cdots & S[K-1] \end{bmatrix}^T$ denote the data vectors of $\mathbf{s}_T$ and $\mathbf{s}$ in the frequency domain after the K-point DFT, respectively, since DFT of the complex conjugate of a sequence is related to DFT of the original sequence through a mirrored relation [85], i.e.,

$$S[k] = \mathcal{F}\{s[n]\}, \quad S^*[(-k)_K] = \mathcal{F}\{s^*[n]\} \qquad 0 \le n \le K-1, 0 \le k \le K-1. \quad \text{(B.1)}$$

Consequently, it can be obtained that

$$S_T[k] = \alpha_T S[k] + \beta_T S^*[k'],$$

where $k' = (-k)_K$.

B.2 Derivation of Receiver I/Q Imbalance Model in Frequency Domain

Let $\mathbf{r} = \begin{bmatrix} r[0] & r[1] & \cdots & r[K-1] \end{bmatrix}^T$ and $\mathbf{n} = \begin{bmatrix} n[0] & n[1] & \cdots & n[K-1] \end{bmatrix}^T$ denote the received data vector and the additive noise vector. After the removal of CP at the

receiver side, according to equation (2.4), it can be obtained

$$\mathbf{r} = \alpha_R^* \mathbf{H}\mathbf{s}_T + \beta_T \mathbf{H}^* \mathbf{s}_T^* + \mathbf{n},$$

where the $K \times K$ matrix $\mathbf{H}$ is circulant. Let $\mathbf{h} = \begin{bmatrix} h[0] & h[1] & \cdots & h[L] \end{bmatrix}^T$ denote the channel vector, and $\tilde{\mathbf{h}} = \begin{bmatrix} \mathbf{h}^T & \mathbf{0}_{K-L+1}^T \end{bmatrix}^T$ denote the zero-padded channel, then $\mathbf{H}$ can be diagonalized by the unitary DFT matrix $\mathbf{W}$ as $\mathbf{H} = \mathbf{W}^H \mathbf{\Lambda}_{\tilde{h}} \mathbf{W}$, with $\mathbf{\Lambda}_{\tilde{h}} = \text{diag}\{\mathbf{W}\tilde{\mathbf{h}}\}$. Since $\mathbf{W}\mathbf{W}^H = \mathbf{I}_K$, then

$$\mathbf{W}\mathbf{r} = \alpha_R^* \text{diag}\{\mathbf{W}\tilde{\mathbf{h}}\}\mathbf{W}\mathbf{s}_T + \beta_T \text{diag}\{\mathbf{W}\tilde{\mathbf{h}}^*\}\mathbf{W}\mathbf{s}_T^* + \mathbf{W}\mathbf{n}.$$

Let

$$\begin{aligned}
\mathbf{W}\mathbf{r} &= \begin{bmatrix} R[0] & R[1] & \cdots & R[K-1] \end{bmatrix}^T, \\
\mathbf{W}\tilde{\mathbf{h}} &= \begin{bmatrix} H[0] & H[1] & \cdots & H[K-1] \end{bmatrix}^T, \\
\mathbf{W}\mathbf{s}_T &= \begin{bmatrix} S_T[0] & S_T[1] & \cdots & S_T[K-1] \end{bmatrix}^T, \\
\mathbf{W}\mathbf{n} &= \begin{bmatrix} N[0] & N[1] & \cdots & N[K-1] \end{bmatrix}^T.
\end{aligned}$$

Using the property given in (B.1), it is not difficult to show that

$$R[k] = \alpha_R^* H[k] S_T[k] + \beta_R H^*[k'] S_T^*[k'] + N[k], \qquad 0 \le k \le K-1, 0 \le k' \le K-1.$$

APPENDIX C

DERIVATION OF THE DIVERSITY AND CODING GAIN WITH SUBCARRIER GROUPING

C.1 Derivation of the Diversity and Coding Gain for $L = 1$

Since $\tilde{\mathbf{S}}[k]$ and $\tilde{\mathbf{S}}'[k]$ are orthogonal matrices, $\mathbf{\Delta}[k]$ is an orthogonal matrices as well, it is straightforward to show that

$$\mathbf{\Delta}[k]\mathbf{\Delta}^H[k] = d[k]\mathbf{I}_2,$$

with $d[k] := \|\tilde{S}_1[k] - \tilde{S}'_1[k]\|^2 + \|\tilde{S}_2[k] - \tilde{S}'_2[k]\|^2$. Hence,

$$\mathbf{\Delta}_e = \sum_{i=1}^{2} d[k_i]\mathbf{\Omega}[k_i]\mathbf{\Omega}^H[k_i].$$

It is easy to show that

$$\mathbf{\Omega}[k]\mathbf{\Omega}^H[k] = \mathbf{I}_2 \otimes \begin{bmatrix} 1 & e^{j\frac{2\pi k}{K}} \\ e^{-j\frac{2\pi k}{K}} & 1 \end{bmatrix}.$$

With the optimal subcarrier grouping, i.e., $k_2 = K/2 + k_1$, $e^{j\frac{2\pi k_2}{K}} = -e^{j\frac{2\pi k_1}{K}}$, then

$$\mathbf{\Delta}_e = \mathbf{I}_2 \otimes \begin{bmatrix} d[k_1] + d[k_2] & e^{j\frac{2\pi k_1}{K}}(d[k_1] - d[k_2]) \\ e^{-j\frac{2\pi k_1}{K}}(d[k_1] - d[k_2]) & d[k_1] + d[k_2] \end{bmatrix}.$$

The determinant of $\mathbf{\Delta}_e$ can be obtained as

$$\begin{aligned} \det(\mathbf{\Delta}_e) &= \left((d[k_1] + d[k_2])^2 - (d[k_1] - d[k_2]^2)\right)^2 \\ &= (4d[k_1]d[k_2])^2. \end{aligned}$$

With the proposed subcarrier grouping, i.e., $k_2 = (-k_1)_K = K - k_1$, $e^{j\frac{2\pi k_2}{K}} = e^{-j\frac{2\pi k_1}{K}}$, then

$$\mathbf{\Delta}_e = \mathbf{I}_2 \otimes \begin{bmatrix} d[k_1] + d[k_2] & e^{j\frac{2\pi k_1}{K}} d[k_1] + e^{-j\frac{2\pi k_1}{K}} d[k_2] \\ e^{-j\frac{2\pi k_1}{K}} d[k_1] + e^{j\frac{2\pi k_1}{K}} d[k_2] & d[k_1] + d[k_2] \end{bmatrix}.$$

Let $\theta = e^{j\frac{2\pi k_1}{K}}$ $(k_1 = 1, \cdots, K/2 - 1)$, then the determinant of $\mathbf{\Delta}_e$ can be obtained as

$$\begin{aligned} \det(\mathbf{\Delta}_e) &= \left((d[k_1] + d[k_2])^2 - (d[k_1])^2 - (d[k_2])^2 - (e^{j2\theta} + e^{-j2\theta}) d[k_1] d[k_2]\right)^2 \\ &= \left(4d[k_1]d[k_2]\left(\frac{1 - \cos(2\theta)}{2}\right)\right)^2. \end{aligned}$$

Note the special pair $\{k_1 = 0, k_2 = K/2\}$ is also the optimal grouping pair, and $\det(\mathbf{\Delta}_e) = (4d[k_1]d[k_2])^2$. Consequently, with the proposed grouping, the determinant of $\mathbf{\Delta}_e$ can be generalized as

$$\det(\mathbf{\Lambda}_e) = \begin{cases} (4d[k_1]d[k_2])^2 & k_1 = 0, k_2 = \frac{K}{2}, \\ \left(4d[k_1]d[k_2]\left(\frac{1-\cos(2\theta)}{2}\right)\right)^2 & \text{others}, \end{cases}$$

C.2 Derivation of the Diversity and Coding Gain for $L = 3$

When $L = 3$, define

$$\begin{gathered} \mathbf{\Delta}[k] := \tilde{\mathbf{S}}[k] - \tilde{\mathbf{S}}'[k] \in \mathbb{C}^{2\times 2}, \\ \mathbf{\Omega}[k] := \mathbf{I}_2 \otimes [1 \;\; e^{-j2k\pi/K} \;\; e^{-j4k\pi/K} \;\; e^{-j6k\pi/K}]^T \in \mathbb{C}^{8\times 2}, \\ \mathbf{\Lambda}_e := \textstyle\sum_{k\in\{k_1,k_2,k_3,k_4\}} \mathbf{\Omega}[k]\mathbf{\Delta}[k]\mathbf{\Delta}^H[k]\mathbf{\Omega}^H[k] \in \mathbb{C}^{8\times 8}, \\ \tilde{\mathbf{\Lambda}}_e := \mathbf{B}_h^T \mathbf{\Lambda}_e \mathbf{B}_h^* \in \mathbb{C}^{8\times 8}. \end{gathered}$$

Since $\mathbf{\Delta}[k_i]\mathbf{\Delta}^H[k_i] = d[k_i]\mathbf{I}_2$, hence

$$\mathbf{\Delta}_e = \sum_{i=1}^{4} d[k_i]\mathbf{\Omega}[k_i]\mathbf{\Omega}^H[k_i], \tag{C.1}$$

and

$$\mathbf{\Omega}[k_i]\mathbf{\Omega}^H[k_i] = \mathbf{I}_2 \otimes \begin{bmatrix} 1 & e^{-j\frac{2\pi k_i}{k}} & e^{-j\frac{4\pi k_i}{k}} & e^{-j\frac{6\pi k_i}{k}} \\ e^{j\frac{2\pi k_i}{k}} & 1 & e^{-j\frac{2\pi k_i}{k}} & e^{-j\frac{4\pi k_i}{k}} \\ e^{j\frac{4\pi k_i}{k}} & e^{j\frac{2\pi k_i}{k}} & 1 & e^{-j\frac{2\pi k_i}{k}} \\ e^{j\frac{6\pi k_i}{k}} & e^{j\frac{4\pi k_i}{k}} & e^{j\frac{2\pi k_i}{k}} & 1 \end{bmatrix}. \tag{C.2}$$

With the optimal subcarrier grouping, for any group $\{k_i\}_{i=1}^4$ ($k_i = (i-1)K/4 + k_1$), according to (C.2), it can be obtained that

$$\begin{aligned} \mathbf{\Delta}_e &= \sum_{i=1}^{4} d[k_i]\mathbf{\Omega}[k_i]\mathbf{\Omega}^H[k_i] \\ &= \Big(\prod_{i=1}^{4} 4d[k_i]\Big)^2. \end{aligned}$$

With the proposed subcarrier grouping, i.e., the subcarriers $\{k, k+K/4, -k+3K/4, -k+K\}$ ($k = 1, \cdots, K/4$) are selected and grouped, according to (C.1) and (C.2), it can be obtained

$$\det(\mathbf{\Lambda}_e) = \Big((\prod_{i=1}^{4} 4d[k_i])(\frac{1-e^{-j4\theta}}{2})^2(\frac{e^{j2\theta}+j}{2})^4\Big)^2.$$

The result of the special group $\{0, K/4, K/2, 3K/4\}$ is the same as the optimal grouping. Consequently, the determinant with the proposed grouping can be generalized as

$$\det(\mathbf{\Lambda}_e) = \begin{cases} \big(\prod_{i=1}^{4} 4d[k_i]\big)^2, & k_i \in \{0, \frac{K}{4}, \frac{K}{2}, \frac{3K}{4}\} \\ \Big((\prod_{i=1}^{4} 4d[k_i])(\frac{1-e^{-j4\theta}}{2})^2(\frac{e^{j2\theta}+j}{2})^4\Big)^2, & \text{others} \end{cases}$$

where $\theta := 2\pi k_1/K$ ($k_1 = 1, \cdots, K/4-1$).

APPENDIX D

DERIVATION OF THE LMMSE FILTER FOR TR-OSTBC SYSTEM WITH I/Q IMBALANCE

The linear filter $\mathbf{F}_{\text{LMMSE}}$ is the solution of the equation

$$E\{\frac{\partial\|\tilde{\mathbf{s}}-\mathbf{F}\tilde{\mathbf{r}}\|^2}{\partial\mathbf{F}}\}=0.$$

Since

$$\begin{aligned}\|\tilde{\mathbf{s}}-\mathbf{F}\tilde{\mathbf{r}}\|^2 &= (\tilde{\mathbf{s}}^T-\tilde{\mathbf{r}}^T\mathbf{F})(\tilde{\mathbf{s}}-\mathbf{F}\tilde{\mathbf{r}})\\ &= \tilde{\mathbf{s}}^T\tilde{\mathbf{s}}-\tilde{\mathbf{s}}^T\mathbf{F}\tilde{\mathbf{r}}-\tilde{\mathbf{r}}^T\mathbf{F}^T\tilde{\mathbf{s}}+\tilde{\mathbf{r}}^T\mathbf{F}^T\mathbf{F}\tilde{\mathbf{r}},\end{aligned}$$

according to [86], it can be obtained

$$\begin{aligned}\frac{\partial(\tilde{\mathbf{s}}^T\mathbf{F}\tilde{\mathbf{r}})}{\partial\mathbf{F}} &= \tilde{\mathbf{s}}\tilde{\mathbf{r}}^T,\\ \frac{\partial(\tilde{\mathbf{r}}^T\mathbf{F}^T\tilde{\mathbf{s}})}{\partial\mathbf{F}} &= \tilde{\mathbf{s}}\tilde{\mathbf{r}}^T,\\ \frac{\partial(\tilde{\mathbf{r}}^T\mathbf{F}^T\mathbf{F}\tilde{\mathbf{r}})}{\partial\mathbf{F}} &= 2\mathbf{F}\tilde{\mathbf{r}}\tilde{\mathbf{r}}^T,\end{aligned}$$

hence $E\{\tilde{\mathbf{s}}\tilde{\mathbf{r}}^T\}=\mathbf{F}E\{\tilde{\mathbf{r}}\tilde{\mathbf{r}}^T\}$. Recall that $\tilde{\mathbf{r}}=\mathbf{H}\tilde{\mathbf{s}}+\tilde{\mathbf{n}}$, then

$$E\{\tilde{\mathbf{s}}\tilde{\mathbf{s}}^T\}\mathbf{H}^T+E\{\tilde{\mathbf{s}}\tilde{\mathbf{n}}^T\}=\mathbf{F}\mathbf{H}(E\{\tilde{\mathbf{s}}\tilde{\mathbf{s}}^T\}\mathbf{H}^T+\mathbf{H}E\{\tilde{\mathbf{s}}\tilde{\mathbf{n}}^T\}+E\{\tilde{\mathbf{n}}\tilde{\mathbf{s}}^T\mathbf{H}\}+E\{\tilde{\mathbf{n}}\tilde{\mathbf{n}}^T\})$$

Since $\tilde{\mathbf{s}}\sim\mathcal{N}(\mathbf{0},\frac{\sigma_s^2}{2}\mathbf{I}_{4K})$ and $\tilde{\mathbf{n}}\sim\mathcal{N}(\mathbf{0},\frac{\sigma_n^2}{2}\mathbf{I}_{4K})$ are independent, then $E\{\tilde{\mathbf{s}}\tilde{\mathbf{s}}^T\}=\frac{\sigma_s}{2}\mathbf{I}_{4K}$, $E\{\tilde{\mathbf{s}}\tilde{\mathbf{n}}^T\}=E\{\tilde{\mathbf{n}}\tilde{\mathbf{s}}^T\}=0$, $E\{\tilde{\mathbf{n}}\tilde{\mathbf{n}}^T\}=\frac{\sigma_n}{2}\mathbf{I}_{4K}$. Consequently, the linear filter can be obtained

$$\mathbf{F}_{\text{LMMSE}}=\mathbf{H}^T(\mathbf{H}\mathbf{H}^T+\sigma_n^2/\sigma_s^2\mathbf{I}_{4K})^{-1}.$$

APPENDIX E

DERIVATION OF THE MMSE-DFE FILTER FOR TR-OSTBC SYSTEM WITH I/Q IMBALANCE

Define $\mathbf{e} := \tilde{\mathbf{s}}' - \tilde{\mathbf{s}}$, where $\tilde{\mathbf{s}}'$ is the output of the equalizer before the slicer, as shown in Fig. 6.3. Assume the past decisions are correct, i.e., $\hat{\tilde{\mathbf{s}}} = \tilde{\mathbf{s}}$, then

$$\mathbf{e} = \mathbf{F}_f \tilde{\mathbf{r}} - (\mathbf{F}_b + \mathbf{I}_{4K})\tilde{\mathbf{s}}. \tag{E.1}$$

The feedforward filter $\mathbf{F}_f$ should be chosen to minimize $E\{\|\mathbf{e}\|^2\}$. In addition, the feedback filter $\mathbf{F}_b$ should be strict upper-triangular so the successive cancelation can be carried out.

By fixing the feedback filter $\mathbf{F}_b$ first, following the similar derivation in Appendix E, it can be obtained that

$$\mathbf{F}_f E\{\tilde{\mathbf{r}}\tilde{\mathbf{r}}^T\} = (\mathbf{F}_b + \mathbf{I}_{4K})E\{\tilde{\mathbf{s}}\tilde{\mathbf{r}}^T\}. \tag{E.2}$$

Note the result can also be obtained using the orthogonal principle, i.e., $E\{\mathbf{e}\tilde{\mathbf{r}}^T\} = \mathbf{0}_{4K}$ [87] [88].

Using the property that $\tilde{\mathbf{s}} \sim \mathcal{N}(\mathbf{0}, \frac{\sigma_s^2}{2}\mathbf{I}_{4K})$ and $\tilde{\mathbf{n}} \sim \mathcal{N}(\mathbf{0}, \frac{\sigma_n^2}{2}\mathbf{I}_{4K})$ are independent, i.e., $E\{\tilde{\mathbf{s}}\tilde{\mathbf{s}}^T\} = \frac{\sigma_s}{2}\mathbf{I}_{4K}$, $E\{\tilde{\mathbf{s}}\tilde{\mathbf{n}}^T\} = E\{\tilde{\mathbf{n}}\tilde{\mathbf{s}}^T\} = 0$, and $E\{\tilde{\mathbf{n}}\tilde{\mathbf{n}}^T\} = \frac{\sigma_n}{2}\mathbf{I}_{4K}$, the feedforward filter $\mathbf{F}_f$ can be obtained as

$$\begin{aligned} \mathbf{F}_f &= (\mathbf{F}_b + \mathbf{I}_{4K})\mathbf{H}^T(\mathbf{H}\mathbf{H}^T + \sigma_n^2/\sigma_s^2\mathbf{I}_{4K})^{-1} \\ &= (\mathbf{F}_b + \mathbf{I}_{4K})\mathbf{F}_{\text{LMMSE}}. \end{aligned}$$

To implement the symbol-by-symbol detection in the optimal sense, the error signal at the input of the slicer should be uncorrelated, i.e., $E\{\mathbf{e}\mathbf{e}^T\}$ should be a diagonal matrix.

Define

$$\begin{aligned}
\mathbf{R}_{ee} : &= E\{\mathbf{e}\mathbf{e}^T\}, \\
\mathbf{R}_{rr} : &= E\{\tilde{\mathbf{r}}\tilde{\mathbf{r}}^T\}, \\
\mathbf{R}_{ss} : &= E\{\tilde{\mathbf{s}}\tilde{\mathbf{s}}^T\}, \\
\mathbf{R}_{sr} : &= E\{\tilde{\mathbf{s}}\tilde{\mathbf{r}}^T\}, \\
\mathbf{R}_{rs} : &= E\{\tilde{\mathbf{r}}\tilde{\mathbf{s}}^T\}, \\
\mathbf{R}_{nn} : &= E\{\tilde{\mathbf{n}}\tilde{\mathbf{n}}^T\}.
\end{aligned}$$

Since $\mathbf{R}_{sr} = \frac{\sigma_n^2}{2}\mathbf{H}^T$, $\mathbf{R}_{rs} = \frac{\sigma_n^2}{2}\mathbf{H}$, hence $\mathbf{R}_{sr} = \mathbf{R}_{rs}^T$. From (E.1) (E.2) it can be obtained that

$$\mathbf{e} = (\mathbf{F}_b + \mathbf{I}_{4K})(\mathbf{R}_{sr}\mathbf{R}_{rr}^{-1}\tilde{\mathbf{r}} - \tilde{\mathbf{s}}).$$

Define $\varepsilon := \mathbf{R}_{sr}\mathbf{R}_{rr}^{-1}\tilde{\mathbf{r}} - \tilde{\mathbf{s}}$, $\mathbf{R}_{\varepsilon\varepsilon} := E\{\varepsilon\varepsilon^T\}$, then

$$\begin{aligned}
\mathbf{R}_{\varepsilon\varepsilon} &= E\{(\mathbf{R}_{sr}\mathbf{R}_{rr}^{-1}\tilde{\mathbf{r}} - \tilde{\mathbf{s}})(\mathbf{R}_{sr}\mathbf{R}_{rr}^{-1}\tilde{\mathbf{r}} - \tilde{\mathbf{s}})^T\} \\
&= \mathbf{R}_{ss} - \mathbf{R}_{sr}\mathbf{R}_{rr}^{-1}\mathbf{R}_{rs} \\
&= \mathbf{R}_{ss} - \mathbf{R}_{ss}\mathbf{H}^T(\mathbf{R}_{nn} + \mathbf{H}\mathbf{R}_{ss}\mathbf{H}^T)^{-1}\mathbf{H}\mathbf{R}_{ss}.
\end{aligned}$$

Using the matrix inversion lemma as follows

$$(\mathbb{A} - \mathbb{C}\mathbb{B}^{-1}\mathbb{D})^{-1} = \mathbb{A}^{-1} + \mathbb{A}^{-1}\mathbb{C}(\mathbb{B} - \mathbb{D}\mathbb{A}^{-1}\mathbb{C})^{-1}\mathbb{D}\mathbb{A}^{-1},$$

Let $\mathbb{A} = \mathbf{R}_{ss}^{-1}$, $\mathbb{B} = \mathbf{R}_{nn}$, $\mathbb{C} = -\mathbf{H}^T$, and $\mathbb{D} = \mathbf{H}$, then

$$\mathbf{R}_{\varepsilon\varepsilon} = (\mathbf{R}_{ss}^{-1} + \mathbf{H}^T\mathbf{R}_{nn}^{-1}\mathbf{H})^{-1}.$$

Consequently,

$$\mathbf{R}_{ee} = (\mathbf{F}_b + \mathbf{I}_{4K})(\mathbf{R}_{ss}^{-1} + \mathbf{H}^T\mathbf{R}_{nn}^{-1}\mathbf{H})^{-1}(\mathbf{F}_b + \mathbf{I}_{4K})^T.$$

Since $\mathbf{R}_{ss} = \frac{\sigma_s^2}{2}\mathbf{I}_{4K}$ and $\mathbf{R}_{nn} = \frac{\sigma_n^2}{2}\mathbf{I}_{4K}$, the Cholesky factorization of $\mathbf{R}_{\varepsilon\varepsilon}^{-1}$ can be performed as follows

$$\mathbf{H}^T\mathbf{H} + \frac{\sigma_n^2}{\sigma_s^2}\mathbf{I}_{4K} = \mathbf{L}\mathbf{\Lambda}_h\mathbf{L}^T.$$

Here $\mathbf{L}$ is a $4K \times 4K$ lower-triangular matrix, and $\mathbf{\Lambda}_h$ is a $4K \times 4K$ diagonal matrix used to normalize the diagonal entries of $\mathbf{L}$.

Let $\mathbf{F}_b = \mathbf{L}^T - \mathbf{I}_{4K}$, then $\mathbf{R}_{ee}$ is diagonalized to be $\mathbf{\Lambda}_h^{-1}$. Consequently,

$$\mathbf{F}_f = \mathbf{L}^T\mathbf{F}_{\text{LMMSE}}.$$

Hence, the derivation of $\mathbf{F}_f$ and $\mathbf{F}_b$ are completed.

REFERENCES

[1] D. Tse and P. Viswanath, *Fundamentals of Wireless Communication.* Cambridge University Press, 2005.

[2] A. Goldsmith, *Wireless Communications.* Cambridge University Press, 2005.

[3] T. S. Rappaport, *Wireless Communications: Principles and Practice*, 2nd ed. Prentice Hall PTR, 2002.

[4] U. Madhow, *Fundamentals of Digital Communication.* Cambridge University Press, 2008.

[5] J. G. Proakis, *Digital Communications.* McGraw-Hill International Edition, 2001.

[6] H. Jafarkhani, *Space-Time Coding.* Cambridge University Press, 2005.

[7] E. G. Larsson and P. Stoica, *Space-Time Block Coding for Wireless Communications.* Cambridge University Press, 2003.

[8] R. N. Arogyaswami Paulraj and D. Gore, *Introduction to Space-Time Wireless Communications.* Cambridge University Press, 2003.

[9] W. Su and X.-G. Xia, "Signal constellations for quasi-orthogonal space-time block codes with full diversity," *IEEE Trans. Inform. Theory*, vol. 50, no. 10, pp. 2331–2347, Oct. 2004.

[10] Y. G. Li and G. L. Stüber, *Orthogonal Frequency Division Multiplexing for Wireless Communications.* Springer Science+Business Media, Inc., 2006.

[11] M. Lei and H. Harada, "Performance comparison of multi-layer STBC OFDM and V-BLAST OFDM," in *IEEE Vehicular Technology Conference (VTC)*, Montreal, Que., Sept. 2006, pp. 1–5.

[12] C.-J. Park and G.-H. Im, "Improved cyclic prefix reconstruction and its application to space-time block coded orthogonal frequency division multiplexing transmission," in *IEEE International Conference on Communications (ICC)*, vol. 1, May 2005, pp. 603–607.

[13] J.-H. Lee and S.-C. Kim, "Efficient ISI cancellation for STBC OFDM systems using successive interference cancellation," *IEEE Commun. Lett.*, vol. 10, no. 8, pp. 629–631, Aug. 2006.

[14] H. Bolcskei and A. J. Paulraj, "Space-frequency codes for broadband fading channels," in *IEEE International Symposium on Information Theory*, Washington, DC, June 2001.

[15] Z. Liu, Y. Xin, and G. B. Giannakis, "Space-time-frequency coded OFDM over frequency-selective fading channels," *IEEE Trans. Signal Processing*, vol. 50, no. 10, pp. 2465–2476, Oct. 2002.

[16] ——, "Linear constellation precoding for OFDM with maximum multipath diversity and coding gains," *IEEE Trans. Commun.*, vol. 51, no. 3, pp. 416–427, Mar. 2003.

[17] D. Wulich, "Definition of efficient PAPR in OFDM," *IEEE Commun. Lett.*, vol. 9, no. 9, pp. 832–834, Sept. 2005.

[18] T. Jiang, M. Guizani, H.-H. Chen, W. Xiang, and Y. Wu, "Derivation of PAPR distribution for OFDM wireless systems based on extreme value theory," *IEEE Trans. Wireless Commun.*, vol. 7, no. 4, pp. 1298–1305, Apr. 2008.

[19] D. Huang and K. B. Letaief, "Carrier frequency offset estimation for OFDM systems using subcarriers," *IEEE Trans. Commun.*, vol. 54, no. 5, pp. 813–823, May 2006.

[20] Y. Jiang, H. Minn, X. Gao, X. You, and Y. Li, "Frequency offset estimation and training sequence design for MIMO OFDM," *IEEE Trans. Wireless Commun.*, vol. 7, no. 4, pp. 1244–1254, Apr. 2008.

[21] E. G. Larsson, P. Stoica, E. Lindskog, and J. Li, "Space-time block coding for frequency-selective channels," in *IEEE International Conference on Acoustics, Speech and Signal Processing (ICASSP)*, vol. 3, May 2002.

[22] N. Al-Dhahir, "Single-carrier frequency-domain equalization for space-time block-coded transmissions over frequency-selective fading channels," *IEEE Commun. Lett.*, vol. 5, no. 7, pp. 304–306, July 2001.

[23] S. Zhou and G. B. Giannakis, "Space-time coding with maximum diversity gains over frequency-selective fading channels," *IEEE Trans. Signal Processing*, vol. 8, no. 10, pp. 269–272, Oct. 2001.

[24] M. Cao and H. Ge, "CP based time-reversal QOSTBC transmissions over frequency-selective fading channels," in *IEEE Military Communications Conference (MILCOM)*, Nov. 2008.

[25] B. Razavi, "RF IC design challenges," in *Design Automation Conference*, Jun. 1998, pp. 408–413.

[26] Y. Zheng, M. Cao, E. K. H. Teo, and H. K. Garg, "An adaptive filtering algorithm for direct-conversion receivers: Architecture and performance analysis," *IEEE Trans. Circuits Syst. I*, vol. 55, no. 4, pp. 1141–1148, May 2008.

[27] A. Baier, "Quadrature mixer imbalances in digital TDMA mobile radio receivers," in *International Zurich Seminar on Digital Communications*, Zurich, Mar. 1990, pp. 147–162.

[28] R. A. Green, R. Anderson-Sprecher, and J. W. Pierre, "Quadrature receiver mismatch calibration," *IEEE Trans. Signal Processing*, vol. 47, no. 11, pp. 3130–3133, Nov. 1999.

[29] L. Yu and W. M. Snelgrove, "A novel adaptive mismatch cancellation system for quadrature IF radio receivers," *IEEE Trans. Circuits Syst. II*, vol. 46, no. 6, pp. 789–801, June 1999.

[30] J. K. Cavers and M. W. Liao, "Adaptive compensation for imbalance and offset losses in direct conversion transceivers," *IEEE Trans. Veh. Technol.*, vol. 42, no. 4, pp. 581–588, Nov. 1993.

[31] I.-H. Sohn, E.-R. Jeong, and Y. H. Lee, "Data-aided approach to I/Q mismatch and DC offset compensation in communication receivers," *IEEE Commun. Lett.*, vol. 6, no. 12, pp. 547–549, Dec. 2002.

[32] M. Cao and H. Ge, "Parametric modeling in mitigating the I/Q mismatch: Estimation, equalization, and performance analysis," in *40th Annual Conference on Information Sciences and Systems (CISS)*, Princeton, NJ, Mar. 2006, pp. 1286–1290.

[33] D. Tandur and M. Moonen, "Joint compensation of OFDM frequency selective transmitter and receiver IQ imbalance," in *IEEE International Conference on Acoustics, Speech and Signal Processing (ICASSP)*, vol. 3, Honolulu, HI, Apr. 2007, pp. 81–84.

[34] E. Lopez-Estraviz, S. De Rore, F. Horlin, and A. Bourdoux, "Pilot design for joint channel and frequency-dependent transmit/receive IQ imbalance estimation and compensation in OFDM-based transceivers," in *IEEE International Conference on Communications (ICC)*, Glasgow, June 2007, pp. 4861–4866.

[35] M. Valkama, M. Renfors, and V. Koivunen, "On the performance of interference canceller based I/Q imbalance compensation," in *IEEE International Conference on Acoustics, Speech, and Signal Processing (ICASSP)*, vol. 5, Istanbul, June 2000, pp. 2885–2888.

[36] ——, "Advanced methods for I/Q imbalance compensation in communication receivers," *IEEE Trans. Signal Processing*, vol. 49, no. 10, pp. 2335–2344, Oct. 2001.

[37] D. Mattera, L. Paura, and F. Sterle, "MMSE WL equalizer in presence of receiver IQ imbalance," *IEEE Trans. Signal Processing*, vol. 56, no. 4, pp. 1735–1740, Apr. 2008.

[38] D. Agrawal, V. Tarokh, A. Naguib, and N. Seshadri, "Gradient-based blind iterative techniques for I/Q imbalance compensation in digital radio receivers," in *IEEE Workshop on Signal Processing Advances in Wireless Communications (SPAWC)*, 2007, pp. 1–5.

[39] L. Anttila, M. Valkama, and M. Renfors, "Circularity-based I/Q imbalance compensation in wideband direct-conversion receivers," *IEEE Trans. Veh. Technol.*, vol. 57, no. 4, pp. 2099 – 2113, July 2008.

[40] P. Rykaczewski and F. Jondral, "Blind I/Q imbalance compensation in multipath environments," in *IEEE International Symposium on Circuits and Systems (ISCAS)*, may. 2007, pp. 29–32.

[41] L. Anttila, M. Valkama, and M. Renfors, "Blind compensation of frequency-selective I/Q imbalances in quadrature radio receivers: Circularity-based approach," in *IEEE International Conference on Acoustics, Speech and Signal Processing (ICASSP)*, vol. 3, Honolulu, HI, 2007, pp. 245–248.

[42] D. Mattera and F. Sterle, "ML estimation of receiver IQ imbalance parameters," in *International Waveform Diversity and Design Conference*, Pisa, June 2007, pp. 160–164.

[43] D. Fu, "A simultaneous TX and RX I/Q imbalance calibration method," in *IEEE International Symposium on Circuits and Systems (ISCAS)*, May 2008, pp. 1264 – 1267.

[44] H.-H. Chen, J.-T. Chen, and P.-C. Huang, "Adaptive I/Q imbalance compensation for RF transceivers," in *IEEE Global Telecommunications Conference (GLOBECOM)*, Dec. 2004, pp. 818–822.

[45] M. Valkama, Y. Zou, and M. Renfors, "On I/Q imbalance effects in MIMO space-time coded transmission systems," in *IEEE Radio and Wireless Symposium*, Jan. 2006, pp. 223–226.

[46] Y. Zou, M. Valkama, and M. Renfors, "Performance analysis of space-time coded MIMO-OFDM systems under I/Q imbalance," in *IEEE International Conference on Acoustics, Speech and Signal Processing (ICASSP)*, vol. 3, Honolulu, HI, Apr. 2007.

[47] S. M. Alamouti, "A simple transmit diversity technique for wireless communications," *IEEE J. Select. Areas Commun.*, vol. 16, no. 8, pp. 1451–1458, Oct. 1998.

[48] A. H. Sayed, W. M. Younis, and A. Tarighat, "An invariant matrix structure in multiantenna communications," *IEEE Signal Processing Lett.*, vol. 12, no. 11, pp. 749–752, Nov. 2005.

[49] L. He and H. Ge, "Reduced complexity maximum likelihood detection for V-BLAST systems," in *IEEE Military Communications Conference (MILCOM)*, vol. 2, 2003, pp. 1386–1391.

[50] J. Tang, A. H. Tewfik, and K. K. Parhi, "Reduced complexity sphere decoding and application to interfering IEEE 802.15.3a piconets," in *IEEE International Conference on Communications (ICC)*, vol. 5, June 2004, pp. 2864–2868.

[51] J. Jalden and B. Ottersten, "On the complexity of sphere decoding in digital communications," *IEEE Trans. Signal Processing*, vol. 53, no. 4, pp. 1474–1484, Apr. 2005.

[52] L. L. Scharf, *Statistical Signal Processing: Detection, Estimation, and Time Series Analysis*. Addison-Wesley Publishing Company, Inc., 1990.

[53] S. M. Kay, *Fundamentals of Statistical Signal Processing: Estimation Theory*. PTR Prentice Hall, 1993.

[54] S. Wu and Y. Bar-Ness, "OFDM systems in the presence of phase noise: consequences and solutions," *IEEE Trans. Commun.*, vol. 52, no. 11, pp. 1988–1996, Nov. 2004.

[55] Q. Zou, A. Tarighat, and A. H. Sayed, "Compensation of phase noise in OFDM wireless systems," *IEEE Trans. Signal Processing*, vol. 55, no. 11, pp. 5407–5424, Nov. 2007.

[56] F. Horlin, S. De Rore, E. Lopez-Estraviz, F. Naessens, and L. Van der Rerre, "MC-CDMA performance in the presence of carrier frequency offset, sample clock offset and IQ imbalance," in *IEEE Global Telecommunications Conference (GLOBECOM)*, vol. 6, Nov./Dec. 2005.

[57] P. Rykaczewski, M. Valkama, and M. Renfors, "Analytical approach to I/Q imbalance in OFDM, CDMA and MC-CDMA based systems," in *IEEE Radio and Wireless Symposium*, Jan. 2006, pp. 555–558.

[58] J. P. Elsner, P. Rykaczewski, C. Korner, and F. K. Jondral, "Orthogonal complex hadamard spreading codes for I/Q imbalance mitigation in MC-CDMA systems," in *IEEE Vehicular Technology Conference (VTC)*, Dublin, Apr. 2007, pp. 2661–2665.

[59] R. Chrabieh and S. Soliman, "IQ imbalance mitigation via unbiased training sequences," in *IEEE Global Telecommunications Conference (GLOBECOM)*, Washington, DC, Nov. 2007, pp. 4280–4285.

[60] J. Tubbax, B. Come, L. Van der Perre, S. Donnay, M. Moonen, and H. De Man, "Compensation of transmitter IQ imbalance for OFDM systems," in *IEEE International Conference on Acoustics, Speech, and Signal Processing (ICASSP)*, vol. 2, May 2004, pp. 325–8.

[61] S. Krone and G. Fettweis, "On the capacity of OFDM systems with receiver I/Q imbalance," in *IEEE International Conference on Communications (ICC)*, Beijing,China, May 2008, pp. 1317–1321.

[62] M. Krondorf and G. Fettweis, "Numerical performance evaluation of impaired OFDM links using Alamouti space time coding," in *IEEE International Conference on Communications (ICC)*, Beijing, May 2008, pp. 4074–4078.

[63] E. Lopez-Estraviz, S. De Rore, F. Horlin, and L. Van der Perre, "Optimal training sequences for joint channel and frequency-dependent IQ imbalance estimation in OFDM-based receivers," in *IEEE International Conference on Communications (ICC)*, vol. 10, Istanbul, June 2006, pp. 4595–4600.

[64] F. Horlin, A. Bourdoux, E. Lopez-Estraviz, and L. Van der Perre, "Low-complexity EM-based joint CFO and IQ imbalance acquisition," in *IEEE International Conference on Communications (ICC)*, Glasgow, June 2007, pp. 2871–2876.

[65] H. Lin, T. Adachi, and K. Yamashita, "Carrier frequency offset and I/Q imbalances compensation in OFDM systems," in *IEEE Global Telecommunications Conference (GLOBECOM)*, Washington, DC, Nov. 2007, pp. 2883–2888.

[66] J. Tubbax, B. Come, L. Van der Perre, S. Donnay, M. Engels, H. D. Man, and M. Moonen, "Compensation of IQ imbalance and phase noise in OFDM systems," *IEEE Trans. Wireless Commun.*, vol. 4, no. 3, pp. 872–877, May 2005.

[67] Q. Zou, A. Tarighat, and A. H. Sayed, "Joint compensation of IQ imbalance and phase noise in OFDM systems," in *Fortieth Asilomar Conference on Signals, Systems and Computers*, Pacific Grove, CA, Oct./Nov. 2006, pp. 1435–1439.

[68] S. Tang, K. Gong, C. Pan, Z. Yang, and K. Peng, "Phase noise suppression in OFDM systems in presence of IQ imbalance," in *International Conference on Communications, Circuits and Systems Proceedings,*, vol. 2, Guilin, June 2006, pp. 1184–1188.

[69] B. Narasimhan, D. Wang, S. Narayanan, N. Al-Dhahir, and H. Minn, "Digital baseband compensation for mobile SFBC-OFDM systems with receiver I/Q imbalance," in *IEEE Global Telecommunications Conference (GLOBECOM)*, New Orleans, LA USA, Nov./Dec. 2008, pp. 1–5.

[70] B. Narasimhan, S. Lu, N. Al-Dhahir, and H. Minn, "Digital baseband compensation of I/Q imbalance in mobile OFDM," in *IEEE Wireless Communications and Networking Conference (WCNC)*, Las Vegas, NV, Mar./Apr. 2008, pp. 646–651.

[71] M. Lipardi, D. Mattera, and F. Sterle, "MMSE equalization in presence of transmitter and receiver IQ imbalance," in *International Waveform Diversity and Design Conference*, Pisa, June 2007, pp. 165–168.

[72] D. Tandur and M. Moonen, "Digital compensation of RF imperfections for broadband wireless systems," in *IEEE Symposium on Communications and Vehicular Technology in the Benelux*, Delft, Nov. 2007, pp. 1–5.

[73] A. Tarighat, R. Bagheri, and A. H. Sayed, "Compensation schemes and performance analysis of IQ imbalances in OFDM receivers," *IEEE Trans. Signal Processing*, vol. 53, pp. 3257–3268, Aug. 2005.

[74] A. Tarighat and A. H. Sayed, "MIMO OFDM receivers for systems with IQ imbalances," *IEEE Trans. Signal Processing*, vol. 53, no. 9, pp. 3583–3596, Sept. 2005.

[75] L. Shao and S. Roy, "Rate-one space-frequency block codes with maximum diversity for MIMO-OFDM," *IEEE Trans. Wireless Commun.*, vol. 4, no. 4, pp. 1674–1687, July 2005.

[76] Z. Latinovic and Y. Bar-Ness, "SFBC MIMO-OFDM peak-to-average power ratio reduction by polyphase interleaving and inversion," *IEEE Commun. Lett.*, vol. 10, no. 4, pp. 266–268, Apr. 2006.

[77] H.-G. Ryu, "System design and analysis of MIMO SFBC CI-OFDM system against the nonlinear distortion and narrowband interference," *IEEE Trans. Consumer Electron.*, vol. 54, no. 2, pp. 368–375, May 2008.

[78] W. Y. Zou and Y. Wu, "COFDM: an overview," *IEEE Trans. Broadcast.*, vol. 41, no. 1, pp. 1–8, Mar. 1995.

[79] Y. Xin, Z. Wang, and G. B. Giannakis, "Space-time diversity systems based on linear constellation precoding," *IEEE Trans. Wireless Commun.*, vol. 2, no. 2, pp. 294–309, Mar. 2003.

[80] M. Cao and H. Ge, "I/Q imbalance mitigation for STBC MIMO-OFDM communication systems," in *IEEE International Conference on Acoustics, Speech and Signal Processing (ICASSP)*, Mar./Apr. 2008, pp. 3093–3096.

[81] N. H. Tran, H. H. Nguyen, and T. Le-Ngoc, "Subcarrier grouping for OFDM with linear constellation precoding over multipath fading channels," *IEEE Trans. Veh. Technol.*, vol. 56, pp. 3607–3613, Sept. 2007.

[82] Y. Li, N. Seshadri, and S. Ariyavisitakul, "Transmitter diversity for OFDM systems with mobile wireless channels," in *IEEE Global Telecommunications Conference (GLOBECOM)*, vol. 2, Sydney,NSW, Nov. 1998, pp. 968–973.

[83] M. Park, H. Jun, J. Cho, N. Cho, D. Hong, and C. Kang, "PAPR reduction in OFDM transmission using hadamard transform," in *IEEE International Conference on Communications (ICC)*, vol. 1, New Orleans, LA, June 2000, pp. 430–433.

[84] K. D. Wong, M. O. Pun, and H. V. Poor, "The continuous-time peak-to-average power ratio of OFDM signals using complex modulation schemes," *IEEE Trans. Commun.*, vol. 56, no. 9, pp. 1390–1393, Sept. 2008.

[85] S. K.Mitra, *Digital Signal Processing: A Computer-Based Approach.* McGraw-Hill Companies, Inc., 2001.

[86] The Matrix Cookbook. [Online]. Available: http://matrixcookbook.com/

[87] B. Farhang-Boroujeny, *Adpative Filters: Theory and Applications.* John Wiley & Sons, 1998.

[88] S. Haykin, *Adaptive Filter Theory.* PTR Prentice Hall, 2001.